1

CHEMISTRY OF REACTIVE SPECIES

Frederick A. Villamena

COPYRIGHTED MATERIAL

1.1 REDOX CHEMISTRY

An electron is an elementary subatomic particle that carries a negative charge. The ease of electron flow to and from atoms, ions, or molecules defines the reactivity of a species. As a result, an atom, or in the case of molecules, a particular atom of a reactive species undergoes a change in its oxidation state or oxidation number. During reaction, oxidation and reduction can be broadly defined as decrease or increase in electron density on a particular atom, respectively. A more direct form of oxidation and reduction processes is the loss or gain of electrons on a particular atom, respectively, which is often referred to as electron transfer. Electron transfer can be a one- or two-electron process. One common example of a one-electron reduction process is the transfer of one electron to a molecule of oxygen (O_2) resulting in the formation of a superoxide radical anion ($O_2^{\bullet -}$) (Eq. 1.1). Further one-electron reduction of $O_2^{\bullet -}$ yields the peroxide anion (O_2^{2-}) (Eq. 1.2), although this is very unlikely to occur without the addition of protons or another supplier of a positive charge.

$$O_2 + e_{aq}^- \rightarrow O_2^{\bullet -} \tag{1.1}$$

$$O_2^{\bullet -} + e_{aq}^- \rightarrow O_2^{2-} \tag{1.2}$$

Conversely, two-electron oxidation of metallic iron (Fe^0) leads to the formation of Fe^{2+} (Eq. 1.3) and further one-electron oxidation of Fe^{3+} leads to the formation of Fe^{3+} (Eq. 1.4). Electrons in this case can be introduced electrochemically or through reaction with reducing or oxidizing agents.

$$Fe^0 \rightarrow Fe^{2+} + 2e_{aq}^- \tag{1.3}$$

$$Fe^{2+} \rightarrow Fe^{3+} + e_{aq}^- \tag{1.4}$$

Another method by which oxidation state on a particular atom can be altered is through change in bond polarity. Electronegative atoms have the capability of attracting electrons (or electron density) toward themselves. Listed below are the biologically relevant atoms according to their decreasing electronegativities (revised Pauling): F (3.98) > O (3.44) > Cl (3.16) > N (3.04) > Br (2.96) > S > (2.58) > C = Se (2.55) > H (2.20) > P (2.19). Therefore, by changing the electronegativity (or electropositivity) of an atom attached to an atomic center of interest can result in the reversal of the polarization of the bond. Applying the "who's-got-the-electron-rule" will be beneficial in identifying atomic centers that undergo changes in their oxidation states. For example, based on the electronegativity listed above, one could examine the relative oxidation states of a carbon atom in a molecule (Figure 1.1). Since carbon belongs to group 14 of the periodic table, the carbon atom has 4 valence electrons. When carbon is bonded to an atom that is less electronegative to it (e.g., hydrogen atom), the carbon atom tends to pull the electron density toward itself making it electron rich. The 2 electrons that it shares with each hydrogen atom are counted toward the number of electrons the carbon atom can claim. In the first example, methane

Molecular Basis of Oxidative Stress: Chemistry, Toxicology, Disease Pathogenesis, Diagnosis, and Therapeutics, Second Edition.
Edited by Frederick A. Villamena and Henry Jay Forman.
© 2025 John Wiley & Sons, Inc. Published 2025 by John Wiley & Sons, Inc.

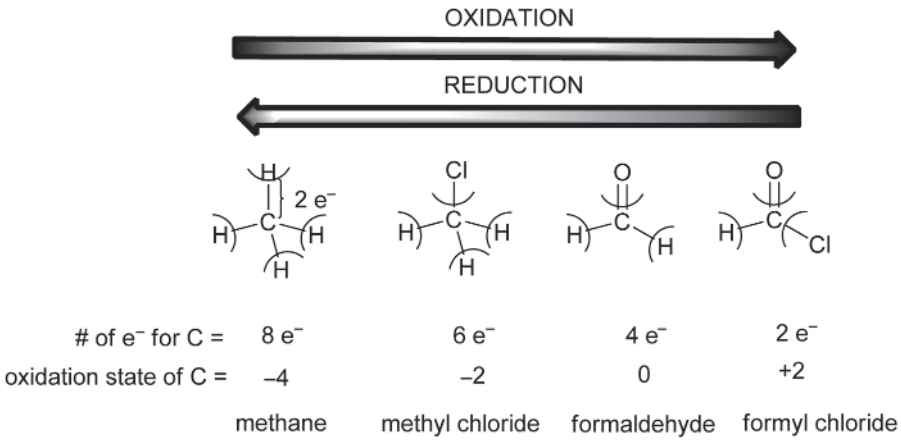


Figure 1.1 Oxidation states of the carbon atom calculated as number of valence electrons for the carbon atom (i.e., 4 e^-) minus the number of electrons that carbon can claim in a molecule. Order of increasing electronegativity: H < C < O < Cl.

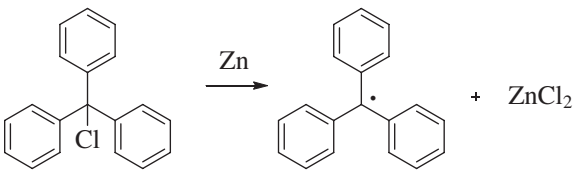
has 4 hydrogen atoms attached to it. A hydrogen is less electronegative than carbon, all 8 shared electrons can be claimed by carbon but since carbon is only entitled to 4 electrons by virtue of its valence electron, it has an excess of 4 electrons making its oxidation state −4. However, when a carbon atom is covalently bound to a more electronegative atom (e.g., oxygen and chlorine), the spin density distribution around the carbon atom decreases and is polarized toward the more electronegative atoms. In this case, the electrons shared by carbon with a more electronegative atom are counted toward the more electronegative atom. In the case of formyl chloride, only the 2 electrons it shares with hydrogen can be counted toward the total number electrons the carbon atom can claim since the 4 electrons it shares with oxygen and the 2 electrons it shares with chlorine cannot be counted toward the carbon because these electrons are polarized toward the more electronegative atoms. Hence, the carbon becomes deficient in electron density, and by virtue of its 4 valence electrons, it can only claim 2 electrons from the hydrogen atom; therefore, the net oxidation state can be calculated to be +2. The increasing positivity of the carbon from methane to formyl chloride indicates oxidation of carbon and, therefore, oxidation can now be broadly defined as: (1) loss of electron; (2) loss of hydrogen atom; and (3) gain of oxygen or halogen atoms; while reduction can be defined as: (1) gain of electron; (2) gain of hydrogen atom; and (3) loss of oxygen or halogen atoms.

1.2 CLASSIFICATION OF REACTIVE SPECIES

Reactive species could be generally classified into two main classes, (1) open-shell; and (2) closed-shell systems. Open-shell systems are those molecular species with an unpaired electron in its valence shell (or orbital) and are usually referred to as free radical (or simply radical), or paramagnets since they are attracted to a magnetic field. Although paramagnetic and free radical species are open-shell systems, the former terminology is commonly used to refer to metal-based molecules while the latter for non-metallic ones. However, open-shell reactive species could have one or more unpaired electron in its orbital; examples of one unpaired electron radicals are hydroxyl ($HO^{\bullet}$), superoxide ($O_2^{\bullet-}$), or nitric oxide ($NO^{\bullet}$) with multiplicity referred to as doublet state (from the expression: $2S+1$ where $S = ½$). Molecular oxygen (O_2), however, has two unpaired electrons in each of its orbitals commonly referred to as biradical and with a triplet multiplicity (where $S = 1$). For the open-shell reactive species, radical species could be atomic, ionic, or neutral molecule. Examples of atomic radical species are $H^{\bullet}$, $Cl^{\bullet}$, or $Br^{\bullet}$, while examples of anionic radicals that are molecular in nature are $O_2^{\bullet-}$, semiquinones ($SQ^{\bullet-}$), or oxidized glutathione radical anion ($GSSG^{\bullet-}$). Closed-shell systems are those species with no unpaired electron, and with filled, or empty valence shells. Since they are not attracted to a magnetic field, they are typically referred to as diamagnetic molecules. Examples of which are hydrogen peroxide (H_2O_2), glutathione (GSH), or peroxynitrite ($ONOO^-$).

Free radicals are an integral part of many chemical and biological processes. They play a major role in determining the lifetime of air pollution in our atmosphere[1] and are widely exploited in the design of polymeric, conductive, or magnetic materials.[2] In biological systems, free radicals have been implicated in the development of various diseases.[3] So what are free radicals? The word "radical" came from the Latin word *radix* meaning "root." In the mid-1800s, chemists began to use the word radical to refer to a group of atoms. How the word "radical" had become a chemical terminology is not clear, but one could only speculate

that these groups of atoms that make up a molecule were figuratively referred to as "roots" or foundation of an entity. In the early 1900s, early literature referred to metallic atoms as basic radicals and nonmetallic ones as acid radicals, for example, in $Mg(OH)_2$ or H_2S, respectively. During this time, radicals were still referred to as group entities that were part of a compound but not until Gomberg had demonstrated during this same time that radicals can indeed exist by themselves as exemplified by his synthesis of the stable triphenylmethyl radical **2** from the reduction of triphenylchloromethane **1** by Zn (Eq. 1.5).[4]



1 **2** (1.5)

In the late 1950s, the electron paramagnetic resonance spectrum of **2** was obtained, further confirming the radical nature of trityl which can indeed be stable enough to exist by itself and be spectroscopically detected.[5] Radical is defined in modern times as a finite chemical entity by its own that is capable of undergoing chemical reaction. Radicals carry an odd number of electrons in the form of an atom, neutral or ionic molecule. By virtue of Pauli's exclusion principle, the number of electrons occupying an atomic or molecular orbital is limited to two if they have different spin quantum number. This pairing of electrons results in the formation of a chemical bond between atoms, existence of lone pair of electrons or completion of the inner core non-bonding electrons. For radicals, electrons are typically on an open-shell configuration in which the atomic or molecular orbitals are not filled with electrons making them thermodynamically more energetic species than atoms or molecules with closed-shell configuration or with filled orbitals. For example, the noble gases He, Ne, or Ar, with filled atomic orbitals, $1s^2$ (He), $1s^22s^22px^22py^22pz^2$ (Ne), $1s^22s^22p^6 3s^23px^23py^23pz^2$ (Ar), are known to be inert, while the atomic H, N, or Cl with electron configurations of $1s^1$ (H), $1s^22s^22px^22py^12pz^0$ (N), and $1s^22s^22p^63s^23px^2 3py^23pz^1$ (Cl) are known to be highly reactive and hence exist as diatomic molecules. Similarly, molecules with open-shell molecular orbital configurations are more reactive than molecules with closed-shell configuration. For example, HO$^\bullet$ has an open-shell configuration of $\sigma_{pz}^2\ p_x^2p_y^1$, while the hydroxide anion has a closed-shell configuration of $\sigma_{pz}^2\ p_x^2p_y^2$, making the former more reactive than the latter.

1.2.1 Type of Orbitals

Radicals can be classified according to the type of orbital (SOMO) that bears the unpaired electron as σ- or π-radicals. Radical stability is governed by the extent of electron delocalization within the atomic orbitals. In general, due to the restricted spin delocalization in the σ-radicals, these radicals are more reactive than the π-radicals. Examples of σ-radicals are H$^\bullet$, formyl-, vinyl-, or phenyl-radicals (Figure 1.2).

Almost all of the radical-based ROS that will be discussed in this chapter fall under the π-type category, but each will differ only on the extent of spin delocalization within the molecule. Examples of π-radicals with restricted spin delocalization are $^\bullet CH_3$, $^\bullet SH$, and HO$^\bullet$ and are relatively less stable than π-radicals with extended spin delocalization (e.g., HOO$^\bullet$, $O_2^{\bullet-}$, and NO$^\bullet$) (Figure 1.3).

1.2.2 Stability of Radicals

Radicals can also be categorized according to their stability as stable, persistent, and unstable (or transient). Although the terms stable and persistent are often used interchangeably, free radical chemists agree that persistent radicals refer to the thermodynamic favorability of being monomeric as opposed to dimer as formed *via*

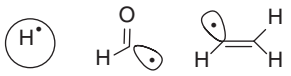


Figure 1.2 Hydrogen, formyl and vinyl σ-radicals.

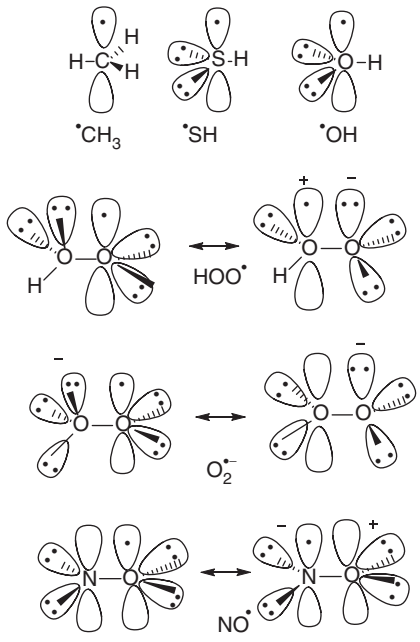


Figure 1.3 Methyl, thiyl, hydroxyl, hydroperoxyl, superoxide and nitric oxides as examples of π-radicals.

radical-radical reaction in solution. Radical-based ROS are not persistent (or stable) making their detection in solution very difficult. ROS detection is commonly accomplished by detecting secondary products arising from their redox or addition reaction with a reagent as will be discussed in the succeeding section. Figure 1.4 shows examples of dimer formation from $HO^{\bullet}$, $HO_2^{\bullet}$, TEMPO, and trityl, and their respective approximate dissociation enthalpies. Rates of ROS decomposition in solution, of course, depend on the type of substrates that are present in solution, but lifetimes of these radicals vary in solution since even one of the most stable radicals such as the trityl radical for example is not stable in the presence of oxido-reductants.

1.2.3 Reactive (O, N, S, X) Species

The classifications mentioned above could be simplified to refer to the specific atom that underwent redox transformation as reactive oxygen, nitrogen, sulfur, or halogen species and are abbreviated as ROS, RNS, RSS, or RXS, respectively. Nitric oxide ($NO^{\bullet}$), for example, could react with $HO^{\bullet}$ to form nitrous acid (HNO_2) but to classify whether $NO^{\bullet}$ is a reactive nitrogen or oxygen species, one has to carefully examine the oxidation states of the relevant atoms of the reactants and the product (Figure 1.5). Using the "who's-got-the-electron-rule" mentioned above, one can assign the oxidation states for each of the species involved in the transformation. The nitrogen atom of $NO^{\bullet}$ underwent an oxidation since its oxidation state has increased from +2 to +3 in HNO_2, while the oxygen of $HO^{\bullet}$ (not of $NO^{\bullet}$) underwent reduction (from −1 to −2). We can therefore classify $NO^{\bullet}$ as reactive nitrogen species (RNS) while $HO^{\bullet}$ as reactive oxygen species (ROS) since it was the nitrogen atom of $NO^{\bullet}$ and the oxygen atom of $HO^{\bullet}$ that underwent oxidation state modification after reaction. However, there is a caveat in this classification since, for example, a few molecules contain more than one atom whose oxidation state could change during a redox reaction. For example, the formation $^{\bullet}NO_2$ and $HO^{\bullet}$ from ONOO(H) would make ONOO(H) both an RNS and ROS since N and O atoms were oxidized and reduced, respectively, during the chemical transformation (Figure 1.5). Figure 1.6 shows the various reactive oxygen, nitrogen, and sulfur species with their respective oxidation states.

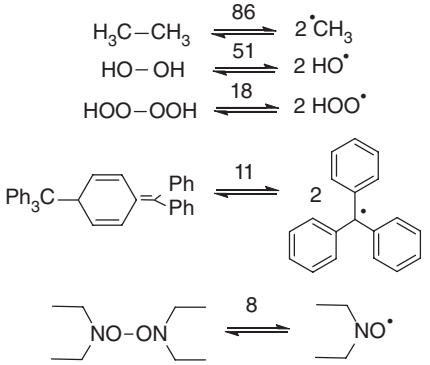


Figure 1.4 Dissociation enthalpies (ΔH^0 in kcal/mol) of various dimers showing nitroxide to be the most stable radical and the methyl radical being the least stable.

1.3 REACTIVE OXYGEN SPECIES

1.3.1 Oxygen Molecule (O_2, Triplet Oxygen, Dioxygen)

The electronic ground state of molecular oxygen is the triplet state, $O_2(X^3\Sigma_g^-)$. Dioxygen's molecular orbital $O_2(X^3\Sigma_g^-)$ has each of the two electrons occupying the two degenerate antibonding π_g-orbitals and whose spins are the same or are parallel with each other (Figure 1.7).

Owing to dioxygen's biradical (open-shell) property, it exhibits a radical-type behavior in many chemical reactions. Elevated physiological concentrations of O_2 (hyperoxia) have been shown to be toxic to cultured epithelial cells via necrosis, while lethal concentrations of H_2O_2 and $O_2^{\bullet-}$ cause apoptosis suggesting that O_2 causes cell death mechanism that is distinct from other oxidants. However, in *in vivo* systems, apoptosis is predominantly the main mechanism of cell death in the lung upon breathing 99.9% O_2.[6]

Chlorinated aromatics have been widely used as biocides and industrial raw materials and are ubiquitous as

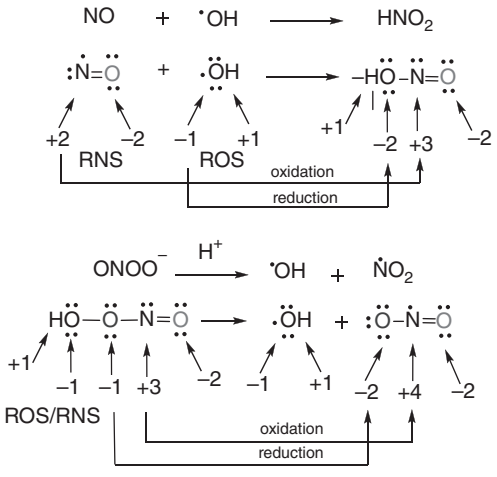


Figure 1.5 Reaction of nitric oxide with hydroxyl radical to produce nitrous acid showing pertinent oxidation states of the atoms undergoing redox transformation.

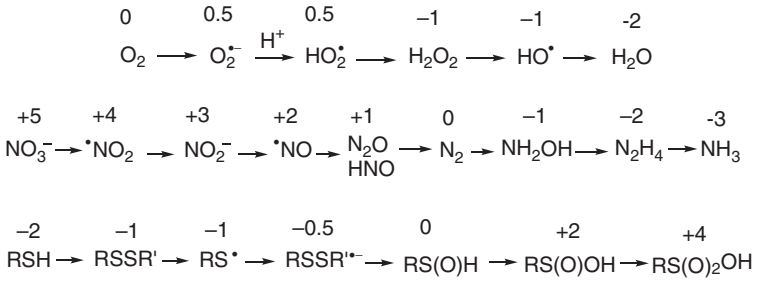


Figure 1.6 Reaction of nitric oxide with hydroxyl radical to produce nitrous acid showing pertinent oxidation states of the atoms undergoing redox transformation.

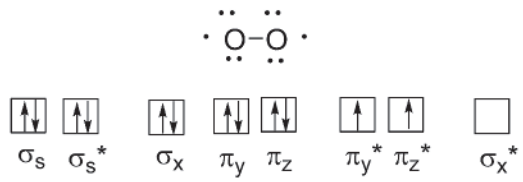
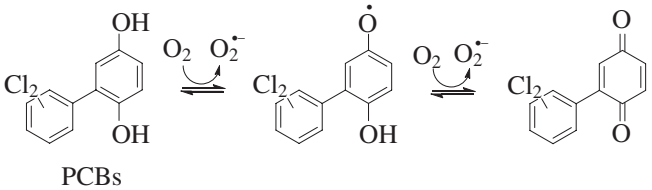
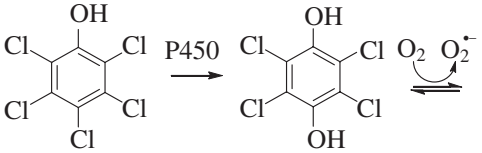


Figure 1.7 Molecular orbital diagram of dioxygen showing its biradical nature.

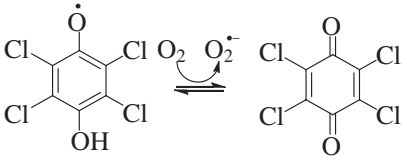
environmental pollutants. The toxicology of polychlorinated biphenyls (PCBs) for example has been shown to be due to the formation H_2O_2 and $O_2^{\bullet-}$ from one-electron oxidation or reduction by molecular oxygen of reactive hydroquinone and quinone products, respectively, via formation of semiquinone radicals (Eq. 1.6).[7] Oxygenation of pentachlorophenol[8] (PCP) also leads to the formation of superoxide via the same mechanisms (Eq. 1.7).



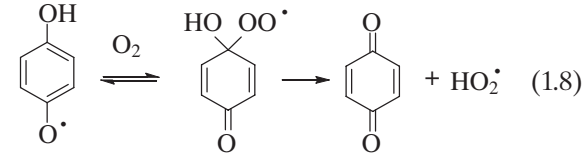
(1.6)



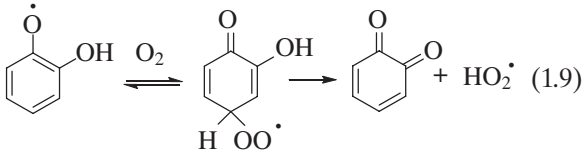
(1.7)



Oxygen addition to 1,4-semiquinone radicals was observed to be more facile than their addition to 1,2-semiquinones with free energies of reaction of 7.4 and 10.3 kcal/mol, respectively (Eqs. 1.8 and 1.9).[9] The experimental rate constants for the reaction of O_2 with 2,5-di-*tert*-butyl-1,4-semiquinone radicals were 2.4×10^5 and $2.0 \times 10^6 M^{-1}\ s^{-1}$ in acetonitrile and chlorobenzene, respectively, similar to that observed aqueous media at pH 7. The formation of quinones was suggested to occur via a two-step mechanism in which O_2 adds to the aromatic ring followed by an intramolecular H-atom transfer to the peroxyl moiety and concomitant release of $HO_2^{\bullet}$. This reactivity of O_2 to semiquinone to yield $HO_2^{\bullet}$ underlies the pro-oxidant activity of hydroquinones.[10]



(1.8)



(1.9)

Perhaps one of the most important reactions of O_2, although reversible in most cases, is its addition to carbon- or sulfur-centered radicals which are relevant in the propagation reaction in lipid peroxidation processes or thiol oxidation, respectively. The reaction of dioxygen with lipid radical and thiyl radicals form peroxyl ($LOO^{\bullet}$) and thiol peroxyl ($RSOO^{\bullet}$) radicals (Eqs. 1.10 and 1.11).

$$L^{\bullet} \overset{O_2}{\rightleftharpoons} LOO^{\bullet} \tag{1.10}$$

$$RS^{\bullet} \overset{O_2}{\rightleftharpoons} RSOO^{\bullet} \tag{1.11}$$

1.3.2 Superoxide Radical Anion ($O_2^{\bullet-}$)

Superoxide is the main precursor of the most highly oxidizing or reducing species in biological system. The one-electron reduction of triplet dioxygen forms $O_2^{\bullet-}$ and initiates oxidative cascade. The molecular orbital of $O_2^{\bullet-}$ shows one unpaired electron in antibonding π_g-orbital (Figure 1.8). The unpaired electron is delocalized between the π^* orbitals of the two oxygen atoms.

1.3.2.1 Dismutation Reaction Superoxide's oxidation state allows it to either get oxidized or reduced to form dioxygen or hydrogen peroxide, respectively (Eq. 1.12), thereby

$$\begin{aligned} O_2^{\bullet-} &\rightarrow O_2 + e^- \quad \text{(oxidation)} \\ O_2^{\bullet-} + e^- + 2H^+ &\rightarrow H_2O_2 \quad \text{(reduction)} \end{aligned} \tag{1.12}$$

allowing $O_2^{\bullet-}$ to dismutate to H_2O_2 and O_2 according to Equation 1.13:

$$2O_2^{\bullet-} + H^+ \rightleftharpoons H_2O_2 + O_2 \quad K_{pH7} = 4 \times 10^{20} \tag{1.13}$$

The dismutation of two $O_2^{\bullet-}$ in the absence of proton is slow with $k = <0.3\,M^{-1}s^{-1}$ due to repulsive effects between the negative charges. However, in acidic medium, the rate $O_2^{\bullet-}$ dismutation significantly increases due to the formation of the neutral $HO_2^{\bullet-}$ (Eqs. 1.14 and 1.15) in which electron transfer between the radicals becomes more facile.

$$O_2^{\bullet-} + HO_2^{\bullet} \rightarrow O_2 + HO_2^- \quad k = 1 \times 10^8\ M^{-1}\ s^{-1} \tag{1.14}$$

$$HO_2^{\bullet} + HO_2^{\bullet} \rightarrow O_2 + H_2O_2 \quad k = 1 \times 10^5\ M^{-1}\ s^{-1} \tag{1.15}$$

The pK_a of the conjugate acid of $O_2^{\bullet-}$ was determined to be 4.69 which indicates that $O_2^{\bullet-}$ is a poor base, but $O_2^{\bullet-}$ has strong propensity to abstract proton from protic substrates. For example, $O_2^{\bullet-}$ addition to water results in the formation of HO_2^- and HO^-, with an equilibrium constant equivalent to 0.9×10^9.[10] This indicates that $O_2^{\bullet-}$ can undergo proton abstraction from substrates to an extent equivalent to a conjugate base of an acid with a pK_a of 24 (Eq. 1.16).[10]

$$2O_2^{\bullet-} + H_2O \rightleftharpoons HO_2^- + O_2 + HO^- \quad K_{pH7} = 0.9 \times 10^9 \tag{1.16}$$

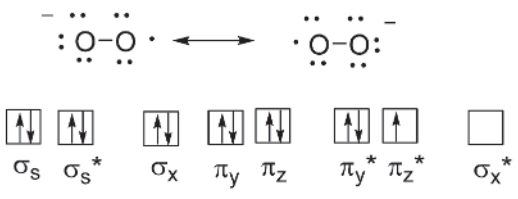


Figure 1.8 Molecular orbital diagram of $O_2^{\bullet-}$.

This ability of $O_2^{\bullet-}$ to act as "strong base" is due to its slow initial self-dismutation to O_2 and peroxide (O_2^{2-}) that can drive the equilibrium further right to form the hydroperoxide, HO_2^-. Since the pK_a of H_2O_2 is ~11.75[11], the basicity of HO_2^- can approach those of RS^-.

Dismutation has also been reported to be catalyzed by SOD mimetics, fullerene derivatives, nitroxides, and metal complexes. Superoxide dismutation should meet the following criteria: (1) no structural or chemical modification of the mimetic upon reaction with $O_2^{\bullet-}$; (2) regeneration of O_2; (3) production of H_2O_2; and (4) absence of paramagnetic primary by-products. Tris-malonyl-derivatives of fullerene (C_{60}) have been shown to exhibit SOD mimetic properties with rate constants in the order of $10^6\,M^{-1}s^{-1}$ compared to dismutation rates imparted by SODs (*i.e.,* ~$10^9\,M^{-1}s^{-1}$).[12] *In vivo* studies using SOD2-/- knockout mice indicate increased lifespan by 300% and show localization in the mitochondria functioning as MnSOD.[13] Computational studies show that electron density around the malonyl groups is low thereby making this region more susceptible to nucleophilic attack by $O_2^{\bullet-}$ *via* electrostatic effects.[13] Osuna et al.[14] suggested a dismutation mechanism by which $O_2^{\bullet-}$ interacts with the fullerene surface and is stabilized by a counter-cation and water molecules. An electron is transferred from $O_2^{\bullet-}$ to the fullerene producing O_2 and fullerene radical anion. Subsequent electron transfer from fullerene radical anion to another molecule of $O_2^{\bullet-}$ gives the fullerene-O_2^{2-} complex and protonation of the peroxide by the malonic acid groups gives fullerene-H_2O_2 where H_2O_2 is released along with the regenerated fullerene (Figure 1.9).

SOD exists in two major forms: CuZnSOD that is primarily present in cytosol, while MnSOD is located in the mitochondria. There is also an FeSOD that has chemical similarities with MnSOD such as being susceptible to deactivation at high pH and resistance to CN^- inactivation. Over the past years, the synthesis of metal-complexes-based SOD mimetics involved the use of Ni(II),[15] Cu(II),[8] Mn(III),[16] Mn(II),[17] Fe(II), and Fe(III).[18] The overall dismutation reaction of metal–SOD/SOD mimetic involves the following redox reaction (Figure 1.10):

Activation of $O_2^{\bullet-}$ by metal ions *via* the formation of metal–peroxo adduct ($M^{(n+1)}$–O_2^{2-}) (Eq. 1.17)

$$Fe(II) + O_2^{\bullet-} \rightarrow Fe(III)\text{-}O_2^{2-} \tag{1.17}$$

Formation of $M^{(n+1)}$–O_2^{2-} can also be achieved through several pathways such as combination of $M^{(n-1)}$ and O_2, $M^{(n+1)}$ and O_2^{2-}, or $M^{(n)}$, O_2 and e^-.[19] Protonation of metal–peroxo adducts can proceed *via* two different pathways depending on the metabolizing enzyme involved. For example with SOD, release of H_2O_2 occurs

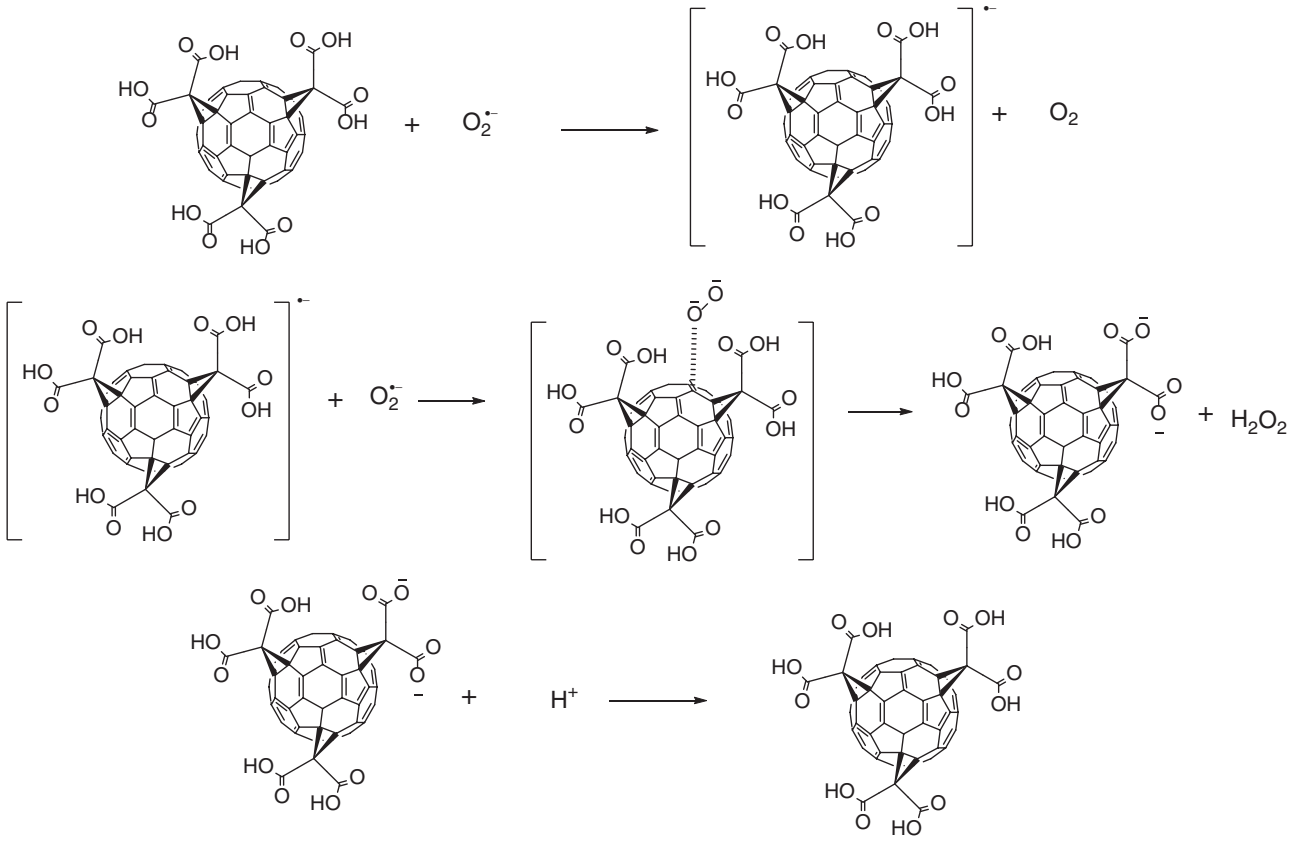


Figure 1.9 SOD mimetic property of tris-malonyl-derivative of fullerene (C_{60}).

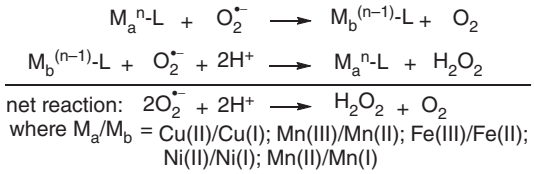


Figure 1.10 SOD mimetic property of metal-complexes.

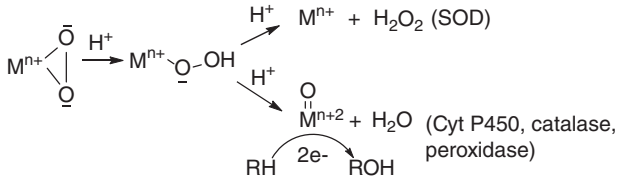
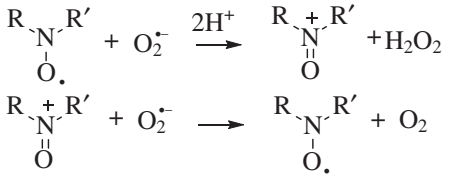


Figure 1.11 Activation of $O_2^{\bullet-}$ by metal ions.

with the metal oxidation state unchanged, while in the case of catalase, peroxidases and cytochrome P450, O–O bond cleavage occurs with the formation of a high valent metal oxo-species (Figure 1.11).[19]

Electrostatic effect plays an important role in enhancing SOD mimetic activity by introducing positively charged moieties.[13] For example, studies show that the presence of guanidinium derivative of an imidazolate-bridged dinuclear copper moiety enhances SOD activity by 30% compared to when the guanidinium is lacking.[8] Also, increasing the number of positive charge on the ligand and its proximity around the metal center gives higher SOD mimetic activity by several-fold compared to the singly charged analogue.[20]

Nitroxide or aminoxyl-type compounds have also been shown to impart SOD-mimetic properties with catalytic rates that are in the order of $10^5 M^{-1} s^{-1}$ at pH 7.[21,22] The mechanism was suggested to be catalyzed by formation of an oxoammonium intermediate which in turn converts $O_2^{\bullet-}$ to molecular O_2 according to the following reactions shown in Equation 1.18:

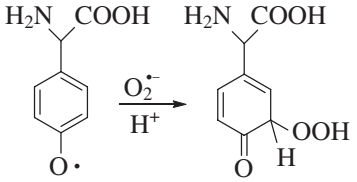


(1.18)

1.3.2.2 Nucleophilic Substitution Reaction Nucleophilic substitution reaction has also been observed for $O_2^{\bullet-}$ with alkyl halides and tosylates in DMSO leading to the formation of alkylperoxy radicals then to peroxy anions via one-electron reduction (Eq. 1.19).[23,24]

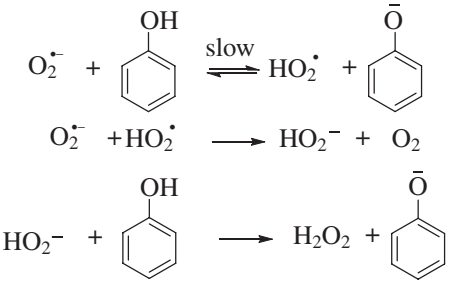
$$\begin{aligned} RX + O_2^{\bullet-} &\longrightarrow ROO^{\bullet} + X^- \\ ROO^{\bullet} &\xrightarrow[H^+]{e^-} ROOH \end{aligned} \qquad (1.19)$$

1.3.2.3 Addition Reactions Reaction of $O_2^{\bullet-}$ with tyrosyl radical generated from sperm whale myoglobin was investigated, and results show that $O_2^{\bullet-}$ prevented myoglobin dimer formation as a mechanism for repairing protein tyrosyl radical.[25] Moreover, an addition product with $O_2^{\bullet-}$ at Tyr151 was identified using mass spectrometry as a more preferred reaction compared to dimer formation, and this addition reaction was enhanced in the presence of exogenously added lysine.[25] This study further supports previous observations on the formation of tyrosyl hydroperoxide generated from $O_2^{\bullet-}$ and tyrosyl radical as enhance by the presence of H-bond donors.[26,27] Addition of $O_2^{\bullet-}$ and tyrosyl radical at the ortho-position is the most thermodynamically preferred addition product (Eq. 1.20).[27] In aprotic solvents, reaction of $O_2^{\bullet-}$ with α-dicarbonyl carbon involves nucleophilic addition to the carbonyl carbon followed by dioxetane formation *via* addition of the terminal O to the other carbonyl carbon. Reductive cleavage by the second $O_2^{\bullet-}$ yields benzoate and oxygen.[28]



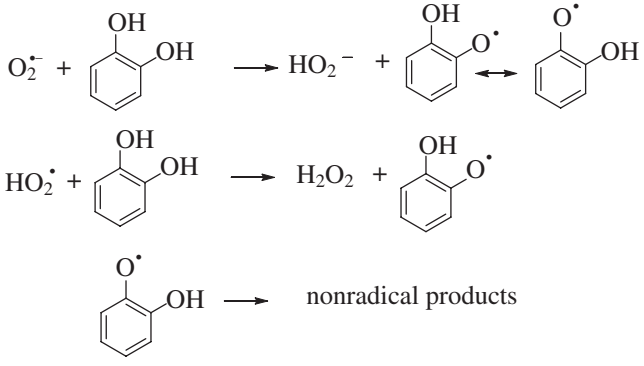
(1.20)

1.3.2.4 Proton-radical Transfer By virtue of the pK_a of the conjugate acid of $O_2^{\bullet-}$ of 4.8, $O_2^{\bullet-}$ is considered a weak base. However, proton and radical transfer pathways have been proposed for the antioxidant property of monophenols and polyphenols, respectively.[29] For mono-phenols, electrogenerated $O_2^{\bullet-}$ acts as weak base and the phenolic compound (PhOH) acting as Bronsted acid according to Equation 1.21 in which the formation of phenoxide PhO^- and $HO_2^{\bullet}$, though thermodynamically unfavorable, can be driven to completion by the subsequent electron-transfer reaction between $HO_2^{\bullet}$ and $O_2^{\bullet-}$, to form HO_2^- (a very strong base) and O_2 in which the former can further abstract proton from phenol to form the phenoxide (PhO^-) according to Equation 1.21.



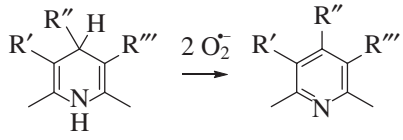
(1.21)

Polyphenols however undergo radical (or H atom) transfer reaction with $O_2^{\bullet-}$ to form the phenoxyl radical ($PhO^{\bullet}$) and HO_2^-; similarly with monophenols, HO_2^- can also abstract proton from PhOH to form phenoxide (PhO^-). The fate of $PhO^{\bullet}$ was shown to form non-radical products via dimerization or oligomerization, or semiquinone formation. The difference in the pathways for monophenols *versus* polyphenol decomposition with $O_2^{\bullet-}$ can be due to the stabilization of the radical in polyphenols *via* resonance as evidenced by the higher reactivity of polyphenols containing o-diphenol rings with $O_2^{\bullet-}$ according to Equation 1.22.



(1.22)

Reactivity of $O_2^{\bullet-}$ was also reported with cardiovascular drugs such as 1,4-dihydropyridine analogues of nifedipine to form pyridine (Eq. 1.23).[30] The proposed mechanism involves a two-electron oxidation of DHP to form the pyridine and hydrogen peroxide.



(1.23)

Reaction of $O_2^{\bullet-}$ with thiols was also reported, and reactivities were found to be highest for acidic thiols with approximated rate constants in the orders of

$10–10^3\,M^{-1}\,s^{-1}$.[31] Oxygen uptake shows concomitant formation H_2O_2 for some thiols such as penicillamine and cysteine *via* a complex radical chain reaction with the formation of oxidized thiols (Figure 1.12), but this mechanism was not observed for GSH, DTT, cysteamine, and *N*-acetylcysteine. This difference in mechanisms among thiols for H_2O_2 formation is not clear but was proposed to be due to the nature of the thiol oxidation products formed during the propagation step and of the termination products; thus, stoichiometry could play an important factor in product formation.

Computational studies show that reaction of $O_2^{\bullet-}$ with MeSH to give $MeSO^\bullet$ and HO^- (Pathway 1) as the most favorable mechanism with ΔG_{aq} of –170.5 kcal/mol compared to the formation of $MeS^\bullet$ and HO_2^- (Pathway 2) with endoergic ΔG_{aq} of 68.2 kcal/mol.[32] However, the free energies for the formation of $MeSO^- + HO^\bullet$ and $MeS^- + HO_2^\bullet$ are $\Delta G_{aq} = –52.5$ and 32.2 kcal/mol, respectively. Therefore, the proposed Pathway 2 is unfavorable unless the reacting species is $HO_2^\bullet$ to give $MeS^\bullet$ and H_2O_2 with $\Delta G_{aq} = –11.3$ kcal/mol, but formation of $MeSO^\bullet$ and H_2O from HO_2^- and MeSH is far more favorable with $\Delta G_{aq} = –278.7$ kcal/mol. As previously suggested,[32] the reactivity of other oxidants such as H_2O_2 and $HO^\bullet$ to thiols should also be considered and may involve a more complex mechanistic pathway.

1.3.2.5 Reaction with Iron–Sulfur [Fe–S] Cluster

Iron–sulfur clusters are important co-factors in biological systems. They serve as active sites in various metalloproteins catalyzing electron-transfer reactions and play a role in other biological functions such as O_2 sensing ability (e.g., by the transcription factor FNR).[33] The ubiquitousness of [Fe–S] clusters in enzymatic systems such as in Complexes II and III of the mitochondrial electron transport chain, ferredoxins, NADH dehydrogenase, nitrogenase, or hydro-lyases underlies their susceptibility for inactivation by ROS specifically by $O_2^{\bullet-}$ through formation of unstable oxidation state of the [Fe–S] cluster and their subsequent degradation (Figure 1.13). For example, hydro-lyase enzymes such as dihydroxy-acid dehydratase, fumarase A and B, and aconitase can be inactivated by $O_2^{\bullet-}$ with a second-order rate constant of $10^6–10^7\,M^{-1}\,s^{-1}$, while the rate of their inactivation by O_2 is orders of magnitude lower ($10^2\,M^{-1}\,s^{-1}$).[34] This difference in the rates of inactivation of $O_2^{\bullet-}$ versus O_2 can be accounted to the favorability of the initial steps in the oxidation of a $[4Fe–4S]^{2+}$ by $O_2^{\bullet-}$ and O_2 with ΔG of −10.1 and 17.6 kcal/mol, respectively.[34] However, these initial steps only represent formation of Fe^{2+}, H_2O_2, or $O_2^{\bullet-}$ and can further undergo redox reactions to form H_2O as end product. The overall free energies of oxidation of $[4Fe–4S]^{2+}$ by $O_2^{\bullet-}$ and O_2 leading to the formation of the most stable product (H_2O) and Fe^{3+} are comparable with ΔG of −27.1 and −23.5 kcal/mol, respectively.

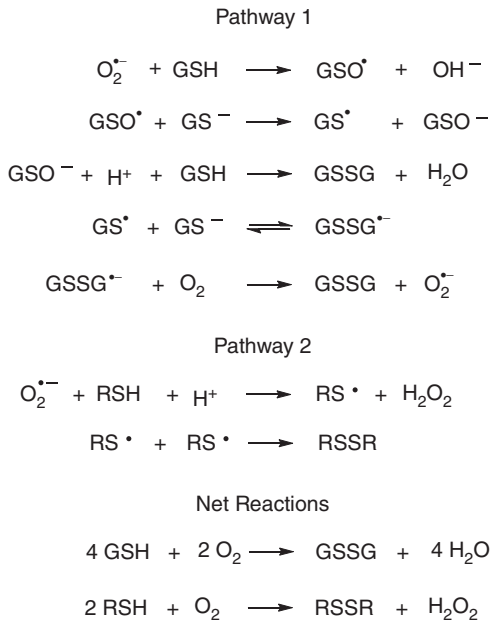
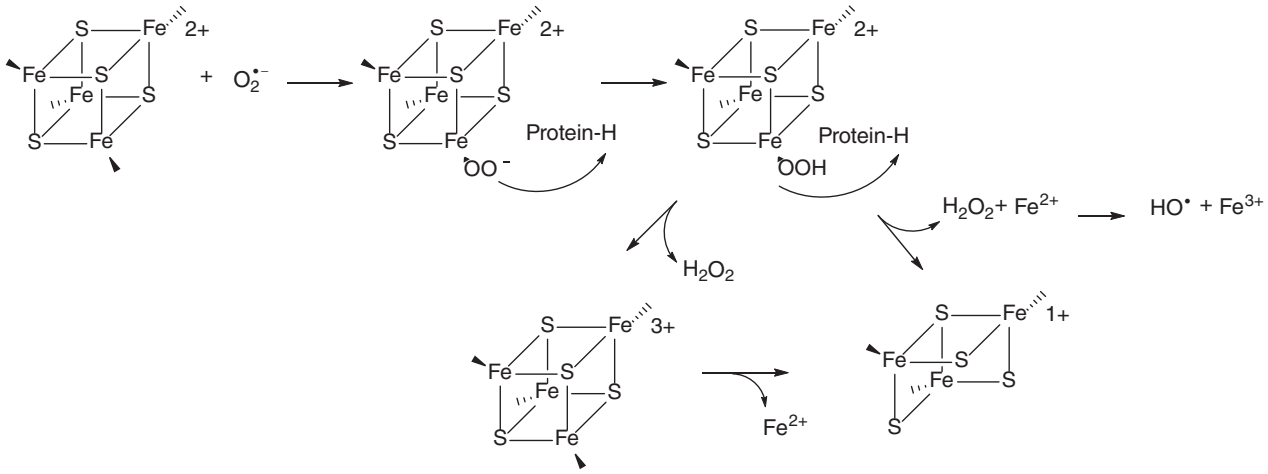


Figure 1.12 Various pathways for the reaction of $O_2^{\bullet-}$ with thiols.

1.3.3 Hydroperoxyl Radical ($HO_2^\bullet$)

Protonation of $O_2^{\bullet-}$ leads to the formation of $HO_2^\bullet$ whose concentration in biological pH exists a hundred times smaller than that of $O_2^{\bullet-}$; however, the presence of small equilibrium concentration of $HO_2^\bullet$ ($pK_a = 4.8$) can contribute to the $O_2^{\bullet-}$ instability in neutral pH due to dismutation reaction shown in Equation 1.14. In acidosis condition, the reactivity of $HO_2^\bullet$ is expected to be more relevant than $O_2^{\bullet-}$. Electrochemical reduction of O_2 in the presence of strong or weak acids such as $HClO_4$ or phenol, respectively, generates $HO_2^\bullet$.[35] Hydroperoxyl radical is a stronger oxidizer than $O_2^{\bullet-}$ with $E^{0\prime} = 1.06$ and 0.94 V, respectively, and due to its neutral charge, it is capable of penetrating the lipid bilayer and, hence, it has been suggested that $HO_2^\bullet$ is capable of H-atom abstraction from PUFAs or from the lipids present in low-density lipoproteins. Cheng and Li[36] argued against the role of $HO_2^\bullet$ in LPO initiation since the concentration of $HO_2^\bullet$ at physiological pH is less than 1% of the generated $O_2^{\bullet-}$ and that SOD have little effect on peroxidation in liposomal or microsomal systems. However, it has been demonstrated that LOOH is more likely the preferred species for $HO_2^\bullet$ attack and not the LPO initiation process. H-atom abstraction from peroxyl-OOH and not from the alkyl C–H backbone is the preferred mechanism of $HO_2^\bullet$ reactivity, and



$$[4Fe\text{-}4S]^{2+} + O_2^{\bullet-} + 2H^+ \xrightarrow{-10.1} [3Fe\text{-}4S]^{1+} + H_2O_2 + Fe^{2+}$$

$$[4Fe\text{-}4S]^{2+} + 2/3\,O_2^{\bullet-} + 8/3H^+ \xrightarrow{-27.1} [3Fe\text{-}4S]^{1+} + 4/3\,H_2O + Fe^{3+}$$

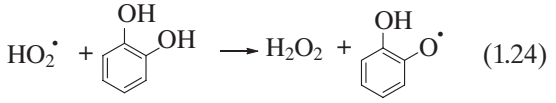
$$[4Fe\text{-}4S]^{2+} + O_2 \xrightarrow{17.6} [3Fe\text{-}4S]^{1+} + O_2^{\bullet-} + Fe^{2+}$$

$$[4Fe\text{-}4S]^{2+} + 1/2\,O_2 + 2H^+ \xrightarrow{-23.5} [3Fe\text{-}4S]^{1+} + H_2O + Fe^{3+}$$

Figure 1.13 Free energies (in kcal/mol) of the reaction of $O_2^{\bullet-}$ and O_2 with $[4Fe\text{-}4S]^{2+}$ cluster.

therefore, $HO_2^\bullet$ is more important than $O_2^{\bullet-}$ in initiating LOOH-dependent LPO, but not as the H-abstraction initiator in LPO.[36]

Relevant to the antioxidant activity of catechols or hydroquinones (QH_2), the reactivity of $HO_2^\bullet$ with QH_2 involves H-atom transfer reaction to form semiquinone radical and H_2O_2 with a rate constant of $4.7\times10^4\,M^{-1}s^{-1}$ for 1,2-dihydroquinone (Eq. 1.24).[37]



(1.24)

1.3.4 Hydrogen Peroxide (H_2O_2)

Perhaps one of the most ubiquitous ROS present in biological systems due to its relative stability with an oxidation potential of 1.8V compared to other ROS such as $O_2^{\bullet-}$, $HO_2^\bullet$, or $HO^\bullet$. Hydrogen peroxide is the protonated form of the 2-electron reduction product of molecular oxygen and is a non-radical ROS with all the anti-bonding orbitals occupied by paired electrons (Figure 1.14). Hydrogen peroxide undergoes highly exoergic disproportionation reaction to form 2 equivalents of water and 1 equivalent of oxygen where the rate of disproportionation is temperature dependent.

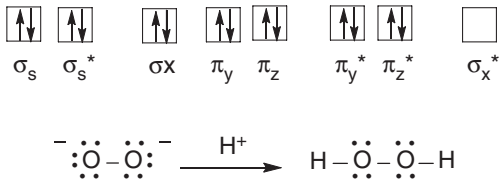


Figure 1.14 Molecular orbital diagram of H_2O_2.

Perhaps the most common reaction of H_2O_2 is its metal-catalyzed reaction to produce $HO^\bullet$ and $HO_2^\bullet$ (the Fenton chemistry) as proposed by Haber and Weiss (Eqs. 1.24–1.31).[38] Perez-Benito[39] proposed that this reaction can undergo propagation in which the $HO^\bullet$ can further react with H_2O_2 to produce $HO_2^\bullet$ according to Equation 1.25. Depending on the pH, the equilibrium concentrations of $HO_2^\bullet$ and $O_2^{\bullet-}$ can vary (Eq. 1.26), and it has been suggested[39] that $HO_2^\bullet$ and $O_2^{\bullet-}$ are involved in the reduction and oxidation of Fe^{3+} (Eq. 1.27) and Fe^{2+} (Eq. 1.29), respectively. Iron(III) reaction with H_2O_2 can also lead to $HO^\bullet$ production in acidic pH via formation of $FeOOH^{2+}$ complex and its subsequent decomposition to Fe^{2+} and $HO_2^\bullet$ (Eqs. 1.30 and 1.31) in which the formed Fe^{2+} can propagate the cycle to produce $HO^\bullet$ as shown in Equations 1.24–1.29.

$$Fe^{2+} + H_2O_2 \rightarrow Fe^{3+} + HO^\bullet + {}^-OH \qquad (1.24)$$

$$HO^{\bullet} + H_2O_2 \rightarrow H_2O + HO_2^{\bullet} \quad (1.25)$$

$$HO_2^{\bullet} \rightleftharpoons H^+ + O_2^{\bullet -} \quad (1.26)$$

$$O_2^{\bullet -} + Fe^{3+} \rightarrow O_2 + Fe^{2+} \quad (1.27)$$

$$2HO_2^{\bullet} \rightarrow H_2O_2 + O_2 \quad (1.28)$$

$$Fe^{2+} + HO_2^{\bullet} \rightarrow Fe^{3+} + {}^{-}OH \quad (1.29)$$

$$Fe^{3+} + H_2O_2 \rightleftharpoons FeOOH^{2+} + H^+ \quad (1.30)$$

$$FeOOH^{2+} \rightarrow Fe^{2+} + HOO^{\bullet} \quad (1.31)$$

Shown in Figure 1.15 is the metal-independent generation of $HO^{\bullet}$ from H_2O_2 proposed from tetrachlorobenzoquinone (TCBQ)[8] through nucleophilic substitution reaction to form the hydroperoxyl-TCNQ and O-O homolytic cleavage to yield $HO^{\bullet}$ and TCBQ-$O^{\bullet}$. Subsequent disproportionation TCBQ-$O^{\bullet}$ yields TCBQ-O^- can further react with excess H_2O_2 to produce $HO^{\bullet}$.

Hydrogen peroxide oxidation of anions is not favorable. For example, oxidation of Cl^- to HOCl by H_2O_2 is highly endoergic with ~30 kcal/mol. However, myeloperoxidase-mediated oxidation of Cl^- in the presence of H_2O_2 gave rate constants that are dependent on the Cl^- concentration. It was proposed that Cl^- reacts with MPO-I (an active intermediate formed from the reaction of MPO with excess H_2O_2) to form the chlorinating intermediate MPO-I-Cl^-. The rate-limiting step is [Cl^-] dependent, that is, at low [Cl^-], k_2 is the rate-limiting step with $k_2 = 2.2 \times 10^6\,M^{-1}\,s^{-1}$, and $k_3 = 5.2 \times 10^4\,s^{-1}$ (Eq. 1.32).[40]

$$\begin{aligned} MPO + H_2O_2 &\underset{k_{-1}}{\overset{k_1}{\rightleftharpoons}} MPO\text{-}I + H_2O \\ MPO\text{-}I + Cl^- &\underset{k_{-2}}{\overset{k_2}{\rightleftharpoons}} MPO\text{-}I\text{-}Cl^- \\ MPO\text{-}I\text{-}Cl^- &\xrightarrow{k_3} MPO + HOCl \end{aligned} \quad (1.32)$$

In the absence of ionic substrates, myeloperoxidase has been reported to degrade H_2O_2 to oxygen and water thereby imparting a catalase activity.[41] Kinetic analysis show that there is one mole of oxygen produced per two moles of H_2O_2 consumed with a rate constant of $2 \times 10^6\,M^{-1}\,s^{-1}$ which is an order of magnitude slower than the rate constant observed for catalase of $3.5 \times 10^6\,M^{-1}\,s^{-1}$. Oxidation of nitrite to nitrate by H_2O_2 in the presence of catalase has been reported.[42] In the absence of catalase, nitrite reacts with H_2O_2 to form peroxynitrite.[43] Hydroxylation and nitration of tyrosine and salicylic acid by H_2O_2 in the presence of nitrite occur between the pHs of 2–4 and 5–6, respectively, as mediated by peroxynitrite formation.[44]

Four major detoxification pathways for H_2O_2 operate intracellularly: (1) catalase; (2) glutathione peroxidase; (3) peroxiredoxin enzymes; and via (4) non-enzymatic mean via oxidation of protein thiol residues.[45] These pathways will be discussed in detail in the succeeding chapters. Probably one of the most important reactions in biological systems is the reaction of H_2O_2 with thiols. The cellular signaling property H_2O_2 is mainly dependent on the oxidation of intracellular protein thiols in which majority of these reactions form protein disulfides as opposed to S-glutathiolation.[45] The H_2O_2 reaction with thiols is free radical mediated, and the rate is dependent on the pK_a of the thiol in which the thiolate (RS^-) is the reacting species to form the sulfenic acid (RSOH) intermediate according to Equation 1.33.[31] The reported rate constant for the reaction of H_2O_2 with thiolates ranges from 18–26 $M^{-1}\,s^{-1}$ which is relatively slow compared to the reaction of $O_2^{\bullet -}$ with thiols ($>10^5\,M^{-1}\,s^{-1}$).[31] Catalysis of RSSR formation with Cu(II) from peroxides has also been reported.[46]

$$\begin{aligned} RS^- + H_2O_2 &\rightarrow RSOH + HO^- \\ RSOH + RSH &\rightarrow RSSR + H_2O \end{aligned} \quad (1.33)$$

1.3.5 Hydroxyl Radical ($HO^{\bullet}$)

Hydroxyl radical originates from the 3-electron reduction of oxygen. Among all the ROS, $HO^{\bullet}$ perhaps is the most reactive and short-lived. Aside from the $HO^{\bullet}$ significant role in controlling atmospheric chemistry, it plays a direct role in the initiation of oxidative damage to macromolecules in biological systems. Unlike $O_2^{\bullet -}$ and H_2O_2 whose reactions are limited due to their lower oxidizing ability, $HO^{\bullet}$ can practically react with almost every organic molecule *via* H-atom abstraction, electrophilic addition, or radical–radical reactions, to name a few. The standard reduction potential for $HO^{\bullet}_{aq}/HO^-_{aq}$ couple was determined to be 1.77 V in neutral solution.[47]

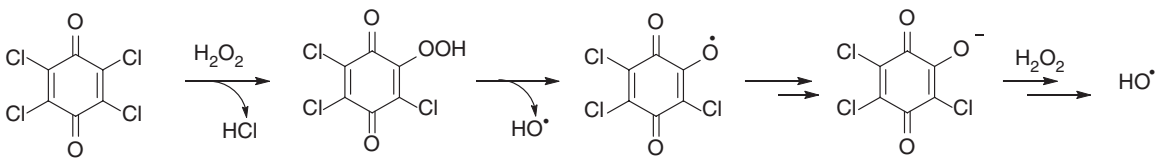


Figure 1.15 Metal-independent generation of $HO^{\bullet}$ from H_2O_2.

The half-life of $HO^{\bullet}$ is ~10^{-9} s compared to ~10^{-5} s and ~60 s for $O_2^{\bullet-}$ and H_2O_2, respectively.

Reactivity with ROS/RNS. Radical–radical reaction of $HO^{\bullet}$ proceeds at diffusion-controlled rate. For example, at neutral pH, reaction of $HO^{\bullet}$ with various ROS and non-ROS radicals ranges between ~10^9 and $10^{10}\,M^{-1}s^{-1}$ (Eq. 1.34). The reactions are characteristic of addition of the hydroxyl-O to the heteroatoms. In the case of $HO^{\bullet}$ reaction to $O_2^{\bullet-}$ and $HO_2^{\bullet}$, oxidation of electron-transfer reactions to form O_2 was observed (Eq. 1.35).

Hydrogen bonding between $HO^{\bullet}$ and H_2O_2 has been computationally demonstrated which forms a five-membered ring-like structure with two distorted hydrogen bonds having a binding energy of ~4 kcal/mol.[48] This $HO^{\bullet}$–H_2O_2 interaction leads to H atom abstraction to yield $O_2^{\bullet-}$. In pyridine, H_2O_2 reaction with $HO^{\bullet}$ has a relatively slower rate of $3\times10^7\,M^{-1}s^{-1}$ compared to most of $HO^{\bullet}$ reactions.[49]

$$\begin{aligned}
HO^{\bullet} + HO^{\bullet} &\rightarrow H_2O_2 && k = 5.2\times10^9\\
HO^{\bullet} + H^{\bullet} &\rightarrow H_2O && k = 7\times10^9\\
HO^{\bullet} + ClO_2^{\bullet} &\rightarrow H^+ + ClO_3^- && k = 4\times10^9\\
HO^{\bullet} + NO &\rightarrow H^+ + NO_2^- && k = 4\times10^9\\
HO^{\bullet} + NO_2 &\rightarrow HO_2NO && k = 1\times10^{10}
\end{aligned} \quad (1.34)$$

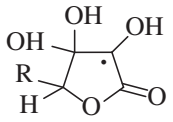
$$\begin{aligned}
HO^{\bullet} + O_2^{\bullet-} &\rightarrow HO^- + O_2 && k = 7\times10^9\\
HO^{\bullet} + HO_2^{\bullet} &\rightarrow H_2O + O_2 && k = 6.6\times10^9
\end{aligned} \quad (1.35)$$

1.3.5.1 Reactivity with Ions Reaction of $HO^{\bullet}$ to anions leads to a one-electron oxidation of the anion. It has been suggested that simple electron-transfer mechanism from the anion to the $HO^{\bullet}$ is not likely the mechanism due to the large energy associated with the formation of the hydrated hydroxide ion.[50] Instead, an intermediate $HOX^{\bullet-}$ adduct is initially formed (Eq. 1.36). Reaction of $HO^{\bullet}$ to cations can also result in an increase in the oxidation state of the ion, but unlike its reaction with anions, the reaction occurs at a much slower rate constant that is no more than ~$3\times10^8\,M^{-1}s^{-1}$ *via* H atom abstraction from the metal-coordinated water (Eq. 1.37).[50]

$$\begin{aligned}
HO^{\bullet} + Cl^- &\rightarrow ClOH^- && k = 4.3\times10^9\\
HO^{\bullet} + CO_3^{2-} &\rightarrow HO^- + CO_3^{\bullet-} && k = 3.7\times10^8\ (\text{pH } 11)
\end{aligned} \quad (1.36)$$

$$\begin{aligned}
HO^{\bullet} + Fe^{2+} &\rightarrow FeOH^{2+} && k = 3.2\times10^8\\
HO^{\bullet} + Cu^{2+} &\rightarrow CuOH^{2+} && k = 3.5\times10^8
\end{aligned} \quad (1.37)$$

1.3.5.2 Modes of Reaction with Organic Molecules There are two main mechanisms of $HO^{\bullet}$ reaction with organic compounds, that is, H-atom abstraction and addition reaction. With protic compounds such as alcohols, reaction of $HO^{\bullet}$ proceeds *via* H-atom abstraction from C–H bond and not from the O–H to form water and the radical species. The general reaction for $HO^{\bullet}$ with alcohol is $HO^{\bullet} + RH \rightarrow R^{\bullet} + H_2O$, and not $HO^{\bullet} + ROH \rightarrow RO^{\bullet} + H_2O$. For example, ascorbate/ascorbic acid (AH^-/AH_2) reacts with $HO^{\bullet}$ to form ascorbate radical anion ($A^{\bullet-}$) and ascorbyl radical ($HA^{\bullet}$) with rate constants of $1.1\times10^{10}\,M^{-1}s^{-1}$ (pH = 7) and $1.2\times10^{10}\,M^{-1}s^{-1}$ (pH = 1), respectively.[50] EPR studies revealed formation of a C-centered radical.[51] Reaction of $HO^{\bullet}$ with aliphatic alcohols such as methanol and ethanol gave rate constants of 9.0×10^8 and $2.2\times10^9\,M^{-1}s^{-1}$, respectively, using pulse radiolysis.[52] Preference to abstract H atom at the alpha position (*i.e.,* the H attached to the C atom that is also attached to the OH group) was shown theoretically and was found to be both kinetically and thermodynamically favorable. For example, the relative energies of H-atom abstraction as calculated at the CCSD(T) level of theory are as follows: α-H = −25.79 kcal/mol > β-H = −16.26 kcal/mol > OH = −15.67 kcal/mol.[53]



Ascorbyl Radical

Reaction of $HO^{\bullet}$ with deoxyribose forms a C-centered radical which further decomposes to form malonaldehyde (MDA) (Figure 1.16).[54] Malonaldehyde is a toxic by-product of polyunsaturated lipid degradation.[55,56] Increased dose of $HO^{\bullet}$ results in increase MDA-like products;[54] therefore, production of MDA in biological systems has become a popular biomarker of oxidative stress using thiobarbituric acid (TBARS) *via* MDA electrophilic addition reaction to form a UV-detectable adduct, TBARS-MDA. Radiolysis of D-glucose for example undergoes H-atom abstraction at the C-6 position, and rearrangement leads to the initial elimination of two water molecules. Fragmentation yields malonaldehyde upon protonation and a dihydroxy-aldehyde radical species which can further undergo dehydration to form another molecule of malonaldehyde.[57]

Reaction of $HO^{\bullet}$ to ketones and aldehydes also gave preference to H-atom abstraction. Rate constants for H-atom abstraction in aqueous phase were faster $2.4–2.8\times10^9\,M^{-1}s^{-1}$ for acetaldehyde and propionaldehyde, compared to acetone with $k = 3.5\times10^7\,M^{-1}s^{-1}$.[58] Computational studies show that for ketones with at least an ethyl

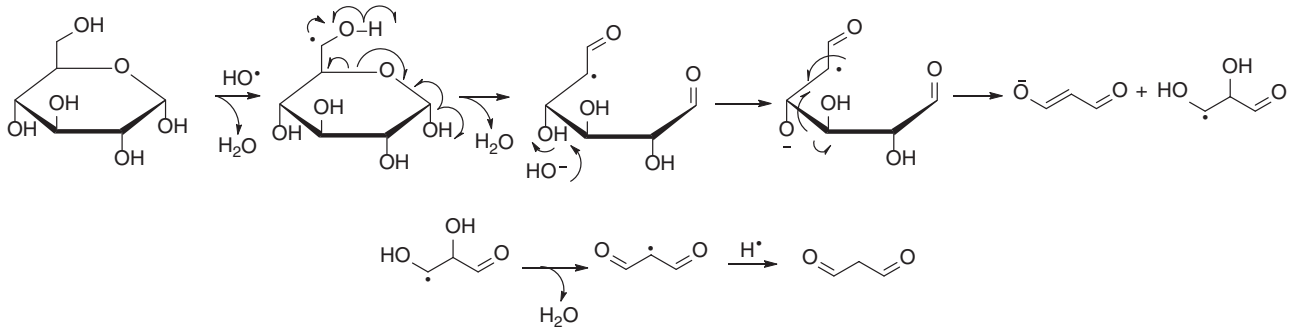


Figure 1.16 Malonaldehdye formation from the reaction of hydroxyl radical to deoxyribose.

group attached to the carbonyl carbon, the preference for H-atom abstraction is at the beta-position rather than the alpha position due to the presence of strong H-bond interaction forming 7-member ring transition state structure (Figure 1.17).[59] In aldehydes, abstraction of the aldehydic-H was shown to be the most favored according to the equation, $RHC{=}O + HO^{\bullet} \rightarrow [RC{=}O]^{\bullet} + H_2O$.[60]

Reaction of $HO^{\bullet}$ to carboxylic acids is also that of H-atom abstraction of the acidic-H and alpha-H. There are two possible reactions in acetic acid/acetate system. One that involves H-atom abstraction from C–H and the other from OH according to Equations 1.38 and 1.39, respectively:

$$CH_3COO^- + HO^{\bullet} \rightarrow {}^{\bullet}CH_2OO^- + H_2O \qquad k = 7.0\times10^7\,M^{-1}s^{-1} \tag{1.38}$$

$$CH_3COOH + HO^{\bullet} \rightarrow CH_2OO^{\bullet} + H_2O \qquad k = 1.7\times10^7\,M^{-1}s^{-1} \tag{1.39}$$

Rate constants for these reactions show that H-atom abstraction from C–H bond is 4× faster than abstraction from O–H in aqueous solution.[61] The same trend in the relative reactivities of $HO^{\bullet}$ with various acids and their respective conjugate base had been observed.[61]

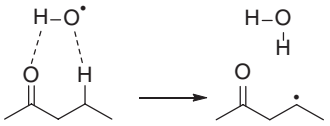


Figure 1.17 Transition state H-bonding interaction of hydroxyl radical to carbonyl leading to H atom abstraction at the beta position.

The reaction of $HO^{\bullet}$ with alkenes is relevant in the initiation of lipid peroxidation processes and will be discussed in detail in the succeeding chapter. It has been demonstrated that increasing alkyl substitution on the C=C bond enhances its reaction rate with $HO^{\bullet}$ by two orders of magnitude.[62] In the gas phase, initial reaction of $HO^{\bullet}$ to alkenes forms the HO–alkene adduct which in the presence of O_2 gives the (β-hydroxylalkyl)peroxy radical. Further reactivity with $NO^{\bullet}$ yields the β-hydroxyalkoxy radical and ${}^{\bullet}NO_2$ according to Figure 1.18.[63]

Reaction of $HO^{\bullet}$ with aromatic hydrocarbons mainly proceeds *via* addition reaction. Laser flash photolytic study in acetonitrile gave rate constants ranging from 1.2 to $7.9\times10^8\,M^{-1}\,s^{-1}$ for one-ringed aromatic hydrocarbons compared to $1.8–5.2\times10^9\,M^{-1}s^{-1}$ for naphthalenic systems.[64] Experimental and computational studies indicate that the electrophilic nature of $HO^{\bullet}$ addition was supported by the higher rate of $HO^{\bullet}$ addition reaction in aqueous solution compared to acetonitrile by a factor of 65. Stabilization of an aromatic ring-OH complex occurs in the transition state in which the aromatic unit assumes a radical cation-like form and the $HO^{\bullet}$ looks more like a hydroxide anion. This can have implication in the $HO^{\bullet}$ reactivity with DNA bases in which stabilization of the radical cation form can increase $HO^{\bullet}$ reactivity to the bases.[65] The same addition mechanism was proposed for benzaldehyde and its methoxy-, chloro-, and nitro-analogues.[66]

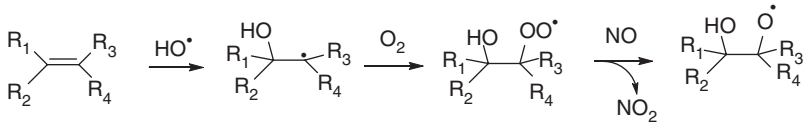


Figure 1.18 Addition reaction of hydroxyl radical to alkenes and subsequent reaction of O_2 and $NO^{\bullet}$ with the formed HO-alkene adduct.

Thiols, such as GSH or thiol-based synthetic antioxidants such as *N*-acetyl cysteine, are important biological species. H-atom abstraction is the main mechanism of $HO^{\bullet}$ reaction with thiols ($RSH + HO^{\bullet} \rightarrow RS^{\bullet} + H_2O$) with rate constants that range from 8.8×10^{9} to $2\times10^{10}\,M^{-1}s^{-1}$.[50] Computational studies also show that H-atom abstraction of the thiyl-H is the main reaction channel[67] via formation of a short-lived, weakly bonded adduct prior to the abstraction process.[68] Using peroxynitrite, formation of $RS^{\bullet}$ species as source of $HO^{\bullet}$ was demonstrated by spin trapping.[69]

1.3.6 Singlet Oxygen ($^1O_2{}^1\Delta_g$ or $^1O_2{}^*$)

Singlet oxygen is the diamagnetic and less stable form of molecular oxygen. The energy separation between $^1O_2(^1\Delta_g)$ and the triplet ground-state oxygen $^3O_2(^3\Sigma_g^-)$ was estimated to be 22.5 kcal/mol (94.3 kJ/mol), corresponding to a near-infrared transition of 1270 nm, while the energy separation between the $^1O_2{}^1\Delta_g$ and the singlet $^1O_2(^3\Sigma_g^+)$ is 15.0 kcal/mol.[70] Electronic configuration of the various spin states of oxygen shows only variation in the electronic distribution at the pi-antibonding (p*) orbitals. As shown in Figure 1.19, unlike the ground-state oxygen ($^3\Sigma_g^-$), the electron distribution in $^1\Delta_g$ and $^3\Sigma_g^+$ has antiparallel spins, where in the former, the two electrons occupy the same orbital, while in the latter, each electron occupies two separate orbitals. Spin-forbidden transition from $^1\Delta_g$ and $^3\Sigma_g^-$ makes $^1O_2{}^*$ a relatively longer-lived species compared to the short-lived $^3\Sigma_g^+$ due to the spin-allowed transition. In solution, lifetime of $^1O_2{}^*$ is solvent dependent and ranges from 10^{-3} to 10^{-6} s, with the shortest lifetime observed in water.[71]

Due to the high energy state of $^1O_2{}^*$, its generation in biological system usually involves photoexcitation *via* direct absorption through vibrationally excited

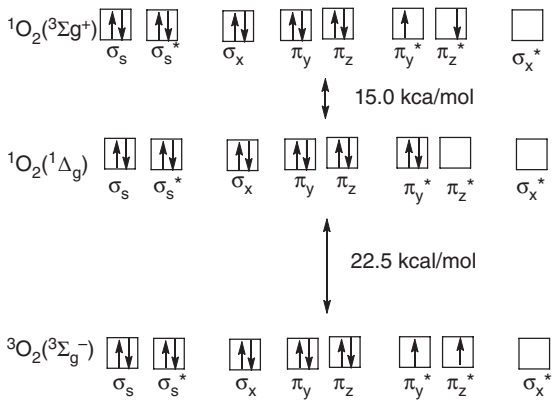


Figure 1.19 Bonding orbitals of singlet oxygens, $^1\Delta_g$ and $^3\Sigma_g^+$, in comparison to the triplet ground state, $^3\Sigma_g^-$.

water at 600 nm, or indirectly through photosensitization. Certain organic molecules absorb photons of a particular wavelength causing transition from singlet ground state (S_0) to one of the higher energy 1st or 2nd excited states, that is, S_1 and S_2, respectively. Through vibrational relaxation (VR) or internal conversion (IC) (a non-radiative transition), $S_2 \rightarrow S_1$ ($\tau_{S1} = 10^{-8}$ s) transition occurs which can further undergo conversion to $S_1 \rightarrow S_0$ via IC, or through emission of fluorescence which is a radiative transition between spin states of the same multiplicity. One must note that these processes do not involve change in multiplicity ($S = 1$) where the lowest energy orbitals still have the two electrons of opposite spins and are usually referred to as "spin-allowed" transitions. Transition from S_0 to excited triplet states (T_1), whereby two electrons with the same spins occupy different orbitals, is "spin forbidden." However, the energy difference between S_1 and the lower-lying T_1 is about ~12 kcal which can facilitate $S_1 \rightarrow T_1$ transition *via* intersystem crossing (ISC), another nonradiative process, for molecules with large spin–orbit coupling. Higher excited states transition ($S_2 \rightarrow T_2$) can also occur and through VR and IC, $T_2 \rightarrow T_1$ is possible. Photosensitizers typically have longer T_1 half-life than S_1 with $\tau_{S1} = 10^{-4}$ to 10^{-3} s and have a quantum yield of 0.7–0.9. Conversion of $T_1 \rightarrow S_0$ emits phosphorescence as a spin-forbidden radiative transition.

The high quantum yield and longer half-life for T_1 state of photosensitizers have significant ramification in the initiation of a variety of chemical reactions. There are two major types of reaction resulting from T_1 quenching (*i.e.*, Types I and II). Type I processes are typically characterized by H-atom abstraction or electron transfer between the excited sensitizer (A) to a substrate (X) (triplet oxygen for example to yield $O_2^{\bullet-}$) and sensitizer $(A)^{\bullet+}$ according to Equation 1.40:

$$A(T_1)_+ O_2 \rightarrow A^{\bullet++} O_2^{\bullet-} \tag{1.40}$$

where $O_2^{\bullet-}$ can further dismutate to H_2O_2 and to form $HO^{\bullet}$. Alternatively, $O_2^{\bullet-}$ can also be produced from $A^{\bullet-}$ as a secondary product depending on the direction of the electron-transfer reaction (Eq. 1.41).

$$\begin{aligned} A(T_1)_+ X &\rightarrow X^{\bullet++} A^{\bullet-} \\ A^{\bullet-+3}O_2 &\rightarrow A^{+} O_2^{\bullet-} \end{aligned} \tag{1.41}$$

Formation of ROS from $O_2^{\bullet-}$ can have implications in the initiation of oxidative damage to key biomolecular systems. Type II processes involve photosensitization of biological or synthetic compounds through energy-transfer mechanism (in contrast to electron-transfer mechanism for Type I) from a sensitizer triplet-state

molecule T_1 to the ground-state triplet O_2, a spin-allowed process (Eq. 1.42).[71]

$$A(T_1) + {}^3O_2 \rightarrow A(S_0) + {}^1O_2{}^* \tag{1.42}$$

Oxidative modification *via* Type I or Type II processes may depend on the O_2 concentration in which the former is more likely to occur at low O_2 concentration.

The generation of singlet oxygen through photosensitization has been widely exploited in photodynamic therapy, environmental remediation, and synthesis.[70] In general, the reactivity of $^1O_2$* was found to be lower than that of HO$^\bullet$ but higher than $O_2^{\bullet-}$, and is ca. 1 V more oxidizing than $^3O_2$.[70] There are two major quenching mechanisms for singlet $^1O_2$*, that is, through physical means where interaction of $^1O_2$* with substance A forms $^3O_2$; or chemical where $^1O_2$* reacts with A to form product B or a combination of both. Physical quenching of $^1O_2$* occurs mainly through its interaction with solvents, or other substrates such as azide, carotene, or lycopene, but its most common reaction is chemical which accounts for its main mode of action in photodynamic therapy. For example, reaction of $^1O_2$* with double bonds results in the formation hydroperoxides *via* "ene"-reactions, or endoperoxides through Diels–Alder-type addition to unsaturated lipids (PUFA or cholesterol), amino acids (e.g., His, Trp, and Met), or nucleic acids (e.g., guanosine).[72] Singlet oxygen has also been shown to be chemically produced from H_2O_2 and hypochlorite, KO_2 reaction with water, and thermal decomposition of aryl peroxides.[71] In biological systems, $^1O_2$* can be endogenously produced from the decomposition of alpha-linolenic acid hydroperoxide by cytochrome c and lactoperoxidase,[73] metabolism of indole-3-acetic acid by horseradish peroxidase and neutrophils,[74] oxidation of NADPH by liver microsomes,[75] from myeloperoxidase-H_2O_2-chloride system,[76] or from horseradish peroxidase-H_2O_2-GSH system.[77]

1.4 REACTIVE NITROGEN SPECIES

1.4.1 Nitric Oxide (NO or NO$^\bullet$)

Nitric oxide is a paramagnetic molecule with a bond order of 2.5 where the unpaired electron occupies an anti-bonding orbital (Figure 1.20). Nitric oxide is non-polar and with solubility in aqueous solution of 1.94×10^{-6} mol cm^{-3} atm^{-1} at 298.[78] The diffusivity (D) at 298 K of NO$^\bullet$ is similar to that of O_2 with D_{NO} in water of 2.21×10^{-5} and 2.13×10^{-5} cm^2 s^{-1} for O_2.[78]

Nitric oxide functions as an intracellular signaling molecule and is the main precursor of highly oxidizing RNSs in biological system. Nitric oxide's toxicity is generally limited to its reaction or oxidation to form the more highly reactive species such as $ONOO^-$ and $^\bullet NO_2$ (Scheme 1.1).[43]

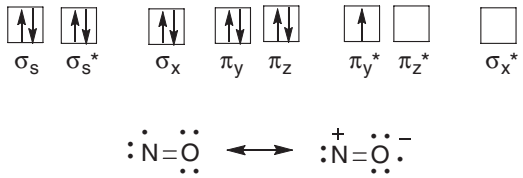


Figure 1.20 Bonding orbitals of nitric oxide.

1.4.1.1 NO$^\bullet$ Radical Reaction Due to NO$^\bullet$'s radical nature, it exhibits rich chemistry and is capable of reacting with radicals or transition metals to form complexes. NO$^\bullet$ is relatively stable and unreactive to non-radical species. Theoretical evidence shows dimerization of NO$^\bullet$ to $(NO)_2$ is only slightly favorable with $\Delta H = -2.3$ kcal/mol.[79] The facile reaction of NO$^\bullet$ with O_2 gave $k_1 = 2.1$–2.9×10^6 M^{-2}s^{-1} at 22 °C (based on the rate law: $4k_1$ [NO$^\bullet$]^2[O_2])[80,81] in aqueous solution and yields a variety of NO_x products such as $^\bullet NO_2$, N_2O_3, and N_2O_4, as well as NO_2^- *via* a complex mechanism. Kinetic model for NO$^\bullet$ reaction with O_2 is shown in Equation 1.43.

$$\begin{aligned}
&2NO + O_2 \rightarrow 2NO_2 \quad (k = 2.9\times10^6\ M^{-1}\ s^{-1})\\
&2NO_2 + 2NO \rightleftharpoons 2N_2O_3 \quad (k_{forward} = 1.1\times10^9\ M^{-1}\ s^{-1})\\
&2N_2O_3 + 2H_2O \rightarrow 4NO_2^- + 4H^+ \quad (k = 530\ s^{-1})\\
&\text{Net:}\quad 4NO + 2H_2O + O_2 \rightarrow 4NO_2^- + 4H^+
\end{aligned} \tag{1.43}$$

The reaction of NO$^\bullet$ with O_2 results in the formation of NO$^\bullet$–O_2 weak complex, a nitrosyldioxyl radical intermediate, and its further reaction to NO$^\bullet$ yields the dimerized $^\bullet NO_2$ (ONOONO) which along with $^\bullet NO_2$ and N_2O_3 are potent oxidants. Subsequent reaction of ONOONO with two equivalents of NO$^\bullet$ yields equimolar amounts of N_2O_3. Since N_2O_3 is not formed in the presence of $^\bullet NO_2$ scavengers, it was assumed that ONOONO formation as a weak oxidant from NO$^\bullet$/O_2 is the rate-limiting step.[81]

Reactions of NO$^\bullet$ with short-lived radicals such as $(SCN)_2^{\bullet-}$, $CO_2^{\bullet-}$, $CO_3^{\bullet-}$, and hydroxyethyl radicals in aqueous solution have been reported with rate constant approaching diffusion controlled limit.[82] Reaction of NO$^\bullet$ with $(SCN)_2^{\bullet-}$ forms the NOSCN intermediate that upon hydrolysis yields NO_2^- (Eq. 1.44).

$$\begin{aligned}
&NO + (SCN)_2^{\bullet-} \rightarrow NO(SCN)_2^{\bullet-} \rightarrow NOSCN + SCN^-\\
&\quad (k = 4.3\times10^9\ M^{-1}\ s^{-1})\\
&NOSCN + H_2O \rightleftharpoons (HO\text{-}NOSCN)^- + H^+\\
&\quad \rightarrow HNO_2 + SCN^-
\end{aligned} \tag{1.44}$$

For $CO_3^{\bullet-}$, O-transfer to $NO^\bullet$ yields NO_2^- and CO_2 as the most preferred mechanism according to Equation 1.45:

$$NO + CO_3^{\bullet-} \rightarrow NO_2^- + CO_2 \quad (k = 3.5\times10^9 M^{-1}s^{-1}) \tag{1.45}$$

Reaction of $NO^\bullet$ with $CO_2^{\bullet-}$ forms the transient $NOCO_2^-$ and its subsequent decomposition yields hyponitrite radical anion and CO_2 (Eq. 1.46)

$$NO + CO_2^{\bullet-} \rightarrow NOCO_2^- \xrightarrow[NO]{} N_2O_2^{\bullet-} + CO_2 \quad (k = 2.9\times10^9 M^{-1}s^{-1}) \tag{1.46}$$

With hydroxyethyl radical (radical derived from ethanol), its reaction with $NO^\bullet$ gives oximes/hydroxamic acids as the main products (Eq. 1.47).

$$CH_3{}^\bullet CHOH + NO \longrightarrow CH_3CH(NO)OH \longrightarrow CH_3\underset{\underset{NOH}{\|}}{C}OH + CH_3\underset{\underset{NHOH}{|}}{C}=O \quad (k = 3.0\times10^9\ M^{-1}\ s^{-1}) \tag{1.47}$$

Reactions of $NO^\bullet$ with lipid alkoxyl ($LO^\bullet$) and peroxyl ($LOO^\bullet$) radicals are relevant in the termination of lipid peroxidation processes since $NO^\bullet$, being more soluble in non-polar solvents, can concentrate in lipid bi-layers, and therefore, can play a role in the regulation of lipid peroxidation. Reaction of $NO^\bullet$ with alkoxyl ($RO^\bullet$) and peroxyl ($ROO^\bullet$) radicals approaches that of diffusion-controlled rate. Reaction of $MeO^\bullet$ with $NO^\bullet$ yields MeONO[83] in aqueous solution, while reaction of $MeOO^\bullet$ with $NO^\bullet$ proceeds at a rate of constants of $3.7\times10^9 M^{-1}s^{-1}$ to yield ROONO and decomposes *via* O-O homolysis to free $RO^\bullet$ and $^\bullet NO_2$ (Eqs. 1.48 and 1.49).[84]

$$RO^\circ + NO \rightarrow RONO \tag{1.48}$$

$$ROO^\bullet + NO \rightarrow ROONO \rightarrow RO^\bullet + {}^\bullet NO_2 \tag{1.49}$$

1.4.1.2 NO•-metal Reaction Metal complexation of $NO^\bullet$ is important in the regulation of protein function. Aside from radicals, metals (mostly heme iron) are $NO^\bullet$'s principal target. A classic example is the activation of the enzyme guanylyl cyclase (sGC) *via* $NO^\bullet$ complexation with the ferro-heme. The formation of nitrosyl-Fe(II) complex results in changes in the electronic property of the heme iron such that the histidine ligand that was initially bound became labile and leads to change in the protein conformation. This change allows for the catalytic formation of the secondary messenger, cGMP from GTP, which then causes relaxation of the smooth muscle tissue. Other metalloenzymes where $NO^\bullet$ plays a crucial role in their regulations are *cyt* P450, cytochrome oxidases, catalase, or peroxidases.[85] There are two major $NO^\bullet$ binding modes to metalloporphyrin depending on the direction of the charge transfer between the metal and $NO^\bullet$: (1) $NO^\bullet$ assumed the NO^+ upon complexation and is characterized by a 180° M–N–O angle; and (2) $NO^\bullet$ assumed the NO^- upon complexation and is characterized by a 120° M–N–O angle (Figure 1.21).

The direction of charge transfer is dependent on several factors such as the oxidation state and type of metal ion, as well as the coordination number and type of co-ligands bound to the metal other than the $NO^\bullet$. The nature of the M–NO bonding mode determines protein conformation and NO–M reactivity (*e.g.,* in the activation of O_2 to yield nitrate). For example, M–N–O bond angles for Fe^{II}(OEP)(NO) and $[Fe^{III}(OEP)(NO)]^+$ (OEP = octaethylporphinato) are 143.6° and 176.9°, respectively.[86] Dependence of $NO^\bullet$ binding mode on the type of metal ions can also be seen with tetraphenylporphyrin complexes of Mn^{II}, Fe^{II}, and Co^{II}, where the M–N–O bond angles are as follows, 176.1°, 142.1°, and 128.5°, respectively.[85]

1.4.2 Nitrogen Dioxide ($^\bullet NO_2$)

Nitrogen dioxide is one of the nitrogen oxides (NO_x) and is a paramagnetic π molecule where the unpaired electron is delocalized between the three atoms (Figure 1.22). The polar property of $^\bullet NO_2$ is due to its bent structure with an O–N–O bond angle of 136° having negative charges on the O atoms and a positive charge on the N.

Nitrogen dioxide is sparingly soluble in water. Surface chemistry of adsorbed $^\bullet NO_2$ in aqueous system leads to its decomposition to H^+, nitrate and nitrous acid (HONO), and the presence of antioxidants such as

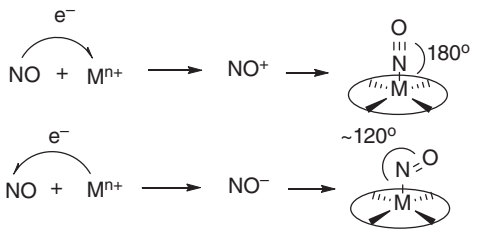


Figure 1.21 Binding modes of nitric oxide to metal ions.

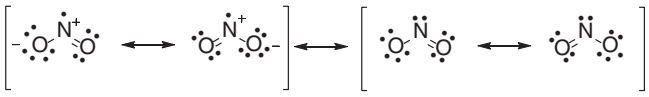


Figure 1.22 Mesomeric structures of nitrogen dioxide.

ascorbate, urate, and glutathione catalyzes this hydrolytic disproportionation.[87] In the gas and aqueous phases, $^{\bullet}NO_2$ dimerizes with a rate constant of $\sim 5\times10^{8}\,M^{-1}s^{-1}$ where it reacts rapidly with water to form nitrites and nitrates.[88] Nitrogen dioxide is a powerful oxidizer with an $E^{0}(^{\bullet}NO_2/NO_2^{-}) = 0.89–1.13\,V$.[89] Among the most important reactions of $^{\bullet}NO_2$ are: (1) H-atom abstraction from C–H bond; (2) addition reaction to C=C bonds; (3) O-transfer reactions; (4) radical–radical addition; (5) electron transfer. Due to the weak H–O bond in HONO having a dissociation energy of ~ 79 kcal/mol compared to C–H bond of ~100 kcal/mol, the H-atom abstraction involving $^{\bullet}NO_2$ is a slow process.[87]

1.4.2.1 Addition to Double Bonds Nitration of PUFA occurs *via* $^{\bullet}NO_2$ addition to C=C bond (Figure 1.23). Nitrated PUFA are important biomarkers of nitrosative stress due to their abundance in biological systems. Reaction of $^{\bullet}NO_2$ with 1,4-pentadiene moiety of ethyl linoleate[90] for example proceeds *via* competition between H-atom abstraction and free radical combination. The formation of vicinal –OH along with $–NO_2$ results from the O-centered addition of another $^{\bullet}NO_2$ to the alkyl radical and the subsequent hydrolysis of the nitrite to form the hydroxyl group. Addition of $^{\bullet}NO_2$ to double bonds has also been observed in xenobiotics, food additives, retinoic acid, 17β-estradiol, or cinnamic acids.[91]

1.4.2.2 Radical–radical Addition The major product in the reaction of $^{\bullet}NO_2$ with $MeO^{\bullet}$ is methyl nitrate ($MeONO_2$) through O-N bond formation.[83] However, reaction of $^{\bullet}NO_2$ with tyrosyl radical ($Tyr^{\bullet}$) forms the 3-nitrotyrosine *via* C-N bond formation which is one of the most studied biomarkers of oxidative damage to protein systems due to their abundance in biological systems. One could initial assume that $HO^{\bullet}$ can abstract H-atom from tyrosine, but its preferred mode of reaction is the ortho-directed addition to the aromatic ring to form the ortho-dihydroxytyrosine with $k = 7.0\times10^{9}\,M^{-1}s^{-1}$.[92] While $^{\bullet}NO_2$ is able to abstract H-atom from Tyr to form $Tyr^{\bullet}$, this reaction is relatively slower ($k = 3.2\times10^{5}\,M^{-1}s^{-1}$)[93] than the H-atom abstraction by $CO_3^{\bullet-}$ with $k = 4.5\times10^{7}\,M^{-1}s^{-1}$ (Figure 1.24). Resonance structure of $Tyr^{\bullet}$ shows localization of the unpaired electron on the phenoxyl-O and the carbon atom ortho to the phenoxyl-O. Subsequent addition of $^{\bullet}NO_2$ to $Tyr^{\bullet}$ yields the 3-nitrotyrosine with $k = 3\times10^{9}\,M^{-1}s^{-1}$.[93] Loss of enzyme function has been correlated with the degree of tyrosyl nitration and has been observed in prostaglandin H2 synthase (PGSH-1),[94] MnSOD,[95] and mitochondrial cytochrome c.[96]

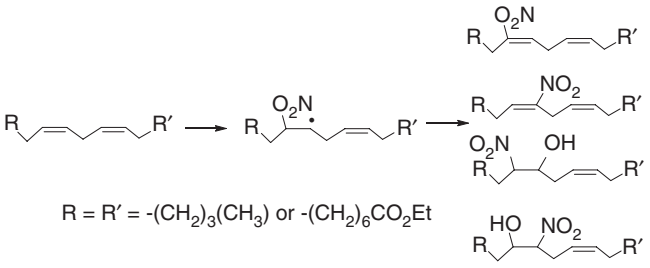


Figure 1.23 Nitration and hydroxylation of PUFA by $^{\bullet}NO_2$.

1.4.2.3 Reaction with Thiols Nitrosation of thiol-containing biomolecules is one of the most important processes in post-translational protein modification. Production of nitrosothiols (RSNO) is an important regulatory function of $NO^{\bullet}$ in cell signaling and pathology. Examination of RSNO production at low micromolar concentrations of $NO^{\bullet}$ indicates N_2O_3 and $^{\bullet}NO_2$ as the nitrosating agents *via* a one-electron oxidation of thiols to $RS^{\bullet}$ and its subsequent radical–radical addition to $NO^{\bullet}$ to form S-nitrosothiols (RSNO).[97] The rate of glutathiyl radical ($GS^{\bullet}$) reaction with $NO^{\bullet}$ to form GSNO is $2.8\times10^{7}\,M^{-1}s^{-1}$ (Eq. 1.50).[98] which is lower than that expected for GSSG formation through radical–radical reaction further demonstrating that $GS^{\bullet}$ does not directly react with $NO^{\bullet}$ to form GSNO.

$$RSH + NO_2 \rightarrow RS^{\bullet} + NO_2^{-} + H^{+} \quad (k = 10^{7}\,M^{-1}s^{-} \tag{1.50}$$

1.4.3 Peroxynitrite ($ONOO^{-}$)

Peroxynitrite is formed from the addition reaction of $NO^{\bullet}$ with superoxide ($O_2^{\bullet-}$) at a diffusion-controlled rate.[43,81] Peroxynitrite is known to exist in the relatively stable cis-conformation, or gain a proton to form peroxynitrous acid (ONOOH, pK_a 6.8). One relevant mechanism for $ONOO^{-}$/ONOOH decay is its homolytic cleavage through $^{\bullet}ONOO^{\bullet-}$ and $^{\bullet}ONO\cdots{}^{\bullet}OH$

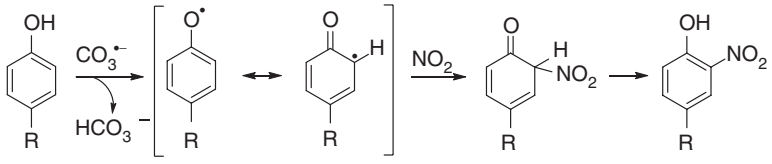


Figure 1.24 Radical-radical addition of $^{\bullet}NO_2$ to tyrosyl radical.

intermediates (Scheme 2).[99] The higher membrane permeability of ONOOH compared to its unprotonated form can result in its homolysis to form HO• and •NO_2 leading to the initiation of oxidation of key biomolecular systems. Technically, therefore, $ONOO^-$ could be both classified as ROS and RNS since both N and O atoms in $ONOO^-$ underwent oxidation and reduction, respectively, to form •NO_2. For $ONOO^-$, the rate of radical cleavage has been reported at $\approx 10^{-6}$ s^{-1}, with negligible •NO_2 and $O^{\bullet -}$ release,[100] while for ONOOH, the rate of radical cleavage has been reported to be $0.35 \pm 0.03\,s^{-1}$, with about 30% of HO•OH and •NO_2 being released at pH < 5 *via* escape from the solvent cage. Like $O_2^{\bullet -}$, $ONOO^-$ is capable of reacting with protein active sites containing Cu, Zn, sulfhydryl, and Fe–S clusters to cause nitration and protein cleavage resulting in enzyme deactivation.[59,101–103] The rate constant for ONOOH isomerization to nitric acid (HNO_3) was found to be $1.1 \pm 0.1\,s^{-1}$.[104] While the low rate of homolytic cleavage of $ONOO^-$ makes the reaction trivial, $ONOO^-$ is known to react with dissolved CO_2 to form nitrosoperoxycarbonate ($ONOOCO_2^-$) at a rate constant of $3.0 \times 10^4\,M^{-1}\,s^{-1}$.[105] $ONOOCO_2^-$ is a two-electron oxidant that undergoes homolytic cleavage to form 30% $CO_3^{\bullet -}$ and •NO_2 (Eq. 1.51).[95,106]

$$ONOO^- + CO_2 \rightarrow ONOOCO_2^- \rightarrow CO_3^{\bullet -} + NO_2 \quad (1.51)$$

The modes of decay of $ONOOCO_2^-$ and ONOOH have been shown to vary depending on the ability of the solvent to hold the intermediate species in the solvent cage, and is therefore, dependent on the viscosity of a solvent.[107] Peroxynitrite is a strong nucleophile, and has been shown to cause β-scission of carbonyl groups,[108,109] where acyl- and H-spin adducts have been observed using EPR spin trapping.[110,111] Peroxynitrite has recently been shown to form peroxynitrate (O_2NOO^-) at neutral pH through combination of $ONOO^-$ and ONOOH to form O_2NOOH and nitrite (NO_2^-).[112]

Reaction of $ONOO^-$ with inorganic radicals such as $CO_3^{\bullet -}$, $^{\bullet}N_3$, $ClO_2^{\bullet}$, and HO• involves a one-electron transfer process. For example, $ONOO^-$ oxidation by the inorganic radicals yields ONOO• and the corresponding anions with varying rate constants (Eqs. 1.52–1.55).[113] With NO•, $ONOO^-$ forms •NO_2 and NO_2^- with highly exoergic free energy of –113 kJ.[114]

$$ONOO^- + CO_3^{\bullet -} \rightarrow ONOO^{\bullet} + CO_3^{2-} \quad (k = 7.7 \times 10^6\ M^{-1}\ s^{-1}) \quad (1.52)$$

$$ONOO^- + {}^{\bullet}N_3 \rightarrow ONOO^{\bullet} + N_3^- \quad (k = 7.2 \times 10^8\ M^{-1}\ s^{-1}) \quad (1.53)$$

$$ONOO^- + HO^{\bullet} \rightarrow ONOO^{\bullet} + HO^- \quad (k = 4.8 \times 10^9\ M^{-1}\ s^{-1}) \quad (1.54)$$

$$ONOO^- + ClO_2^{\bullet} \rightarrow ONOO^{\bullet} + ClO_2^- \quad (k = 3.2 \times 10^4\ M^{-1}\ s^{-1}) \quad (1.55)$$

Peroxynitrite acts as a two-electron oxidant with thiols. Thiolates from low-molecular-weight thiols or protein thiols react with ONOOH to form sulfenic acid (RSOH). With low-molecular-weight thiols, the rates of thiol oxidation increase with decreasing thiol pK_a,[115] consistent with the mechanism of nucleophilic attack of the thiolate-O to the peroxyl-O of ONOOH with nitrite as the leaving group according to the following mechanism shown in Equation 1.56:

$$RS^- \; O{=}N{-}O{-}OH \longrightarrow RSOH + NO_2^- \quad (1.56)$$

Rate constants for the reaction of $ONOO^-$ with free cysteine and the single thiol of albumin were reported to be in the order of $10^3\,M^{-1}\,s^{-1}$.[116] The formation of RSSR' from RSOH in the presence of RS^- is fundamental to the regulation of protein function. With peroxidoxin thiol ($PrxS^-$), the reaction with ONOO to yield NO_2^- and PrxSOH is faster ($10^7\,M^{-1}\,s^{-1}$)[117] than $ONOO^-$ reaction with small-molecular-weight thiols. Decomposition of $ONOO^-$ *via* one-electron or two-electron reduction processes can be catalyzed by metalloporphyrins of iron and manganese which can have protective effects against $ONOO^-$-induced damage. One-electron reduction leads to the formation of •NO_2 , while its two-electron reduction forms NO_2^-.[101] The formation of •NO_2 from $ONOO^-$ is shown to cause tyrosine nitration to form 3-nitrotyrosine.[118]

1.5 REACTIVE SULFUR AND CHLORINE SPECIES

1.5.1 Thiyl or Sulfhydryl Radical (RS•)

Thiyl radicals are analogous to alkoxyl radicals (RO•), but there are important differences between the bonds involving S and O atoms. For example, the S–H bond in thiols is weaker than the O–H bond in alcohols with experimental bond dissociation energies of 88.0 and 104.4 kcal/mol for CH_3S–H and CH_3O–H, respectively.[119] The bond length for S–H is 1.33 Å compared to O–H of 0.96 Å. These differences in the structural and physical properties of thiols compared to alcohols play an important role in the reactivity of thiols compared to alcohols in which the S is more accessible. Since S is less electronegative than O, therefore, thiyls

are more electrophilic than alkoxyl radicals with a longer C–S bond length of 1.81 Å compared to C–O of 1.42 Å.

Generation of RS$^\bullet$ in biological systems occurs *via* one-electron oxidation of thiols (RSH) by metal ions such as Cu^{2+} or Fe^{3+}, HO$^\bullet$, peroxynitrite, DNA, or protein radicals. Disulfide formation (GSSG) from GS$^\bullet$ *via* radical–radical addition is fast with rate constant of 1.5×10^9 M^{-1} s^{-1}.[120] The susceptibility of RSH to oxidation is the basis of thiol antioxidant or repair mechanisms. GSH for example is the predominant intracellular antioxidant with cytosolic concentrations of up to 10 mM. Due to the high GSH concentration, the formation of disulfide is regulated. Glutathione reacts with tyrosyl radical Tyr$^\bullet$ to yield GS$^\bullet$ and TyrOH ($k = 2\times10^6$ M^{-1} s^{-1}) as a repair mechanism but at a 220x slower rate than Tyr$^\bullet$ reaction with ascorbate. Ascorbate, being more abundant in tissues, makes GSH a minor player in this type of repair mechanism.[121]

Thiyl radicals can catalyze conversion of cis-to-trans isomerism in unsaturated systems. In lipid systems, the conversion of the naturally occurring *cis* unsaturated fatty acids to *trans* can cause morphological changes in the lipid bi-layers.[122] Reaction of thiyl with unsaturated compounds can also result to addition reaction where the preference for radical attack is the one with the highest electron density such as double bonds demonstrating the electrophilic nature of thiyl radicals which is due to the ability of the d-orbitals of sulfur to accommodate the negative charge. The rate constant for thiyl radical addition to monounsaturated fatty acid esters such as methyl oleate, methyl palmitoleate, methyl Z-vaccenate, and oleic acid in *tert*-butyl alcohol is in the order of k_a^Z and $k_a^E \sim 10^5$ M^{-1} s^{-1}, while the rate constant for the β-elimination to Z or E configurations is higher with k_f^Z and k_f^E of ~10^7 and 10^8 s^{-1}, respectively.[123] Thiyl-radical-induced isomerization for linoleic acid, linolenic acid, and arachidonic acid gave k_a^Z and k_a^E of ~10^6 M^{-1} s^{-1} and k_f^Z and k_f^E of ~10^5 s^{-1}, respectively (Figure 1.25).[51]

Relevant to the oxidation PUFA, thiyl can also undergo H-atom abstraction in bisallylic systems, and like HO$^\bullet$ (Eq. 1.57), demonstrates their pro-oxidative role in the initiation of lipid peroxidation. The rate

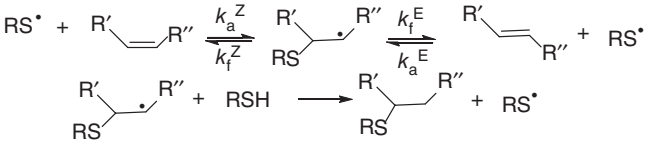
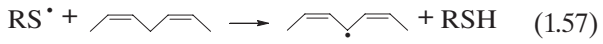


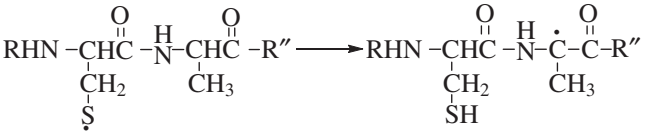
Figure 1.25 Thiyl radical mediated E and Z isomerization of monosaturated fatty acid.

constant for H-atom abstraction by thiyl radicals with PUFAs was in the order of 10^7 M^{-1} s^{-1}.[124]



(1.57)

H-atom abstraction from aliphatic alcohols and ethers has been shown to occur at a rate constant of 10^3 to 10^4 M^{-1} s^{-1}.[125] In peptidic systems, intramolecular H-atom transfer between cysteine thiyl radical and the $^\alpha$C–H bond occurs with rate constants that are in the order of 10^3 to 10^5 M^{-1} s^{-1}.[126] The favorability of this reaction was shown to be dependent on peptide and protein sequence as well as structure and can have implications in the catalysis of protein damage due to its potential irreversibility resulting in protein fragmentation and/or epimerization.[127] Interconversion between $^\alpha$C-, $^\beta$C-, and S-centered radicals in GS$^\bullet$ (Eq. 1.58) has been shown to proceed favorably and is pH dependent with an overall rate constant of $k_{forward} = 3.0\times10^5$ s^{-1}, $k_{reverse} = 7.0\times10^5$ s^{-1}, and $K = 0.4$, with an equilibrium ratio at pH 7 of 8:3:1 for S:$^\beta$C:$^\alpha$C-, centered radicals.[128]



(1.58)

H-atom abstraction by thiyl radical from carbohydrates has been reported.[129] H-atom transfer of C^1–H of 2-deoxy-D-ribose, 2-deoxy-D-glucose, α-D-glucose, and inositol by cysteine-derived thiyl radical gave rate constants that are in the order of 10^4 M^{-1} s^{-1}.

Quenching of thiyl radicals by ascorbate results in the formation of ascorbyl radical and RSH, while thiyl reaction with radicals such as NO$^\bullet$, O_2, and R$^\bullet$ showed varying reactivity. Formation of S-nitrosothiols in biological systems is one of the most established paradigms in cell signaling. The rate constant for the reaction of NO$^\bullet$ with thiyl radicals of glutathione (Eq. 1.59), cysteine, and penicillamine was in the range of $2–3\times10^9$ M^{-1} s^{-1}.[130]

$$GS^\bullet + NO \rightarrow GSNO \quad k = 2.7\times10^9\,M^{-1}\,s^{-1} \tag{1.59}$$

Reaction of thiyl radicals with O_2 yields RSOO$^\bullet$, but the presence of excess RSH leads to the formation RSO$^\bullet$ and RSOH under normal conditions.[131] The reported rate constants for the reaction of GS$^\bullet$ with O_2 vary from 3.0×10^{7132} to 2.0×10^9 M^{-1} s^{-1},[133] indicating a more complex mechanism resulting from this addition reaction (Eq. 1.60).

$$GS^\bullet + O_2 \underset{k_{-1}}{\overset{k_1}{\rightleftharpoons}} GSOO^\bullet \qquad k_1 = 2.0\times10^9\ M^{-1}\,s^{-1};\ k_{-1} = 6.2\times10^5\ s^{-1} \tag{1.60}$$

Reaction of GS^- with $GS^\bullet$ forms $GSSG^{\bullet-}$ with a rate constant of $4.5\times10^8\ M^{-1}\ s^{-1}$ (in the case of GSH) with an equilibrium constant of $2.25\times10^3\ M^{-1}$.[134] Decay kinetics of $RSSR^{\bullet-}$ forms RS^- and $RS^\bullet$, with $RS^\bullet$ further undergoing intramolecular H-atom abstraction mechanism to form the α-amino carbon-centered radical with rate constants ranging in the order of 10^4 to $10^5\ s^{-1}$ for cysteine, homocysteine, and glutathione at pH 10.5.[134] Protonation of $RSSR^{\bullet-}$ leads to its decomposition to $RS^\bullet$ and RSH and ultimately to RSSR with rate constants in the order of 10^5 to $10^6\ s^{-1}$.[135] Reaction of $GSSG^{\bullet-}$ with O_2 gave a rate constant of $1.6\times10^8\ M^{-1}\ s^{-1}$ (Eq. 1.61).[136]

$$GS^\bullet + GS^- \rightleftharpoons GSSG^{\bullet-} \xrightarrow{O_2} GSSG + O_2^{\bullet-} \qquad (1.61)$$

1.5.2 Disulfide (RSSR)

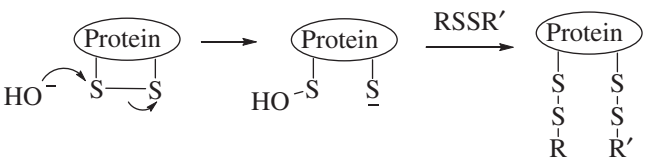
Unlike the S–H bond dissociation energy being lower than the O–H, the S–S bond dissociation energy is higher compared to O–O. Reported BDE for MeS–SMe is 74 kcal/mol compared to MeO–OMe of 37.6 kcal/mol.[119,137] Thiol-disulfide interchange as described by Equations 1.62 and 1.63 shows formation of a mixed disulfide intermediate RSSR′ from the oxidation of RSH and reduction of R′SSR′.[138] Thiol-disulfide interchange is an important biochemical process and occurs in many metabolic reactions of thiols either endogenous or thiol-based drugs such as penicillamine. The rate constants for the symmetrical thiol-disulfide exchange reaction have been determined for several thiols such as GSH, Cys, or homocysteine in aqueous basic medium (pH > 10) giving k in the range of 12–60 $M^{-1}\ s^{-1}$.[138]

$$RSH + R'SSR' \rightleftharpoons RSSR' + R'SH \qquad (1.62)$$

$$RSH + RSSR' \rightleftharpoons RSSR + R'SH \qquad (1.63)$$

$$2\,RSH + R'SSR' \rightleftharpoons RSSR + 2\,R'SH$$

Disulfide bonds play a major role in protein thermal stability, but through chemical means, disulfide bonds can be broken down *via* several mechanisms. Under basic or neutral conditions, hydroxide (HO^-) is shown to attack the sulfur atom to form sulfenic acid and thiolate anion and can ultimately results into post-translational protein modification to form complex disulfides (Eq. 1.64) or mixed sulfenic acid/disulfides with another protein/s.



(1.64)

Hydroxide can also abstract the α- or β-protons of the Cys residue leading to C–S or S–S bond breakage, respectively, followed by β- or α-elimination according to Figure 1.26.[139]

Disulfide can be further oxidized to disulfide-S-monoxide and disulfide-S-dioxide. Oxidation of one of the sulfur atoms leads to the weakening of the S–S bond and is therefore more susceptible to reaction with RSH to form sulfenic (RSOH) and sulfenic acids (RSO_2H) to generate the mixed disulfide (Figure 1.27).[140]

Disulfides can also be enzymatically reduced to RSH by glutathione reductase[141] or thioredoxin reductases[142] in the presence of NADPH, or chemically, by small molecules such as dithiothreitol, hydrazine, or sulfones.[143]

1.5.3 Hypochlorous Acid (HOCl)

Hypochlorous acid is usually formed from the reaction of Cl_2 gas with water; however in biological systems, their formation has been mediated by a secreted heme protein, myeloperoxidase (MPO), which can convert H_2O_2 to HOCl in the presence of chloride ion (Cl^-) according to Equation 1.65.[144]

$$H_2O_{2+}\,Cl^{-+}\,H^+ + MPO \rightarrow HOCl + H_2O \qquad (1.65)$$

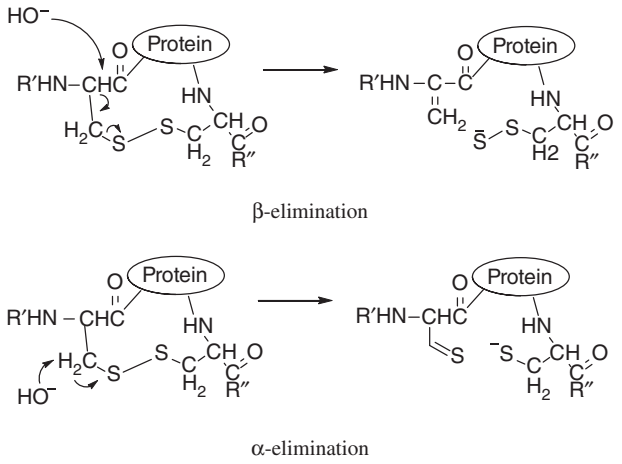


Figure 1.26 β- or α-elimination reactions of hydroxide anion on protein with cysteine residues.

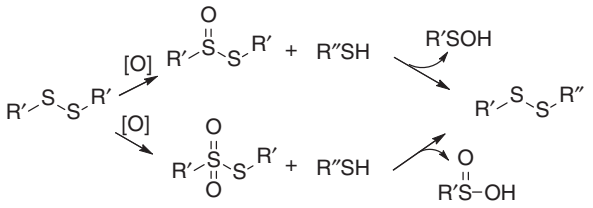
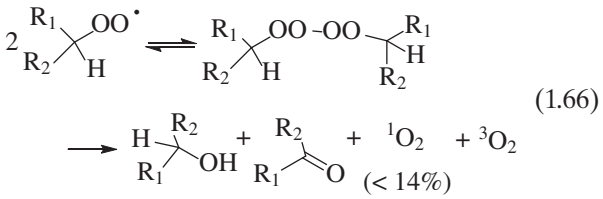


Figure 1.27 Oxidation of disulfide leading to the formation of mixed disulfides.

HOCl has a pK_a of 7.5; therefore, it co-exists with the ionized hypochlorite ($^-$OCl) in solution at physiological pH. The HOCl produced has been shown to be a potent 2-electron oxidant capable of chlorinating electron-rich substrates and oxidation of heme, tyrosine or cysteine residues in proteins, DNA, and lipids.

Hypochlorous acid reacts with various ROS such as H_2O_2 to generate stoichiometric amounts of [O_2 ($^1\Delta_g$)],[145] with $O_2^{\bullet-}$ to generate HO$^\bullet$,[146] and with HO$^\bullet$ to form ClO$^\bullet$ (Figure 1.28).[147]

Reaction of HOCl with hydroperoxide such as linoleic acid hydroperoxide (LA-OOH) mimics that of its reaction with H_2O_2 producing [O_2 ($^1\Delta_g$)] (13% yield) at physiological pH (Eq. 1.66).[148]


(1.66)

With anions such as NO_2^-, HOCl is capable of forming a reactive intermediate that can nitrate phenolic substrates such as tyrosine and 4-hydroxyphenyl acetic acid with high yield at physiological pH.[149,150] The nitrating intermediates were identified to be $^\bullet NO_2$ and nitryl chloride (NO_2-Cl) based on Equation 1.67.

$$\begin{aligned} HOCl + NO_2^- &\rightarrow HO^- + Cl\text{-}NO_2\,(Cl\text{-}ONO) \\ &\rightarrow Cl^+ \cdots NO_2^- + {}^\bullet Cl + {}^\bullet NO_2 \end{aligned} \quad (1.67)$$

Sulfite reaction with HOCl gives the intermediate, Cl-SO_3^- and its subsequent hydrolysis forms Cl^- and SO_4^{2-}.[151] Reaction rate of HOCl with low-molecular-weight antioxidant such as ascorbate (AH^-) is $6\times10^6\,M^{-1}s^{-1}$.[152]

$$AH^- + HOCl \rightarrow A + Cl^- + H_2O \quad (1.68)$$

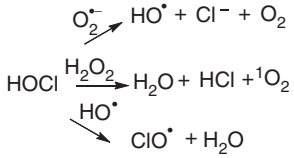


Figure 1.28 Reactions of hypochlorous acid with various reactive oxygen species.

Electron-transfer reaction between Fe^{2+} and HOCl occurs with the generation of HO$^\bullet$ and Cl$^\bullet$ according to Equations 1.69 and 1.70,

$$HOCl + Fe^{2+} \rightarrow Fe^{3+} + HO^\bullet + Cl^- \quad (1.69)$$

$$HOCl + Fe^{2+} \rightarrow Fe^{3+} + HO^- + Cl^\bullet \quad (1.70)$$

where the formation of HO$^\bullet$ predominates due to the electron-transfer reaction between Cl$^\bullet$ and H_2O to further form HO$^\bullet$.[153]

Reaction of HOCl with free amino acid backbone generates chloramine species at the free amino moiety. Chloramine undergoes further decomposition to nitrogen-centered radicals which subsequently undergo further decomposition pathways such as (1) intra- and inter- molecular H-atom abstraction; (2) decarboxylation; (3) β-scission according to Figure 1.29.[154]

Analogous to the reaction of amines with HOCl, GSH forms S-chloro derivative with HOCl which can hydrolyze to yield the corresponding sulfenic acid (GSOH) (*via* formation of thiyl radical)[154] with an estimated rate constant of $>10^7\,M^{-1}s^{-1}$ (Eqs. 1.71–1.73).[153] With amino acids containing thiols, methionine or cysteine the rates was estimated to be in the order of $\sim10^{4-5}\,M^{-1}s^{-1}$).[155]

$$GSH + HOCl \rightarrow GSCl + H_2O \rightarrow GS^{\bullet+}\,Cl^\bullet \quad (1.71)$$

$$Cl^{\bullet+}\,H_2O \rightarrow HO^\bullet + Cl^{-+}\,H^+ \quad (1.72)$$

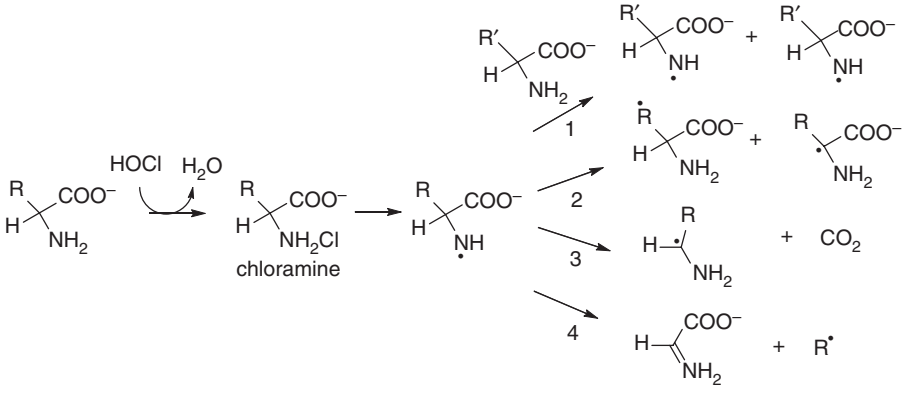
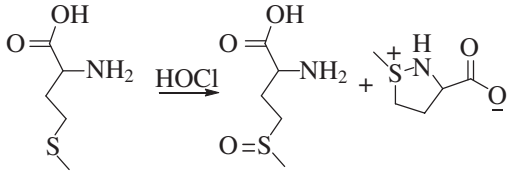


Figure 1.29 Reaction of hypochlorous acid with amino acids.

$$GS^{\bullet+} + HO^{\bullet} \rightarrow GSOH \qquad (1.73)$$

The formation of sulfonamide (RSO_2NHR) but not the formation of GSSG from HOCl and GSH *via* intramolecular cyclization reaction has also been observed.[156] Methionine oxidation by HOCl forms methionine sulfoxide and dehydromethionine according to Equation 1.74:[157]



(1.74)

Reaction of HOCl with tyrosine and peptidyl-tyrosyl residues yielded 3,5-dichlorotryosine (diCl-Tyr) in addition to Cl-Tyr. Further reaction of the mono- and dichlorinated tyrosines gave the corresponding mono- and dichlorinated 4-hydroxyphenylacetaldehydes, Cl-HPAA and diCl-HPAA, respectively, according to Figure 1.30.[158]

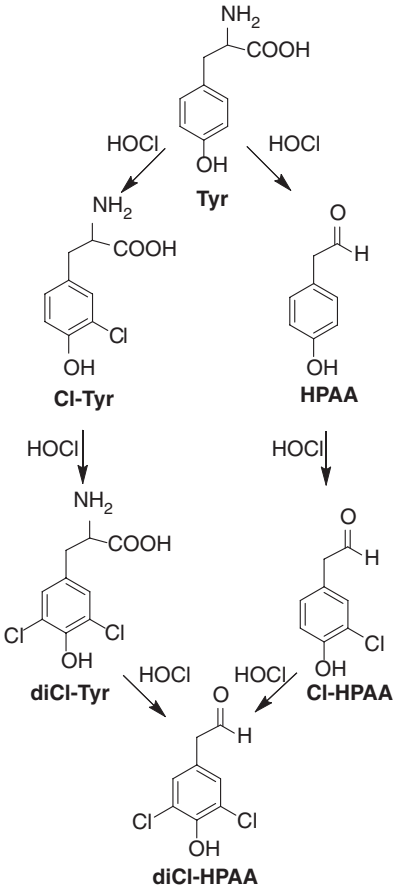
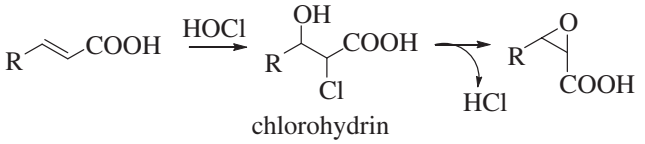


Figure 1.30 Reactions of hypochlorous acid with tyrosine.

Oxidation of cytochrome *c* by HOCl has rate constant of $>3\times10^5\,M^{-1}s^{-1}$. This reaction is not selective toward the heme iron but also involves *N*-halogenation of the side chain amino groups and with concomitant generation of $HO^{\bullet}$.[159]

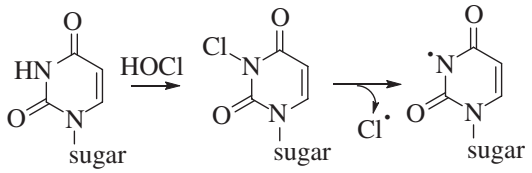
$$Fe(II)cyt\,c + HOCl \rightarrow Fe(III)cyt\,c + HO^{\bullet+}\,Cl^{-+} \qquad (1.75)$$
other products

HOCl reaction with lipids occurs at either the lipid head group or the unsaturated portion of the fatty acid side chain. For example, reaction of HOCl with phosphoryl-serine and phosphoryl-ethanolamine is rapid with $k \sim 10^5\,M^{-1}s^{-1}$ yielding chloroamines as the major products.[44] Reaction with unsaturated fatty acid chains involves initial formation of chlorohydrins[160] followed by secondary dehydrohalogenation reactions to yield the epoxide (Eq. 1.76). The formed epoxide can further react with HOCl to form ROS and lipid peroxidation products.



(1.76)

Reaction of HOCl with nucleotide bases occurs primarily on the exocyclic free amino group (e.g., of cytosine, adenosine, and guanosine) or nitrogen atoms of the heterocyclic ring (e.g., of thymidine, uridine, and guanosine) which contain lone pairs to form N–Cl bond. These adducts can result in miscoding and have been identified in tissues under inflammatory conditions. The rate constant for reactions within the heterocyclic ring is in the order of 10^3 to $10^4\,M^{-1}s^{-1}$. With uridine, for example, N–Cl formation leads to the formation of N–centered radical (Eq. 1.77).[161]



(1.77)

Direct chlorination on the carbon atom by HOCl of the heterocyclic ring was also observed to give chlorinated products such as 5-chloro-2′-deoxycytidine, 5-chloro-uracil,8-chloro-2′-deoxyguanosine,and5-chloro-2′-deoxyadenosine[162] as well as hydroxylation of the pyrimidine moiety to give thymine glycol (cis/trans),

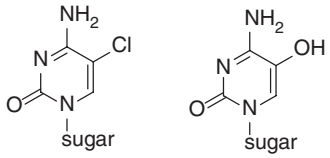


Figure 1.31 Chlorination and hydroxylation of pyrimidine by hypochlorous acid.

5-hydroxycytosine, 5-hydroxyuracil, 5-hydroxyhydantoin (Figure 1.31).[163]

Reaction of related compounds such as NADPH with HOCl is characterized by an initial fast reaction with $k = 4.2 \times 10^5\,M^{-1}s^{-1}$ leading to the formation of a stable pyridine product (Py/Cl). Subsequent reaction with HOCl ($k = 3 \times 10^3\,M^{-1}s^{-1}$) leads to the total loss of the aromatic pyridine ring absorbance.[164]

1.6 REACTIVITY

As in all chemical reactions, reactions involving reactive species are governed thermodynamically and kinetically, and these two inter-related forces can offer insights into the favorability and rate of reaction, respectively.

1.6.1 Thermodynamic Consideration

The favorability of redox reaction involving reactive species is governed by the overall change in the potential energy whereby the energy is released (in this case of an exothermic reaction) or addition of energy (endothermic reaction) to the system for the reaction to proceed. The thermodynamic favorability is defined by an entity called free energy (ΔG) which is either introduced or given off in a reaction. One can envision that reactants and products have stored energy in them. Calculation of ΔG can be theoretically and experimentally performed. As an example for the formation $ONOO^-$ from $O_2^{\bullet -}$ and $NO^\bullet$, one can calculate the favorability of this reaction by taking into account the potential energies of the individual species. One important theoretical consideration in determining the free energy of reaction (ΔG_{rxn}) is that the type and number of atoms in the product and reactant sides should be conserved as shown in the equation: $O_2^{\bullet -} + NO^\bullet \rightarrow ONOO^-$. Each of these species carries a potential energy originating from the separation of the individual nuclei and electrons from the molecule. For example, the following are the total electronic energies (ε_o) (with thermal free energies, G_{corr}) for $O_2^{\bullet -}$, $NO^\bullet$, and $ONOO^-$ formed from nuclei and electrons.

$$O_2^{\bullet -} \rightarrow 2O^{8+} + 17e^- \qquad -150.482170 \text{ hartrees}$$

$$NO^\bullet \rightarrow O^{8+} + N^{7+} + 15e^- \qquad -129.907204 \text{ hartrees}$$

$$ONOO^- \rightarrow 3O^{8+} + N^{7+} + 32e \qquad -280.402251 \text{ hartrees}$$

The $\Delta G^o_{rxn,298K}$ for the reaction: $O_2^{\bullet -} + NO^\bullet \rightarrow ONOO^-$ can then be calculated using the equation:

$$\Delta G^o_{rxn,298K} = \Sigma\,(\varepsilon_o + G_{corr})_{products} - \Sigma\,(\varepsilon_o + G_{corr})_{reactants}$$

$$\Delta G^o_{rxn,298K} = ((-280.402251) - (-150.482170 + -129.907204) * 627.5095$$

$$\Delta G^o_{rxn,298K} = -8.08 \text{ kcal/mol}$$

The ΔG for the formation of $ONOO^-$ from $O_2^{\bullet -}$ and $NO^\bullet$ is therefore exothermic since the total energy of the reactant is greater than the reactants, and therefore, excess energy is given off. The reaction is said to proceed spontaneously. In contrast, the dismutation reaction of two $O_2^{\bullet -}$ to form O_2^{2-} and O_2 according to the equation: $2O_2^{\bullet -} \rightarrow O_2^{2-} + O_2$, gave $\Delta G^o_{rxn,298K}$ 35.7 kcal/mol, which is endoergic and does not proceed spontaneously due to repulsion between the two $O_2^{\bullet -}$. The two contrasting equations demonstrate the relative thermodynamic stability of the two reactions in which the formation of $ONOO^-$ is preferred due to the less repulsion between reactants and the radical–radical nature of the reaction.

However, ΔG of formation for ROS/RNS can also be obtained experimentally. Koppenol had compiled a series free energies as shown in Table 1.1.[114]

The ΔG is defined by Equation 1.78,

$$\Delta G = \Delta H - T\Delta S \tag{1.78}$$

where ΔH is the change in entropy, T is the absolute temperature, and ΔS is the change in entropy. Although the exoergicity or endoergicity of a reaction is determined by the minimization of the total enthalpy (*i.e.,* net heat change), the minimization of the total free energy of the system at constant temperature and pressure is the driving force for all reactions. Therefore, the sign of ΔG indicates favorability of a reaction, that is,

$\Delta G < 0$ (favored or spontaneous)
$\Delta G = 0$ (equilibrium, neither forward nor backward reactions are favored)
$\Delta G > 0$ (not favorable, nonspontaneous)

The concept presented above assumes that the reaction is unidirectional, meaning that the products are perfectly thermodynamically stable and do not revert toward the formation of the reactant. However, there are reactions involving reactive species that are not unidirectional. These reactions contain significant quantities of reactants and products at equilibrium, a state

TABLE 1.1 Gibbs Energies of Formation for Various ROS/RNS.[114,165]

Compounds	$\Delta_f G^o$ (kcal/mol)
$HO^\bullet$	15.7 (12.7)[166]
H_2O	−56.7
H_2O_2	−14.1
$HO_2^\bullet$	10.7 (1.7)[165]
HO_2^-	−7.6
HO^-	−28.1
$NO^\bullet$	24.4
NO^+	52.3
NO^- (singlet)	32.5
NO^- (triplet)	15.3
$^\bullet NO_2$	15.1
NO_2^+	52.1
NO_2^-	−7.7
$^\bullet NO_3$	31.3
NO_3^-	−26.6
N_2	4.2
N_2O	27.2
$N_2O_2^{\bullet-}$	33.7
N_2O_3	35.1
$ONOO^\bullet$	20.1
$ONOO^-$	10.1 (16.6)[167]
O_2	3.9
$O_2^{\bullet-}$	7.6
ONOOH	7.5

Adopted from Ref. 114.

in which the composition of the reactant and products remain unchanged.

$$A \underset{k_2}{\overset{k_1}{\rightleftharpoons}} B$$

The relationship between free energy and thermodynamic equilibrium (K_{eq}) constant is described by Equation 1.79:

$$\Delta G^o = -RT \ln K_{eq} \tag{1.79}$$

where R is the universal gas constant and T is the absolute temperature. Since K_{eq} represents the ratio of the molar concentrations of A relative to B, and of k_1 and k_2 *at equilibrium*, that is, $K_{eq} = [B]/[A] = k_1/k_2$, it is expected that ΔG^o will obviously be dependent on temperature as temperature affects the direction of the equilibrium. Example of temperature-dependent reversible reaction is the transnitrosation reaction between thiol and S-nitrosothiol (Eq. 1.80):

$$RSH + R'SNO \rightleftharpoons R'SH + RSNO \tag{1.80}$$

with R′SNO as S-nitroso-*N*-acetyl-penicillamine (SNAP), and with glutathione or L-cysteine as RSH, the K_{eq}s were determined to be 3.69 and 3.66, at 25 °C. Using Equation 1.79, ΔG^o can be calculated to be −0.77 kcal/mol. With ΔG being negative, it is exoergic; hence, the equilibrium is shifted to the product side of the equation. At higher temperature (*i.e.,* 33 °C) for glutathione or L-cysteine, the K_{eq} is lower with 3.0 and 2.58, which correspond to ΔG^o of −0.66 and −0.58 kcal/mol, respectively, indicating the equilibrium is shifted to the right. Conversely, K_{eq} can be determined based on ΔG^o of formations. In the ionization of ONOOH to $ONOO^-$ for example,

$$ONOOH \rightarrow H^+ + ONOO^-$$

using Table 1.1, the ΔG^o for the formation of ONOOH and $ONOO^-$ is 7.5 and 16.6 kcal/mol, respectively. The free energy of ionization is then equal to $\Delta G^o(ONOO^-) - \Delta G^o(ONOOH) = (16.6\,\text{kcal/mol}) - (7.5\,\text{kcal/mol}) = 9.1\,\text{kcal/mol}$ using $\Delta G^o = 0\,\text{kcal/mol}$ for H^+. Using Equation 1.79 and $RT = 0.593\,\text{kcal/mol}$ at 25 °C, one can calculate the pK_a to be 6.7 which is consistent to that observed experimentally of 6.5 by absorption spectroscopy measurements.[168]

Free energy can also be described as a function of the cell potential (E^o_{cell}) which is characterized by electron-transfer or redox reaction. Using Equation 1.81,

$$\Delta G^o = -nFE^o_{cell} \tag{1.81}$$

where n = is the number of electrons transferred in a half-reaction and F = Faraday's constant (23.06 kcal/mol/V), one can predict the spontaneity of a reaction based on the standard electrode potential of a half-cell reaction. Buettner had complied an extensive list of one-electron reduction potential for a variety of half-cell reactions at pH 7.[169] Table 1.2 lists some of the reduction potentials of half reaction couples. Half-cell reactions are presented such that the species on the right side is the reduced form of the species in the left side. For example, the half-cell reaction, $HO^\bullet$, e^-, H^+/H_2O, can be written as $HO^\bullet + e^- + H^+ \rightarrow H_2O$ with a reduction potential of $E^o = 2.31\,V$ at standard conditions. Oxidation of H_2O can be written in reverse, that is, $H_2O \rightarrow HO^\bullet + e^- + H^+$, but the sign has to be reversed, that is, $E^o = -2.31\,V$. It should be noted that half-cell reaction potentials involving H^+ or HO^- can be pH dependent. Table 1.2 generally shows that the species with the most positive reduction potential (in this case $HO^\bullet$) is the most reducing and is therefore the easiest to oxidize.

To predict the spontaneity of a reaction based on reduction potentials, one can write two half-cell reactions where one is a reduction and the other is an oxidation process. For example in Fenton chemistry, the reaction of Fe(II) with H_2O_2 is represented below. Note that the

TABLE 1.2 Reduction Potentials for Various Half-cell Reactions Showing 1-Electron and 2-Electron Oxidants.[114]

Half-cell reactions	ΔE^{o} (vs NHE) At pH 7 in V at 25 °C
$HO^{\bullet}, e^{-}, H^{+}/H_2O$	2.31
$CO_3^{\bullet-}, e^{-}, H^{+}/HCO_3^{-}$	2.10
$RO^{\bullet}, e^{-}, H^{+}/ROH$	1.60
$2NO^{\bullet}, 2e^{-}, 2H^{+}/N_2O, H_2O$	1.59
$H_2O_2, 2e^{-}, 2H^{+}/2H_2O$	1.35 (1.78)[89]
$HOO^{\bullet}, e^{-}, H^{+}/H_2O_2$	1.05
$ROO^{\bullet}, e^{-}, H^{+}/ROOH$	1.00
$NO_3^{-}, e^{-}, 4H^{+}/NO^{\bullet}, 2H_2O$	0.96
$NO_3^{-}, 2e^{-}, 3H^{+}/HNO_2, H_2O$	0.93
$RS^{\bullet}, e^{-}/ RS^{-}$	0.92
$O_2^{\bullet-}, e^{-}, 2H^{+}/H_2O_2$	0.91
$N_2O_4, 2e^{-}/2NO_2^{-}$	0.87
$O_2, 4e^{-}, 4H^{+}/2H_2O$	0.85 (1.23)[89]
$^1O_2, e^{-}/O_2^{\bullet-}$	0.81
$PUFA^{\bullet}, e^{-}, H^{+}/PUFA\text{-}H$	0.60
$^{\bullet}NO_2, e^{-}/NO_2^{-}$	0.60
α-Tocopheroxyl$^{\bullet}$, e^{-}, H^{+}/α-Tocopherol	0.50
$H_2O_2, e^{-}, H^{+}/H_2O\ HO^{\bullet}$	0.39
$O_2, 2e^{-}, 2H^{+}/H_2O_2$	0.36
ascorbate$^{\bullet}$, e^{-}, H^{+}/ascorbate^{-}	0.28
Fe(III), e^{-}/Fe(II)	0.11
$NO_3^{-}, 2e^{-}, H_2O/NO_2^{-} + 2HO^{-}$	0.01
$O_2, e^{-}/O_2^{\bullet-}$	−0.18
FAD, $2e^{-}, 2H^{+}/FADH_2$	−0.22
$NADP^{+}, 2e^{-}, H^{+}/NADPH$	−0.32
$NAD^{+}, 2e^{-}, H^{+}/NADH$	−0.32
$O_2, e^{-}, H^{+}/HOO^{\bullet}$	−0.46
$NO^{\bullet}, e^{-}/^3NO^{-}$	−0.81
$2NO_3^{-}, 2e^{-}, 2H_2O/N_2O_4 + 4HO^{-}$	−0.85
GSSG, $e^{-}/GSSG^{\bullet-}$	−1.5

Adopted from Refs. 89, 114.

sign for the reduction potential of Fe(II) is negative since Fe(II) is oxidized to Fe(III) in this reaction.

$$\text{Fe(II)} \rightarrow \text{Fe(III)} + e^{-} \quad \Delta E^{o} = -0.11\,\text{V}$$
$$H_2O_2 + e^{-} + H^{+} \rightarrow H_2O + HO^{\bullet} \quad \Delta E^{o} = +0.39\ \text{V}$$
$$H_2O_2 + \text{Fe(II)} + H^{+} \rightarrow H_2O + HO^{\bullet} + \text{Fe(III)} \quad \Delta E^{o} = +0.28\,\text{V}$$

The net equation gave a positive ΔE^{o} value of +0.28 V. For a reaction to occur spontaneously, the ΔG^{o} must be negative. However, according to Equation 1.81, E^{o} must be positive to meet the requirement for spontaneity, and therefore, reaction of H_2O_2 with Fe(II) is considered highly favorable.

1.6.2 *Kinetic Consideration*

Although free energies are useful entities to predict if a reaction will take place, it does not address the rate at which the process will occur. Thermodynamics only describes the relative stability of the reactants versus products. The rate of reaction is proportional to the molar concentration of a component (Eq. 1.82),

$$-d[\text{reactant}]/dt \text{ or } +d[\text{product}]/dt \qquad (1.82)$$

at isothermal and constant volume. As the reaction proceeds, the reactant/s concentrations decrease, and this is accompanied by a decrease in the rate of the reaction as they usually tend to slow down over time. Since rates have variability, a way to quantify the rate of a chemical reaction is by an experimental measure of a reaction rate which is usually referred to as rate constants (k). (Note that by convention, small letter k is referred to as the rate constant and the capitalized K as equilibrium constant). Rate constant is independent of how far the reaction proceeded and its scale. Reactive species in biological systems could exhibit unimolecular, bimolecular, or higher-order reactions, and each of these types of reaction is described by a rate constant.

1.6.2.1 *Unimolecular or First-order Reactions*

Only one reactant in which the rate of its reaction is solely proportional to its concentration at constant volume where the reaction is described in Equation 1.83,

$$\text{A} \rightarrow \text{products} \qquad (1.83)$$

and where the rate law is described in Equation 1.84:

$$\text{Rate of reaction} = -d[\text{A}]/dt = k_1[\text{A}] \qquad (1.84)$$

Experimentally, one can determine the first-order rate constant (k_1) by monitoring the formation or decay of A as a function of time (Eq. 1.85).

$$\ln\left(\frac{[\text{A}]_t}{[\text{A}]_0}\right) = -k_1 t \text{ or } \log\left(\frac{[\text{A}]_t}{[\text{A}]_0}\right) = \frac{-k_1 t}{2.303} \qquad (1.85)$$

where $[\text{A}]_0$ and $[\text{A}]_t$ are concentrations at time = 0 and time = t, respectively. The first-order rate constant has a dimension of time^{-1} and is usually expressed in s^{-1} unit. The half-life ($t_{1/2}$) of a first-order reaction which is the time required for the [A] to decrease by 50% is described as,

$$k_1 t_{1/2} = 0.693$$

Therefore, based on this equation, by knowing $t_{1/2,}$ one will be able to determine k_1. Example of this reaction is the decomposition of $GSSG^{\bullet-}$ to form GS^{-} and $GS^{\bullet}$, or ONOOH to form $^{\bullet}NO_2$ and $HO^{\bullet}$.

1.6.2.2 Bimolecular or Second-order Reactions This reaction occurs from two reactants that are the same species (Eq. 1.86). The rate law is described in Equation 1.87.

$$\mathrm{A} + \mathrm{A} \rightarrow \text{products} \tag{1.86}$$

$$\text{Rate of reaction} = -d[\mathrm{A}]/dt = k_2[\mathrm{A}]^2 \tag{1.87}$$

where the rate is proportional to the instantaneous concentration of A. The second-order rate constant is usually expressed in M^{-1} s^{-1} unit.

Experimentally, one can determine the second-order rate constant (k_2) by monitoring the formation or decay of A as a function of time (Eq. 1.88).

$$\frac{1}{[\mathrm{A}]_t} - \frac{1}{[\mathrm{A}]_0} = k_2 t \tag{1.88}$$

The half-life for second-order reaction is described by Equation 1.89,

$$k_2 t_{1/2} 1/[\mathrm{A}] \tag{1.89}$$

which indicates that the $t_{1/2}$ of the second-order rate constant is inversely proportional to [A]. Examples of this reaction are the bimolecular reaction between two $HO^{\bullet}$ to form H_2O_2, or the dismutation of $HOO^{\bullet}$ to form H_2O_2 and O_2.

Majority of reactions, however, are between two different species (Eq. 1.90) as described by the rate law (Eq. 1.91):

$$\mathrm{A} + \mathrm{B} \rightarrow \text{products} \tag{1.90}$$

$$\text{Rate of reaction} = -d[\mathrm{A}]/dt = -d[\mathrm{B}]/dt = k_2[\mathrm{A}][\mathrm{B}] \tag{1.91}$$

The integrated rate law for k_2 determination is described by Equation 1.92:

$$\mathrm{In}\left(\frac{[\mathrm{A}]_t}{[\mathrm{B}]_t}\right) = \left([\mathrm{A}]_0 - [\mathrm{B}]_0\right)k_2 t + \mathrm{In}\left(\frac{[\mathrm{A}]_0}{[\mathrm{B}]_0}\right) \tag{1.92}$$

To simplify the kinetic measurements, second-order kinetics can be investigated using first-order rate law by making one of the reagents in large excess. For example, if A is in large excess over B, that is, $[A]_0 >>> [B]_0$, then $[A]_t \sim [A]_0$; therefore, Equation 1.92 can be re-written as $k_2[A]_0 = k_1'$ where k_1' is the pseudo-first-order rate constant that is related to the concentrations of B according to Equation 1.93,

$$\mathrm{In}\left(\frac{[\mathrm{B}]_t}{[\mathrm{B}]_0}\right) = -k_1' t \tag{1.93}$$

Using the known initial concentration of the reactant that is in excess, that is $[A]_0$, the second-order rate constant k_2 can be calculated from k_1'.

1.6.2.3 Transition State Theory, Reaction Coordinates, and Activation Energies Transition state theory is the current model used to describe a chemical reaction in terms of physical processes. It assumes that reactions are in equilibrium between the reactants and an activated transition state structure. By determining the reaction rate constants (k_c), the standard Gibbs free energy of activation ($\Delta G^{\neq}$) can be calculated using Equation 1.94,

$$k\mathrm{c} = \frac{k_\mathrm{B}\mathrm{T}}{\mathrm{h}} \mathrm{e}^{-\Delta G^{\ddagger}/\mathrm{RT}} \tag{1.94}$$

where $k_B T/h$ is the universal factor composed of Boltzmann (k_B) and Planck (h) constants and the absolute temperature (T).

In a simple reaction coordinate composed of reactants (A + B), activated complex ($AB^{\neq}$) and products, the potential energy diagram for an exothermic reaction is shown in Figure 1.32. The activated complex lies at the saddle point (highest energy of a potential energy surface) and is in "quasi-equilibrium" with the reactant molecules which is later converted into products.

The magnitude of $\Delta G^{\neq}$ therefore determines the rate of the reaction, that is, the higher the activation barrier, the slower the reaction rate will be. One also must consider that free energy is temperature dependent and hence the kinetics of a reaction. Several external factors can affect the magnitude of $\Delta G^{\neq}$ and the rate of reactions. For example, increased temperature, concentration, and pressure can increase the probability of collision between two particles and, therefore, the rate of reaction

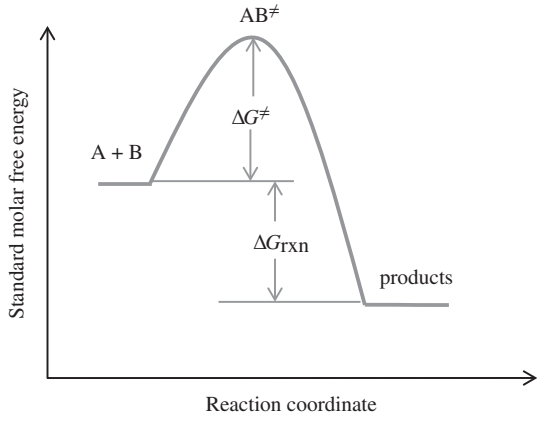


Figure 1.32 Classical reaction coordinate for an exothermic reaction showing the free energies of activation ($\Delta G^{\neq}$) and reaction (ΔG_{rxn}).

increases. Catalysts such as enzymes provide lower activation barrier by increasing the collision rate between reactants, arranging the orientation of the reactants for optimal reactivity, changing the electronic property of the reactants through increased electrophilicity or nucleophilicity, changes in intramolecular forces of attraction that can hinder reactants reactivity or simply providing alternative pathways for the reaction mechanism.

The range of rates by which reactions in biological system occurs is wide from very slow (<1) to diffusion-controlled rate (10^9 to 10^{10}). Table 1.3 shows the various biologically relevant reactions and their experimental rate constants.

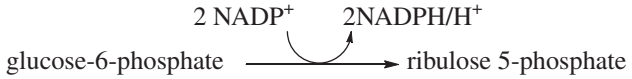
Based on Table 1.3, the fastest reactions (10^9 to 10^{10}) involve either addition reaction or electron-transfer reaction between two radicals. Intermediate rate reactions (10^5 to 10^8) are mostly characterized by H-atom abstraction, reaction between radical anions, or electron transfer between the pi-radicals such as in the case of $NO^{\bullet}$ and O_2. Slow reactions (10^{-2} to 10^4) are mostly unimolecular decomposition that involves bond breaking of N–O, O–O, or N–N bonds and electron transfer between anions and neutral molecules.

1.7 ORIGINS OF REACTIVE SPECIES

1.7.1 Biological Sources

Among the numerous reactive species formed in biological systems, $O_2^{\bullet-}$ and $NO^{\bullet}$ are the two major precursors. The enzymatic generation of $O_2^{\bullet-}$ and $NO^{\bullet}$ has been shown to originate from O_2 and arginine, respectively, as substrates. These radicals are formed in various subcellular compartments such as membrane, mitochondria, endoplasmic reticulum[170], or Golgi apparatus.[171] Below are the common sources of $O_2^{\bullet-}$ and $NO^{\bullet}$, but the mechanistic details will be left in the succeeding chapters, and the list below only offers a general overview of the different enzymes responsible for their generation.

1.7.1.1 NADPH Oxidase Superoxide radical anions are generated through stimulated professional phagocytes (e.g., neutrophils, macrophages monocytes, dendritic cells, and mast cells). Pentose phosphate pathway generates NADPH during the oxidative phase in which two molecules of $NADP^+$ are reduced to NADPH though the utilization of glucose-6-phosphate into ribulose 5-phosphate according to Equation 1.95,



(1.95)

TABLE 1.3 Various Reactions of Reactive Species and Their Respective rate Constants at Normal Conditions

Reaction	Rate Constants
$O_2^{\bullet-} + NO^{\bullet} \rightarrow ONOO^-$	1.9×10^{10} M^{-1} s^{-1}
$O_2^{\bullet-} + HO^{\bullet} \rightarrow O_2 + HO^-$	1.0×10^{10} M^{-1} s^{-1}
$NO^{\bullet} + HO^{\bullet} \rightarrow HNO_2$	1.0×10^{10} M^{-1} s^{-1}
$^{\bullet}NO_2 + HO^{\bullet} \rightarrow {}^{\bullet}NO_2 + HO^-$	1.0×10^{10} M^{-1} s^{-1}
$NO^{\bullet} + R^{\bullet} \rightarrow RNO$	1.0×10^{10} M^{-1} s^{-1}
$2O_2^{\bullet-} + 2H^+ \rightarrow O_2 + H_2O_2$ (SOD catalyzed)	1.0×10^{9} M^{-1} s^{-1}
$O_2^{\bullet-} + {}^{\bullet}NO_2 \rightarrow O_2NOO^-$	4.5×10^{9} M^{-1} s^{-1}
$^{\bullet}NO_2 + {}^{\bullet}NO \rightarrow N_2O_3$	1.1×10^{9} M^{-1} s^{-1}
$NO^{\bullet} + TyrO^{\bullet} \rightarrow$ Tyr-ONO	1.0×10^{9} M^{-1} s^{-1}
$^{\bullet}NO_2 + TyrO^{\bullet} \rightarrow$ Tyr-NO_2	1.3×10^{9} M^{-1} s^{-1}
$NO_2^- + HO^{\bullet} \rightarrow {}^{\bullet}NO_2 + HO^-$	5.3×10^{9} M^{-1} s^{-1}
$GSSG^{\bullet-} + O_2 \rightarrow GSSG + O_2^{\bullet-}$	5×10^{9} M^{-1} s^{-1}
$2GS^{\bullet} \rightarrow GSSG$	1.5×10^{9} M^{-1} s^{-1}
$NO^{\bullet} + GS^{\bullet} \rightarrow GSNO$	3×10^{9} M^{-1} s^{-1}
$^{\bullet}NO_2 + GS^{\bullet} \rightarrow GSNO_2$	3×10^{9} M^{-1} s^{-1}
$GS^{\bullet} + GSNO \rightarrow GSSG + NO^{\bullet}$	1.7×10^{9} M^{-1} s^{-1}
$GS^{\bullet} + O_2 \rightarrow GSOO^{\bullet}$	2×10^{9} M^{-1} s^{-1}
$GSOO^{\bullet} + {}^{\bullet}NO_2 \rightarrow GSOONO_2$	1×10^{9} M^{-1} s^{-1}
$GSOO^{\bullet} + NO^{\bullet} \rightarrow GSOONO$	3×10^{9} M^{-1} s^{-1}
$CO_3^{\bullet-} + NO^{\bullet} + HO^- \rightarrow HCO_3^- + NO_2^-$	3.9×10^{9} M^{-1} s^{-1}
$GSOO^{\bullet} + GSNO \rightarrow GSSG + O_2 + NO^{\bullet}$	3.8×10^{8} M^{-1} s^{-1}
$CO_3^{\bullet-} + O_2^{\bullet-} + H^+ \rightarrow HCO_3^- + O_2$	4.0×10^{8} M^{-1} s^{-1}
$N_2O_3 + RH \rightarrow RNO + H^+ + NO_2^-$	1.8×10^{8} M^{-1} s^{-1}
$CO_3^{\bullet-} + Tyr \rightarrow HCO_3^- + TyrO^{\bullet}$	4.5×10^{7} M^{-1} s^{-1}
$2TyrO^{\bullet} \rightarrow$ diTyr	8.05×10^{7} M^{-1} s^{-1}
$N_2O_3 + GSH \rightarrow GSNO + H^+ + NO_2^-$	6.6×10^{7} M^{-1} s^{-1}
$^{\bullet}NO_2 + GSH \rightarrow GS^{\bullet} + H^+ + NO_2^-$	2×10^{7} M^{-1} s^{-1}
H_2O_2 + Catalase-Fe(III) $\rightarrow$ Compound 1	$k_1 = 1.7\times10^{7}$;
Compound 1 + $H_2O_2 \rightarrow$ Cat Fe(III) + $2H_2O + O_2$	$k_2 = 2.6\times10^{7}$ M^{-1} s^{-1}
$UH_2^- + {}^{\bullet}NO_2^{\bullet} \rightarrow NO_2^- + UH^{\bullet-} + H^+$	1.8×10^{7} M^{-1} s^{-1}
$2NO^{\bullet} + O_2 \rightarrow 2{}^{\bullet}NO_2$	2×10^{6} M^{-1} s^{-1}
$4NO^{\bullet} + O_2 + 2H_2O \rightarrow 4HNO_2$	8.0×10^{6} M^{-1} s^{-1}
$GS^{\bullet} + GS^- \rightarrow GSSG^{\bullet-}$	9.6×10^{6} M^{-1} s^{-1}
$CO_3^{\bullet-} + GSH \rightarrow HCO_3^- + GS^{\bullet}$	5.3×10^{6} M^{-1} s^{-1}
$LOO^{\bullet} + TOH \rightarrow LOOH + TO^{\bullet}$	2.5×10^{6} M^{-1} s^{-1}
$UH^{\bullet-} + Asc^- \rightarrow UH_2^- + A^{\bullet-}$	1×10^{6} M^{-1} s^{-1}
$ROO^{\bullet} + UH_2^- \rightarrow ROO^- + UH^{\bullet-} + H^+$	3×10^{6} M^{-1} s^{-1}
$CO_3^{\bullet-} + RH \rightarrow HCO_3^- + R^{\bullet}$	4×10^{5} M^{-1} s^{-1}
$^{\bullet}NO_2 + Tyr \rightarrow NO_2^- + TyrO^{\bullet}$	3.2×10^{5} M^{-1} s^{-1}
$GSSG^{\bullet-} \rightarrow GS^{\bullet} + GS^-$	1.6×10^{5} s^{-1}
$GSOO^{\bullet} \rightarrow GS^{\bullet} + O_2$	6×10^{5} s^{-1}
$^{\bullet}NO_2 + RH \rightarrow NO_2^- + R^{\bullet} + H^+$	3.2×10^{5} M^{-1} s^{-1}
$GSH + TyrO^{\bullet} \rightarrow GS^{\bullet} + Tyr$	3.5×10^{5} M^{-1} s^{-1}
$GS^{\bullet} + Tyr \rightarrow GSH + TyrO^{\bullet}$	3.5×10^{5} M^{-1} s^{-1}
$2O_2^{\bullet-} + 2H^+ \rightarrow O_2 + H_2O_2$	2.54×10^{5} M^{-1} s^{-1}
$N_2O_3 \rightarrow NO^{\bullet} + {}^{\bullet}NO_2$	8.1×10^{4} s^{-1}
$ONOO^- + CO_2 \rightarrow NO_3^- + CO_2$	2×10^{4} M^{-1} s^{-1}
$ONOO^- + CO_2 \rightarrow {}^{\bullet}NO_2 + CO_3^{\bullet-}$	1×10^{4} M^{-1} s^{-1}
Tyr-ONO $\rightarrow NO^{\bullet} + TyrO^{\bullet}$	1×10^{3} s^{-1}
Urate + $ONOO^- \rightarrow$ products	4.8×10^{2} M^{-1} s^{-1}
$ONOO^- + GSH \rightarrow NO_2^- + GSOH$	6.6×10^{2} M^{-1} s^{-1}
$LOO^{\bullet} + LH \rightarrow LOOH + L^{\bullet}$	10–50 M^{-1} s^{-1}
$GSOONO_2 \rightarrow GSOO^{\bullet} + {}^{\bullet}NO_2$	0.75 s^{-1}
$ONOO^- + H^+ \rightarrow H^+ + HNO_3$	0.568
$ONOO^- + H^+ \rightarrow {}^{\bullet}NO_2 + HO^{\bullet}$	0.232 s^{-1}
$UH^{\bullet-} + O_2 \rightarrow$ no measurable reaction	$<10^{-2}$ M^{-1} s^{-1}

Adopted from Refs. 278, 279.

where NADPH subsequently reduces O_2 to $O_2^{\bullet-}$ via the NADPH oxidase pathway (Eq. 1.96). The details are discussed in the succeeding chapter.[172]

$$\text{NADPH} \xrightarrow[O_2 \quad O_2^{\bullet-}]{} \text{NADP}^+ \tag{1.96}$$

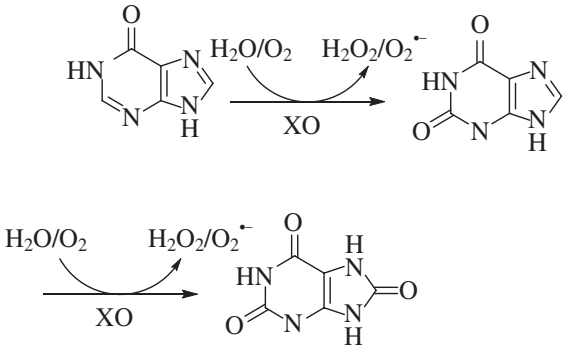
1.7.1.2 Xanthine Oxidoreductase or Oxidase During ischemia, ATP is metabolized to adenosine and through adenosine deaminase, while adenosine is converted to inosine which further decomposes to hypoxanthine (Eq. 1.97). Although hypoxanthine can be converted to xanthine by xanthine oxidase (XO) *via* a reductive half-reaction, xanthine can be independently formed from GMP through purine metabolism. This catalytic purine degradation is also associated with the formation of H_2O_2 and $O_2^{\bullet-}$.[173]

$$\text{ATP} \rightarrow \text{ADP} \rightarrow \text{AMP} \rightarrow \text{adenosine} \rightarrow \text{inosine} \rightarrow \text{hypoxanthine} \tag{1.97}$$

XO belongs to a family of molybdoflavoenzymes and is released by a calcium-triggered protease during hypoxia (Eq. 1.98).

$$\text{xanthine dehydrogenase} \xrightarrow{Ca^{2+}/\text{protease}} \text{xanthine oxidase (XO)} \tag{1.98}$$

Hypoxanthine or xanthine can undergo reductive half-reaction with XO at the Mo–Co. Two electrons are transferred to XO from xanthine thereby reducing Mo(VI) to Mo(IV). The oxidative half-reaction then takes place at FAD where electron transfer between the reduced Mo–Co occurs with FAD as mediated by Fe_2–S_2 centers thus maintaining Mo to be as Mo(VI) and FAD as $FADH_2$. Transfer of electrons from $FADH_2$ to NAD^+ or O_2 occurs during the reoxidation of fully six electron-reduced XO. First two processes involve 2-electron reduction of O_2 to form H_2O_2, then the remaining two electron are each used to reduced O_2 to $O_2^{\bullet-}$. The total ROS produced is, therefore, two molecules of each H_2O_2 and $O_2^{\bullet-}$ (Eq. 1.99).



(1.99)

1.7.1.3 Mitochondrial Electron Transport Chain (METC) Metabolism of O_2 involves a series of electron transfer between an electron donor (NADH) and an electron acceptor, O_2, via the METC, with concomitant transfer of protons from the inner mitochondrial membrane. This process involves transfer of four electrons from cytochrome *c* oxidase to O_2 to form two molecules of water and four molecules of H^+ according to Equation 1.100:[174]

$$4\,\text{Cyt}\,c_{\text{red}} + O_2 + 8\,H^+ \rightarrow 4\,\text{Cyt}\,c_{\text{ox}} + 2H_2O + H^+ \tag{1.100}$$

However, partial metabolism of O_2 occurs prior to its full reduction to water by cytochrome *c* oxidase. Although it is estimated that under normal conditions, 1–2% of O_2 consumed by mitochondria are converted to ROS. This phenomenon called *electron leakage* may be more prevalent in pathophysiological conditions.

The major sources of radical generation within the mitochondria have been identified to be the NADH dehydrogenase and ubiquinone. Figure 1.33 shows the ubiquinone cycle in which ubiquinone (Q) reduces cytochrome *b* through multiple processes that also leads to the oxidation of NADH dehydrogenase. The cycle is coupled to the electron-transfer process that occurs between ubiquinol (QH_2) and cytochrome *c1* via proteins containing Fe–S clusters. At the site of this electron-transfer process, an electron is "leaked" to the O_2 molecule to give $O_2^{\bullet-}$ then subsequently forming H_2O_2. Studies on heart and nonsynaptic brain mitochondria of mammals and birds show that oxygen radicals are generated at complex I in heart and brain mitochondria in States 4 and 3, while complex III (ubiquinone cytochrome *c* reductase) generates radicals only in heart mitochondria and only in State 4.[175] Other sources of ROS in the mitochondria are the dehydrogenases, quinone oxidoreductase, and monoamine oxidase B.

1.7.1.4 Hemoglobin (Hb) Oxygen binds to the heme Fe(II) on a reversible and stable manner and is the basis of Hb function. However, the Fe(II) heme can undergo auto-oxidation (~3 within 24-hour period) to form Fe(III) and $O_2^{\bullet-}$ (Eq. 1.101) and is a common mechanism of oxidative stress in red blood cells.[176]

$$\text{Hb(II)}O_2 \rightarrow \text{Hb}^+ + O_2^{\bullet-} \tag{1.101}$$

1.7.1.5 Nitric Oxide Synthases Nitric oxide synthase catalyzes the production of nitric oxide from L-arginine via an electron flow from NADPH → FAD → FMN → heme → oxygen based on Equation 1.102.[177]

$$\text{L-Arginine} + \frac{3}{2}\,\text{NADPH} + H^+ + 2O_2 \rightarrow \text{citrulline} + \text{NO} + \frac{3}{2}\,\text{NADP}^+ \tag{1.102}$$

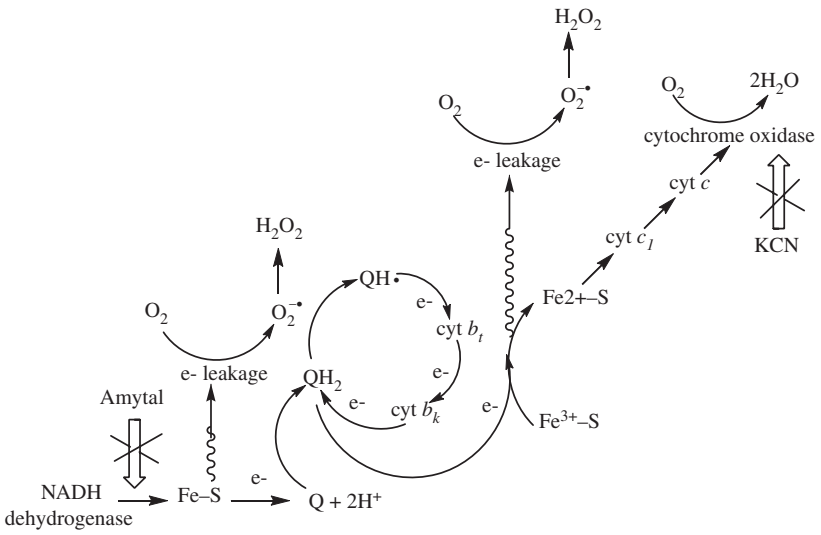


Figure 1.33 The ubiquinone cycle of the mitochondrial electron transport chain showing the formation of reactive oxygen species.

The Fe(III) heme upon reduction by $FMNH_2$ to Fe(II) enables binding to O_2 to form the ferrous-dioxy complex or $Fe(III)O_2^-$ (species 1). Species 1 can presumably further undergo a one-electron reduction by tetrahydrobiopterin (H_4B) to form the iron-peroxo species (species II) and O–O bond cleavage yields water (Figure 1.34) and iron-oxo species which is thought to hydroxylate the guanidino nitrogen of the L-arginine and ultimately leading to the generation of NO• (Figure 1.35).

Under oxidative conditions such as in the presence of $ONOO^-$, the oxidation state for H_4B is altered such that conversion of species 1 to 2 is hampered. The peroxo group of species 1 then decomposes to $O_2^{\bullet-}$ and Fe(III).

1.7.1.6 Cytochrome P450 (CYP) CYP is one of the most important class of enzymes responsible for the oxidation of organic substances using lipids and steroids as well as xenobiotics as substrates.[178,179] The catalytic action of CYP mirrors that of NOS enzymes where the formation of oxo-ferryl (Fe^{IV}=O), species II (shown in Figure 1.34) is the oxidizing form of the heme. Like in NOS, non-reduction of $Fe(III)O_2^-$ results in the production of $O_2^{\bullet-}$.

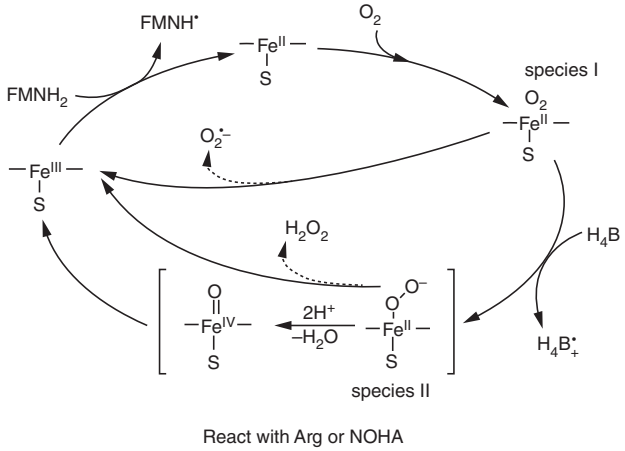


Figure 1.34 Production of superoxide radical anion from nitric oxide synthase. (Adapted with permission from Ref. 177. Copyright 2003 American Chemical Society).

1.7.1.7 **Cyclooxygenase (COX) and Lipoxygenase (LPO)** Arachidonic metabolism can mediate several important cellular events such as inflammation, chemotaxis, and regulation of muscle tone. However, the

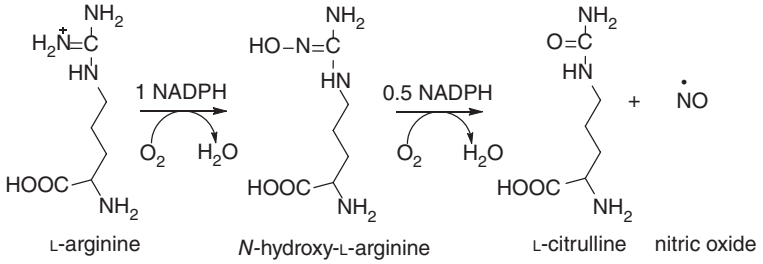


Figure 1.35 Production of nitric oxide from L-arginine, NADPH and O_2.

formation of metabolites such as prostaglandins, thromboxane, and leukotriene generates ROS. The formation of PGG_2 and HpETEs hydroperoxides has been shown to be mediated by COX and LPO. These unstable peroxides can yield $HO^{\bullet}$ and $RO^{\bullet}$ via O-O bond cleavage.[180]

1.7.1.8 Endoplasmic Reticulum (ER) ER is an organelle responsible for protein folding and maturation. Along with Golgi complex, it is involved in the transport of new proteins, lipids, and other small molecules to their proper destination. Recently, ER has been implicated in hypoxia- and diabetes-mediated oxidative stress. During accumulation of newly synthesized unfolded proteins, the unfolded protein response (UPR) is activated and causes a variety of inflammatory and stress signaling responses. The mechanism of radical production from ER was proposed to originate from an enzyme Ero1p, a flavin-containing oxidase, due to its ability to reduce molecular O_2 to yield H_2O_2 when acting on thiol substrates according to Equations 1.103–1.104.[170,181]

$$\text{E-FAD} + 2\,\text{RSH} \rightarrow \text{EFADH}_2 + \text{RSSR} \quad (1.103)$$

$$\text{EFADH}_2 + \text{O}_2 \rightarrow \text{EFAD} + \text{H}_2\text{O}_2 \quad (1.104)$$

Ero1p is an enzyme responsible for the disulfide bond formation in eukaryotic cells under aerobic and anaerobic conditions. The ability of Ero1p to transfer electrons to other small molecules and macromolecular electron acceptor has also been demonstrated.

1.7.2 Non-biochemical Sources

1.7.2.1 Photolytic Shown in Equations 1.105–1.106 is the generation of $O_2^{\bullet-}$ during ionizing radiation of air-saturated sodium formate using stopped-flow radiolysis apparatus on line with a Van de Graaff electron generator at 2-MeV.[182]

$$\begin{aligned} &\text{H}_2\text{O} \rightarrow \text{H}_2\text{O}_2 + \text{H}_3\text{O}^+ + \text{H}^{\bullet} + \text{HO}^{\bullet} + \text{H}_2 + \text{e}_{\text{aq}}^- \\ &\text{H}^{\bullet} + \text{O}_2 \rightarrow \text{HO}_2^{\bullet} \\ &\text{e}_{\text{aq}}^- + \text{O}_2 \rightarrow \text{O}_2^{\bullet-} \qquad 2.3 \times 10^{10}\,\text{M}^{-1}\text{s}^{-1} \end{aligned} \quad (1.105)$$

$$\begin{aligned} &\text{HO}_2^{\bullet} \rightleftharpoons \text{O}_2^{\bullet-} + \text{H}^+ \\ &\text{HCOO}^- + \text{HO}^{\bullet} \rightarrow \text{CO}_2^{\bullet-} + \text{H}_2\text{O} \qquad 2.5\times10^9\,\text{M}^{-1}\text{s}^{-1} \\ &\text{CO}_2^{\bullet-} + \text{O}_2 \rightarrow \text{O}_2^{\bullet-} + \text{CO}_2 \qquad 4.6\times10^9\,\text{M}^{-1}\text{s}^{-1} \end{aligned} \quad (1.106)$$

Superoxide can also be formed in O_2-saturated aqueous formate solution upon short UV irradiation by Xe or Ar lamp. The main process involves photochemical decomposition of water through its dissociation into $HO^{\bullet}$ and $H^{\bullet}$ (Eq. 1.107). In the presence of O_2, electron transfer occurs to produce $O_2^{\bullet-}$ (Eq. 1.108). Moreover, formate ($HCOO^-$) can react with $H^{\bullet}$ or $HO^{\bullet}$ to form a common product $CO_2^{\bullet-}$, where $CO_2^{\bullet-}$ can further reduce O_2 to $O_2^{\bullet-}$ (Eq. 1.109).[183]

$$\text{H}_2\text{O} + h\nu \rightarrow \text{HO}^{\bullet} + \text{H}^{\bullet} \quad (1.107)$$

$$\text{H}^{\bullet+}\,\text{O}_2 \rightarrow \text{HO}_2^{\bullet} = \text{H}^+ + \text{O}_2^{\bullet-} \qquad 1.6\times10^{10}\,\text{M}^{-1}\,\text{s}^{-1} \quad (1.108)$$

$$\begin{aligned} &\text{H}^{\bullet+}\,\text{HCOO}^- \rightarrow \text{H}_2 + \text{CO}_2^{\bullet-} \qquad 1.5\times10^8\,\text{M}^{-1}\,\text{s}^{-1} \\ &\text{HO}^{\bullet+}\,\text{HCOO}^- \rightarrow \text{H}_2\text{O} + \text{CO}_2^{\bullet-} \qquad 2.5\times10^9\,\text{M}^{-1}\,\text{s}^{-1} \\ &\text{CO}_2^{\bullet-+}\,\text{O}_2 \rightarrow \text{CO}_2^{+}\,\text{O}_2^{\bullet-} \qquad 1.0\times10^{10}\,\text{M}^{-1}\,\text{s}^{-1} \end{aligned} \quad (1.109)$$

Photolysis of H_2O_2 solution can also convert $HO^{\bullet}$ and $H^{\bullet}$ to $HO_2^{\bullet}$ *via* reactions shown in Equations 1.110–1.111:[183]

$$\text{H}^{\bullet} + \text{H}_2\text{O}_2 \rightarrow \text{HO}^{\bullet} + \text{H}_2\text{O} \quad (1.110)$$

$$\text{HO}^{\bullet} + \text{H}_2\text{O}_2 \rightarrow \text{HO}_2^{\bullet} + \text{H}_2\text{O} \quad (1.111)$$

UV-photolysis of H_2O_2 yields $HO^{\bullet}$ via O-O bond homolytic cleavage,[184] while photolysis of alkyl disulfides results in C–S and S–S homolytic bond cleavage.[185]

1.7.2.2 Sonochemical Acoustic cavitation involves the nucleation, growth, and violent collapse of gas-filled microbubbles in a liquid. The bubble collapse is associated with the creation of a transient region with very high temperature (>1000 K) and pressure (>100 atm) in pressure. It is known that the collapse of the bubbles is accompanied by the emission of light, a process known as sonoluminescence. Ultrasound-induced pyrolysis of argon-purged water showed formation of $H^{\bullet}$ and $HO^{\bullet}$ using spin-trapping technique.[186,187] Sonolysis in the presence of drugs also known as sonosensitizers can yield $ROO^{\bullet}$ and $RO^{\bullet}$ exhibiting enhanced therapeutic action against cancer cells for example.[188]

1.7.2.3 Photochemical There are three major pathways for the photochemical generation of $O_2^{\bullet-}$ as shown in Figure 1.36: (1) *via* photoionization of a sensitizer molecule which generates hydrated electron (e_{aq}^-) which in turn directly reduces O_2 to $O_2^{\bullet-}$; (2) use of excited-state acceptor (Sen) that can accept electron from a ground-state electron donor such as an amine or other electron-rich substrates to form ($Sen^{\bullet-}$) which then leads to the reduction of O_2 by $Sen^{\bullet-}$ to form $O_2^{\bullet-}$; (3) and through

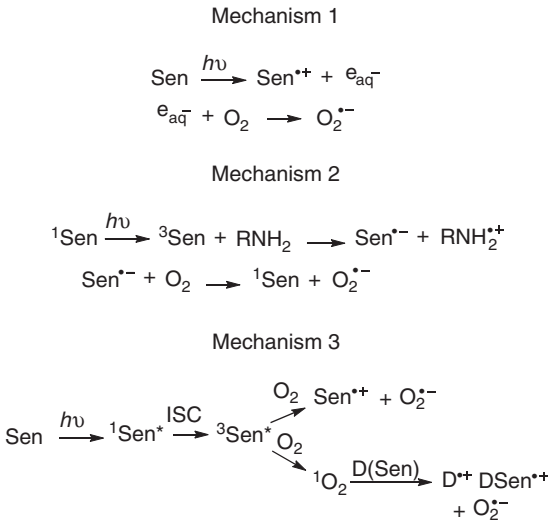


Figure 1.36 Various photochemical mechanisms for the formation of reactive oxygen species.

electron transfer with O_2 or $^1O_2$ by a sensitized excited- or ground-state donor, respectively.[189]

Mechanisms 1, 2, and 3 require O_2 to produce $O_2^{\bullet-}$. For Mechanism 1, tryptophan and other amino acids as well as other aromatic compounds (such as amines, phenols, methoxybenzenes, and indoles) are capable of generating $O_2^{\bullet-}$ under photoionizing conditions in near-UV light. Mechanism 2 involves charge-transfer mechanisms which are very common among flavin and its analogues which usually occurs in the presence of an electron donor such as EDTA. Triplet-state methylene blue in the presence of alkylamines results in electron transfer to generate $O_2^{\bullet-}$. Mechanism 3 shows the formation of $O_2^{\bullet-}$ from $^1O_2$ ($^1O_2$ is generated from O_2 sensitization by rose bengal) using furfuryl alcohol,[190] fullerenes,[191] or quinones[192] as specific $^1O_2$ quenchers.

1.7.2.4 Electrochemical The standard potential of $O_2/O_2^{\bullet-}$, $E^0 = -0.284$V (vs. NHE). Using this potential, $O_2^{\bullet-}$ can be electrochemically generated from one-electron reduction of O_2 in alkaline aqueous solution,[193] DMSO[194,195], or ionic liquids.[196]

1.7.2.5 Chemical Tetramethylammonium salt of $O_2^{\bullet-}$ (Me_4NO_2) can be prepared from solid-state metathesis combination of KO_2 and Me_4NOH with high purity.[197] Also, Me_4NO_2 can be prepared from NH_3 treatment of KO_2 with Me_4NF or reaction of $Me_4NOH{\bullet}5H_2O$ with excess KO_2.[198]

Quinones are active sites of mitochondrial *bc* complex (III) or as active moieties of xenobiotics.[199] One-electron reduction of quinone leads to the formation of semiquinone. In general, reduction of quinone to hydroquinone can be accomplished non-enzymatically *via* two-electron reduction with the reducing equivalents of NADPH, or by one-electron reduction to semiquinone with microsomal or mitochondrial enzymes (Figure 1.37). Semiquinone can reduce O_2 to form $O_2^{\bullet-}$ and the original quinone. The process is repeated until ROS production is at its maximum and semiquinone begins to accumulate, at which time the system becomes depleted with O_2. This process is usually referred to as redox cycling. The diagram below shows the redox cycling of ROS by quinone as mediated by an electron donor, NADPH. Redox cycling has also been observed in ortho-benzoquinones.

Nitric oxide can be generated from chemical sources directly or indirectly by enzymatic or non-enzymatic systems. The most common $NO^{\bullet}$ donors that can directly generate $NO^{\bullet}$ *via* the action of light or heat are metal–NO complexes, *N*-nitrosamines, *N*-hydroxyl nitrosamines, nitrosoimines, nitrosothiols, C-nitrosothiols, and diazetine dioxides. $NO^{\bullet}$ can also be generated indirectly through enzymatic metabolism of organic nitrates/nitrites, guanidines, hydroxyureas, oximes, oxatriazole-5-imines, or furoxans.[200]

Stable $ONOO^-$ solution can be generated directly from ozone and sodium azide,[201] nitrite and H_2O_2,[43] or organic nitrite and H_2O_2.[202] Since 3-*N*-morpholinosydnonimine (SIN-1) comes in solid form, the use of SIN-1 is the most common form of $ONOO^-$ delivery due to its ease of handling. Figure 1.38 shows the proposed decomposition pathway for SIN-1 involves electron-transfer reaction with O_2 to form $O_2^{\bullet-}$. The oxidized SIN-1 intermediate decomposes to form $NO^{\bullet}$. Combination of $NO^{\bullet}$ and $O_2^{\bullet-}$ in solution then yields $ONOO^-$.[203]

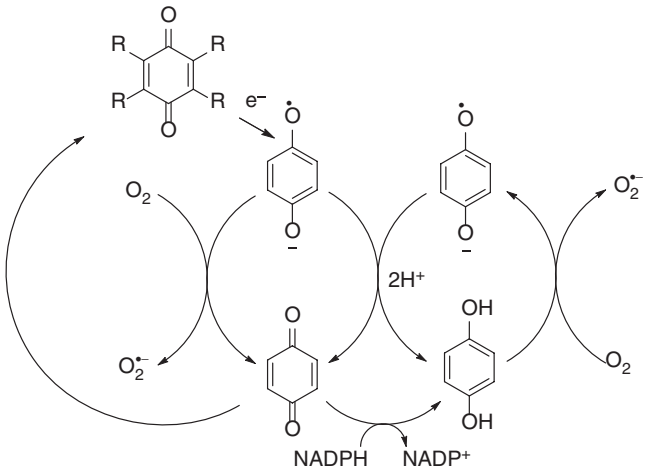


Figure 1.37 NADPH-mediated redox cycling of ROS by quinones.

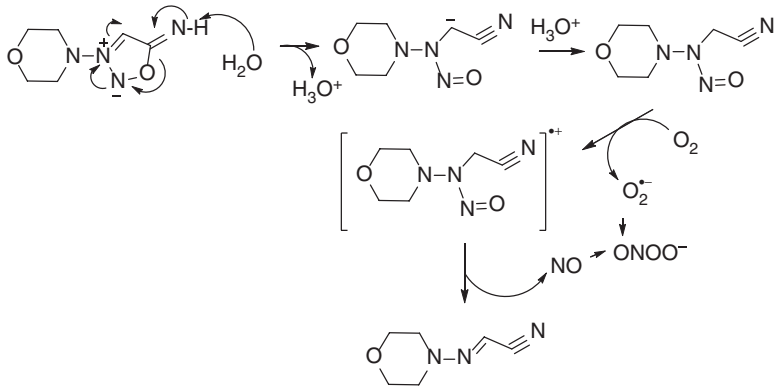


Figure 1.38 Proposed mechanism for the generation of peroxynitrite from SIN-1.

1.8 METHODS OF DETECTION

Reactive species in *in vitro* and *in vivo* systems can be directly or indirectly detected. Due to the instability and short half-lives of the common radicals, reagents are needed for their detection. By exploiting the chemistry of radical addition or electron-transfer reactions to some reagents, one can use this process as an analytical tool to detect ROS production. In particular, the detection of $O_2^{\bullet-}$ is the most relevant since it is the major precursor of most reactive species, and it signals the first sign of oxidative burst in biological systems. However, in *in vitro* and *in vivo* systems where the flux of $O_2^{\bullet-}$ can be below the detection limit of the commonly used analytical techniques, secondary products such as the formation of other ROS, RNS, RSS as well as the formation of biomolecular radicals such as protein or nucleotide radicals can be directly or indirectly detected. Analysis of the primary or secondary addition products of radicals to substrates can be analyzed using various methods such as chromatography, electrochemistry, mass spectrometry, spectrophotometry, or by magnetic resonance spectroscopy.

1.8.1 In Vitro

1.8.1.1 Fluorescence and Chemiluminescence Fluorescence (FL) occurs when light is absorbed by a fluorophore (excitation) with subsequent emission of light, while chemiluminescence (CL) occurs with the emission of light as a result of a chemical reaction, the latter is more sensitive than former by 2 orders of magnitude. Although FL and CL are among the most sensitive techniques for radical detection *in vitro* (*i.e.,* >1 nM), caution is needed for their application. FL and CL probes can detect various ROS/RNS *via* 2-electron oxidation, and therefore, suffer from selectivity and may compete with endogenous intracellular antioxidants such as ascorbate, urate, and thiols. Moreover, these probes can generate $O_2^{\bullet-}$ via formation of an active intermediate after reaction with ROS/RNS. Due to the lack of selectivity to a particular reactive species, FL and CL are more appropriately called redox probes to indicate their general reactivity to various reactive species. Some of the most common FL probes are dichlorodihydrofluorescein ($DCFH_2$), rhodamine (RhH_2), and ethidine (DHE) (Figure 1.39). $DCFH_2$ and RhH_2 react with $O_2^{\bullet-}$ or H_2O_2 poorly, and fluorescence arising from this reaction could be catalyzed by metal ion impurities and therefore are not suitable probes for ROS. Carbonate radical anion and $^{\bullet}NO_2$ are better detected using $DCFH_2$ due to their higher reactivity and higher fluorescence yield; however, this is not true for $HO^{\bullet}$ and HOCl. RhH_2 gives fluorescence with all of the reactive species. Unlike $DCFH_2$ and RhH_2, DHE is highly reactive to $O_2^{\bullet-}$ but yields two fluorescent products: (1) specific to $O_2^{\bullet-}$ (*i.e.,* 2-hydroxyethidium, 2-OH-E^+); and (2) non-specific to $O_2^{\bullet-}$ that can be formed photochemically (E^+). To differentiate between 2-OH-E^+ and E^+, the use of HPLC/FL assay has been suggested and provides unequivocal differentiation of the two products.[204,205] In spite of this complication, DHE is perhaps the most specific FL probe for $O_2^{\bullet-}$ at the moment.

Lucigenin (LC) is the most used CL probe for $O_2^{\bullet-}$ but like $DCFH_2$, it can also generate $O_2^{\bullet-}$ and is not specific for $O_2^{\bullet-}$ because it also gives luminescence in the presence of nucleophiles and reducing agents to form $LC^{\bullet+}$. Addition of $O_2^{\bullet-}$ to $LC^{\bullet+}$ (formed from its enzymatic reduction) forms a dioxetane intermediate that cleaves to form the excited-state *N*-methylacridone which later can emit light (Figure 1.40). Other reductants that can generate $LC^{\bullet+}$ are H_2O_2, flavoproteins, eNOS, NADPH reductases, and cyt P450.[204]

Boronates have been shown to react with $ONOO^-$, HOCl, and H_2O_2 imparting fluorescence but with varying rates of reaction.[206,207] The second-order rate constants show $ONOO^-$ to be the most reactive (~10^5–$10^6\,M^{-1}s^{-1}$) followed by HOCl (~10^3–$10^4\,M^{-1}s^{-1}$)

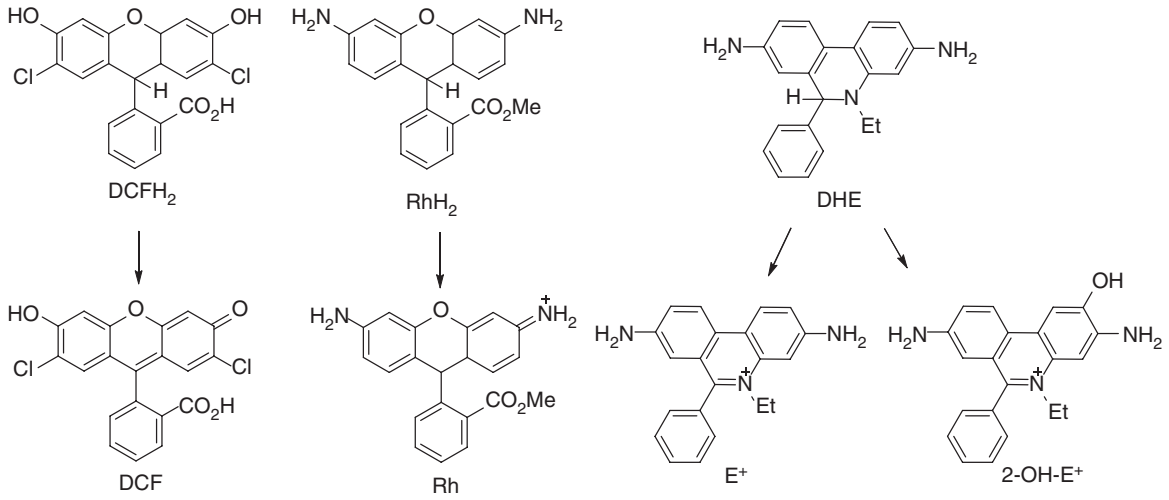


Figure 1.39 Fluorescence probes for ROS and their various products.

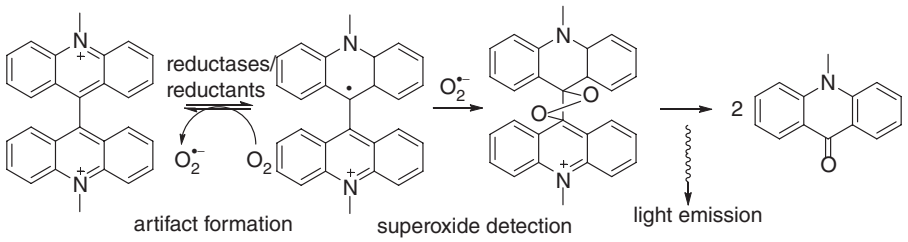
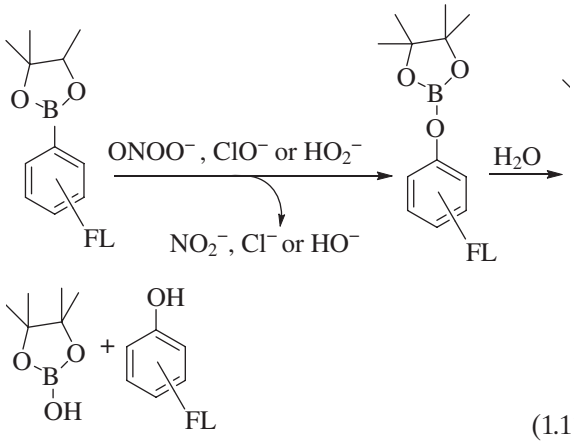


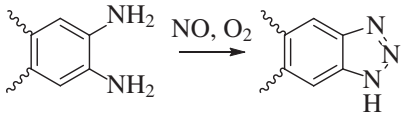
Figure 1.40 Formation of superoxide radical anion from lucigenin$^{\bullet+}$ and its reaction with superoxide resulting in chemiluminescence.

and by H_2O_2 (~2 $M^{-1}s^{-1}$).[207] The mechanism of oxidant reaction to boronates involves nucleophilic addition of the oxidant to the boron atom followed by the heterolytic cleavage of the X–O bond to form the respective ion. Intramolecular rearrangement of the B–O yields the final fluorescent phenolic products (Eq. 1.112).



(1.112)

For NO$^{\bullet}$ detection, fluorescence probes have been employed such as those containing the vicinal diamines (e.g., fluorescein based, DAF-2; rhodamine-based, DAR-4M; BODIPY-based, DAMBO; and cyanine-based, DACs). Reaction of NO$^{\bullet}$ with diamine proceeds in the presence of oxygen to form the highly fluorescent *N*-nitrosated product (Eq. 1.113).[208]



(1.113)

The reaction of NO$^{\bullet}$ with ozone imparts chemiluminescence and has been exploited to detect NO$^{\bullet}$ formation. This ozone-based detection of NO$^{\bullet}$ in the gas phase involves light emission along with the formation of $^{\bullet}NO_2$ (Eqs. 1.114 and 1.115).[209] This technique, although very sensitive, requires the use of an NO$^{\bullet}$ analyzer equipped with ozone generator and sensitive photomultiplier tube and purging of NO$^{\bullet}$ from the sample is required.

$$NO^{\bullet} + O_3 \rightarrow NO_2^{*} + O_2 \qquad (1.114)$$

$$NO_2^{*} \rightarrow NO_2 + h\nu \qquad (1.115)$$

1.8.1.2 UV–Vis Spectrophotometry and HPLC Several assays for $O_2^{\bullet-}$ based on 1-electron transfer reaction have been employed due to the high rate constants observed for this type of reaction. Cytochrome (cyt) c^{3+} can be reduced to cyt c^{2+} by $O_2^{\bullet-}$ and can be detected spectrophotometrically. Due to the relatively low rate constant of this reaction ($\sim 10^5 M^{-1} s^{-1}$), the amount of $O_2^{\bullet-}$ generated can be underestimated. Another popular spectrophotometric technique for $O_2^{\bullet-}$ detection is using p-nitrotetrazolium blue (NBT) which forms a colored monoformazan anion. However, the use of cyt c and NBT has limitations such that their reduction is not specific to $O_2^{\bullet-}$ and cannot be applied in *in vivo* systems.[210]

Nitric oxide can be measured by using reduced hemoglobin according to Equation 1.116. Oxidation of hemoglobin to methemoglobin can be detected spectrophotometrically with a detection threshold of 1 nmol.

$$NO^{\bullet} + Hb\left(Fe^{2+}\right)O_2 \rightarrow Hb\left(Fe^{3+}\right) + NO_3^- \qquad (1.116)$$

Also, by using thioproline, $NO^{\bullet}$ can be trapped and the adduct formed can be detected using mass spectroscopy.[211] Nitrite as an oxidation end product of $NO^{\bullet}$ can also be detected spectrophotometrically using Griess assay. Nitrite is detected as red, pink coloration produced from the reaction of sulfanilic acid with NO_2^- where the product formed reacts further with an azo dye (alpha-naphthylamine) giving a colored product. In systems where NO_3^- are present, prior reduction of NO_3^- to NO_2^- is required to obtain the total NO_2^-/NO_3^- content by treatment of the sample with sodium formate and nitrate reductase.[212]

Hypochlorous acid can be trapped by taurine forming taurine chloramine. Taurine chloramine can then be spectrophotometrically assayed using 5-thio-2-nitrobenzoic acid (TNB)[213] but has some limitations such as the need to predetermine the chloramine concentration for accurate measurements, poor selectivity as other oxidants can bleach TNB, and the light sensitivity of TNB. Iodide was proposed to be an alternative to TNB and by using 3,3′,5,5′-tetramethylbenzidine (TMB) as chromophore due to its ability to be oxidized by hypoiodous acid with a sensitivity of 1 μM of taurine chloramine. Dihydrorhodamine was also used as chromophore giving 10-fold greater sensitivity than TMB.[214]

Other radicals such as $HO^{\bullet}$, $^{\bullet}NO_2$, or $HO_2^{\bullet}$ have been shown to form adducts with various substrates such as amino acids, DNA bases, or lipids *via* hydroxylation, nitration, and hydroperoxide formation, respectively, which can be detected using a variety of analytical methods such as HPLC, electrochemical, spectrophotometric, or by MS. Hydroxyl radical for example adds to 8-hydroxyguanine of the DNA to yield the 8-hydroxy-2-deoxygianosine (8-OHdG) which can be isolated and analyzed using HPLC/electrochemical methods.[215] Recently, more improved methods using HPLC/electrochemical detection for hydroxylation were proposed using 4-hydroxybenzoic acid and terephthalate assays which do not have the drawbacks associated with the use of salicylate or phenylalanine.[216] Using tandem mass spectroscopic techniques, nitration of amino acid residues in peptides[217] has been demonstrated, while proteomic approach has been successful in identifying nitration in proteins.[218,219]

Ferrous oxidation-xylenol orange (FOX) assay has been used as a conventional technique for hydroperoxide formation in lipids,[220,221] and peptide/protein systems.[27,222,223] FOX assay technique uses the Fenton chemistry to generate the $HO^{\bullet}$ from the O–O homolytic cleavage from the ROOH which decolorizes the xylenol orange dye. RNS adduct of lipids has been characterized using HPLC coupled with UV and MS detection.[224] Malonaldehyde (MDA), being one of the end-products of lipid hydroperoxide formation, can be measured using TBARS assay with thiobarbituric acid (TBA) as a reagent. Caution is required in interpreting TBARS data since MDA participates in other reactions other than TBA and is not exclusively formed from lipid peroxidation. Moreover, MDA is only formed from a particular lipid peroxidation process out of a myriad of several lipid peroxidation decomposition reactions.[225] Analysis of F_2-isoprostanes (F_2-IPs) is a more reliable marker of lipid peroxidation which possesses a 1,3-dihydroxycyclopentane ring with the OH groups in the *syn* position and is mainly formed from the arachidonic acid oxidation. Analysis of F_2-IPs can be carried *ex vivo* using LC/MS/MS or GC/MS.[48,226]

1.8.1.3 Immunochemical Formation of macromolecular radical systems such as protein and DNA radicals is a relevant intermediate for the initiation of oxidative stress in biological systems. Nitrone spin traps, for example 5,5,dimethyl pyrroline *N*-oxide (DMPO), add to protein radicals to form a longer-lived protein spin adduct. This radical adduct can later form the diamagnetic analogue; nitrone–protein adduct (formed *via* a variety of oxidative pathways mostly mediated by heme iron centers) which can be detected at 1 μM sensitivity using polyclonal antibodies against DMPO coupled to octanoic acid antiserum. This immune-spin-trapping (ISP)[227] approach combines the specificity of spin trapping to free radical formation and antigen–antibody interactions (Figure 1.41). Coupled with MS/MS technique, one would be able to also identify the specific site/s of radical formation. Immunochemical detection using ISP has been employed in various radical

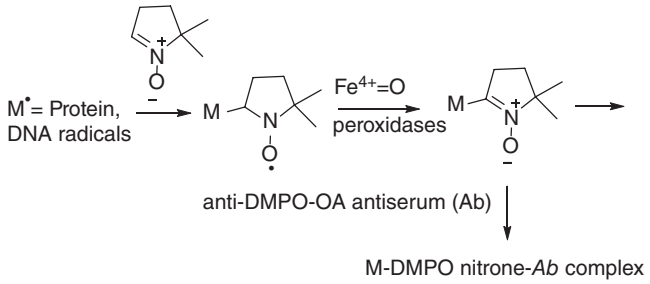


Figure 1.41 Immuno-spin trapping of macromolecular radicals using DMPO and anti-DMPO octanoic acid antiserum.

systems formed from hemoglobin-tyrosyl,[228] myoglobin-tyrosyl,[229] Cu,Zn-SOD,[230] thyroid peroxidase,[231] catalase-peroxidase,[232] and DNA.[233–235]

1.8.1.4 **Electron Paramagnetic Resonance (EPR) Spectroscopy** EPR spectroscopy exploits the magnetic moment of an electron through absorption of microwave radiation in the presence of external magnetic field. As shown in Figure 1.42, there are three major approaches for the detection of $O_2^{\bullet-}$ using EPR and various probes, that is, (1) spin quenching (or spin-loss) using trityl; (2) spin formation using hydroxylamine; (3) spin trapping using nitrones. The use of trityl involves loss of signal and the latter two involve signal formation. Due to the inherent stability of trityl radicals, they have been employed as probes for the detection of $O_2^{\bullet-}$. The most common are the triarylmethyl (trityl)-based radicals[236–238] which can undergo electron-transfer reaction with $O_2^{\bullet-}$ to yield O_2 and the EPR silent trityl anion. The synthetic trityl radicals, TAM OX063 and perchlorotriphenylmethyl (PCM-TC), have been shown to give high reactivity to $O_2^{\bullet-}$ with second-order rate constants of 3.1×10^3 and $8.3\times10^8\,M^{-1}s^{-1}$, respectively.[236,237] Trityl radicals show inertness toward a majority of the common oxido-reductant species; however, they exhibit reactivity with other radical species, such as $HO_2^{\bullet}$, $RO_2^{\bullet}$, and $HO^{\bullet}$.[237]

Although trityls offer some degree of specificity to $O_2^{\bullet-}$, the loss of signal also brings concern about other unknown factors that can result in the loss of signal, and therefore, other non-EPR technique is recommended to confirm the results from using trityl as reagent. A spin-generating system uses diamagnetic probes such as hydroxylamines and nitrone spin traps which involves electron-transfer or addition reactions with $O_2^{\bullet-}$, respectively, forming an EPR-detectable paramagnetic aminoxyl (or commonly called nitroxides) species. Hydroxylamines are oxidized by $O_2^{\bullet-}$ *via* a simple electron-transfer mechanism to yield a paramagnetic aminoxyl species and H_2O_2. Figure 1.43 shows the commonly used hydroxylamines, TPO-H,

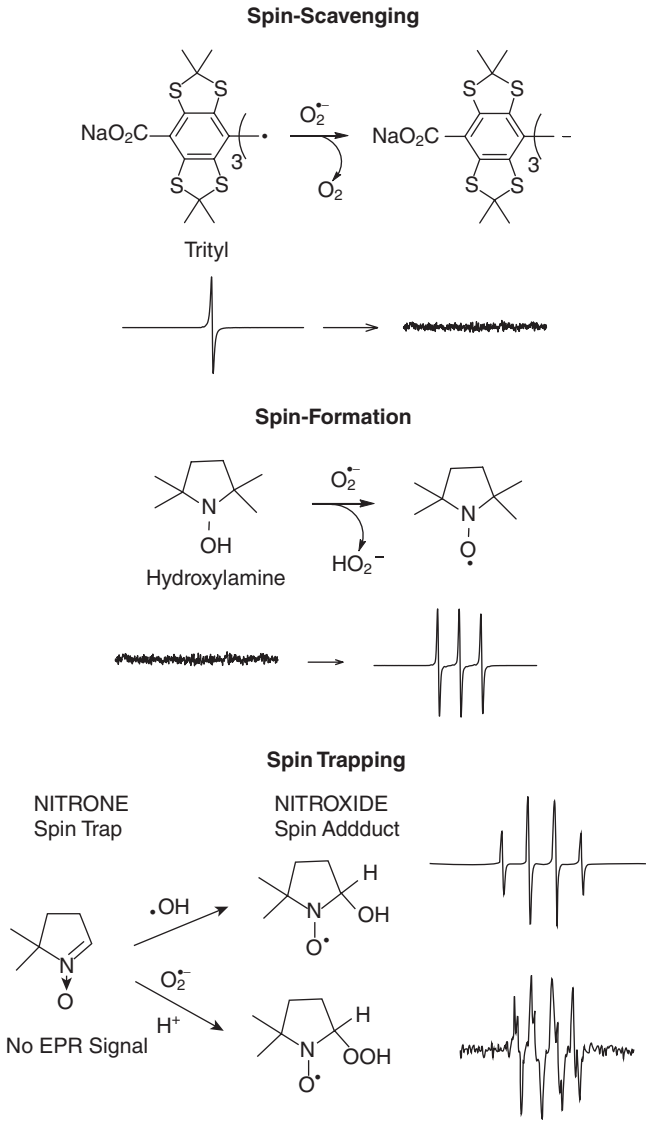


Figure 1.42 Radical detection using EPR spectroscopy and various radical probes.

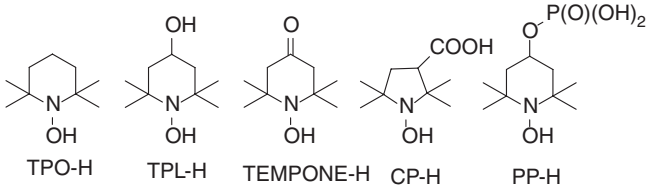
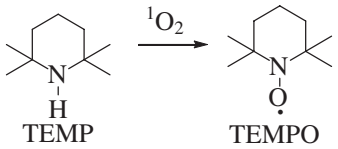


Figure 1.43 Various *N*-hydroxy-pyrrole or piperidine derivatives used as probes for superoxide.

TPL-H, TEMPONE-H[239], CP-H[240], and PP-H[241] which are *N*-hydroxy-pyrrole or piperidine derivatives able to react with $O_2^{\bullet-}$. Rate constants for hydroxylamine probe reaction with $O_2^{\bullet-}$ are dependent on the structure of the

probe. In the case of the negatively charged probe, PP-H, its rate of reaction to $O_2^{\bullet-}$ was found to be slower with $k = 840 \pm 60\,M^{-1}\,s^{-1}$ due mostly to repulsive effect, while the neutral probes, TPO-H and TPL-H, have higher rate constants in the range of $1–2 \times 10^3\,M^{-1}\,s^{-1}$.[107] The redox reaction of $O_2^{\bullet-}$ with the hydroxylamine produces H_2O_2 and can be considered an artifactual source of other ROS. Since other ROS/RNS species as well as metal ions and O_2 can also give the exact same EPR triplet signal, caution should be practiced in data interpretation using hydroxylamine probes.

Detection of $^1O_2$ can be accomplished using the amine 2,2,6,6-tetramethyl-4-piperidone (TEMP). Reaction of $^1O_2$ with TEMP leads to the formation of the nitroxide 2,2,6,6-tetramethyl-4-piperidone-*N*-oxyl (TEMPO) which can be detected using EPR as shown in Equation 1.117.[242]



(1.117)

Spin traps are nitrone-based molecules. Although hydroxylamines exhibit 10- to 1000-fold higher reactivity to $O_2^{\bullet-}$ than the nitrones, the paramagnetic species generated from hydroxylamine does not allow discrimination between the different radicals generated.[241] Spin traps, however, add to a free radical at its α-carbon (C-2) position to form an aminoxyl adduct (or spin adduct), except that the signal is more complex than the ones observed from hydroxylamines.[243] The complex spectrum of the spin adduct is due to the presence of a β-H and the nature of the radical moiety, and is the basis for their popularity not only in free radical detection but also in their identification. Shown in Figure 1.44 are the commonly used spin traps and are divided into two major classes, the cyclic nitrones, 5,5-dimethyl-1-pyroline *N*-oxide (DMPO), 5-(ethoxycarbonyl)-5-methyl-1-py rroline *N*-oxide (EMPO), and 5-(diethoxyphosphoryl)-5-methyl-1-pyrroline *N*-oxide (DEPMPO), and the linear, *N-tert*-Butyl-α-phenylnitrone (PBN). Aside from $O_2^{\bullet-}$, other radicals that can also be identified using spin trapping are $HO^{\bullet}$, $RO^{\bullet}$, $RS^{\bullet}$, $^{\bullet}NO_2$, $CO_3^{\bullet-}$, $CO_2^{\bullet-}$, $N_3^{\bullet-}$, etc. The half-life of the spin adducts varies significantly which range from seconds to hours depending on the type of the radical and nitrone used. The least stable are the $O_2^{\bullet-}$ adducts of DMPO and PBN with a half-life of <1 minute in aqueous solution. However, C-5 derivatized spin traps such as EMPO and DEPMPO exhibit longer $O_2^{\bullet-}$ adduct half-lives of ~8 and ~14 minutes, respectively. One major disadvantage of this technique, despite the improved $O_2^{\bullet-}$ adduct half-lives, is

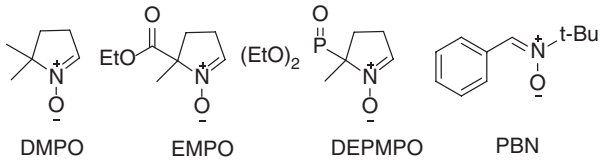


Figure 1.44 Commonly used spin traps for radical detection and identification.

the slow reactivity of these spin traps with $O_2^{\bullet-}$ with rate constants ranging from <1–10 $M^{-1}\,s^{-1}$ which requires the use of high concentrations (typically 10-100 mM) of these reagents in solution for $O_2^{\bullet-}$ detection. However, other radicals exhibit significantly fast reactivity and long adduct half-lives with spin traps.

Spin trapping has been employed to detect $O_2^{\bullet-}$ from xanthine oxidase,[236,244] the mitochondrial ETC,[245,246] and NADPH oxidase.[247] Nitrones have also been successfully used to detect $O_2^{\bullet-}$ generation in human epithelial cells,[248] human neutrophils,[249] reperfused cardiac tissue,[250] and small animals using *ex vivo* techniques.[251,252] *Ex vivo* spin trapping was also demonstrated in ischemia-reperfusion studies where the spin trap was administered to the animals before the onset of ischemia. Reperfusates were then collected and radical adduct generation was detected by EPR spectroscopy.[250,253]

Nitric oxide does not add to nitrone spin traps, but they undergo redox reaction with nitronyl nitroxides (NN) and addition reaction with iron-thiocarbamate complexes with fast rates of reaction whose products are detectable by EPR. Reaction of $NO^{\bullet}$ with NN is an oxidation process, while that of $O_2^{\bullet-}$ reaction with hydroxylamine is a reduction one. There are two commonly used NNs, the 2-phenyl-4,4,5,5-tetramethylimidazoline-l-oxyl 3-oxide (PTIO) and its water-soluble analogue 2-(4-carboxyphenyl)-4,4,5,5-tetramethylimidazoline-1-oxyl 3-oxide (C-PTIO) (Figure 1.45).

Nitric oxide reacts with NN via addition reaction to the nitroxyl-O and subsequent liberation of $^{\bullet}NO_2$ to form the imino nitroxide (IN) as shown in Figure 1.45. The detection of $NO^{\bullet}$ through the use of NN shows clear distinction between the spectral profile imparted by the NN *versus* the IN product formed (Figure 1.46). By virtue of symmetry, the spectral profile of NN is characterized by two equivalent N hyperfine splitting constants with $a_{N1,3} = 8.2$ G, while the IN gives asymmetrical product with the two nitrogens giving two different hfscs of $a_{N1} = 9.8$ G and $a_{N3} = 4.4$ G. The rate constant for the reaction of $NO^{\bullet}$ with NN is in the order of $\sim 10^3\,M^{-1}\,s^{-1}$ which is fast enough to compete with O_2 but not with $O_2^{\bullet-}$. Moreover, nitroxyl (HNO) also reacts with NN to form the similar IN product and that the $^{\bullet}NO_2$ formed can participate with other reactions involving NN and

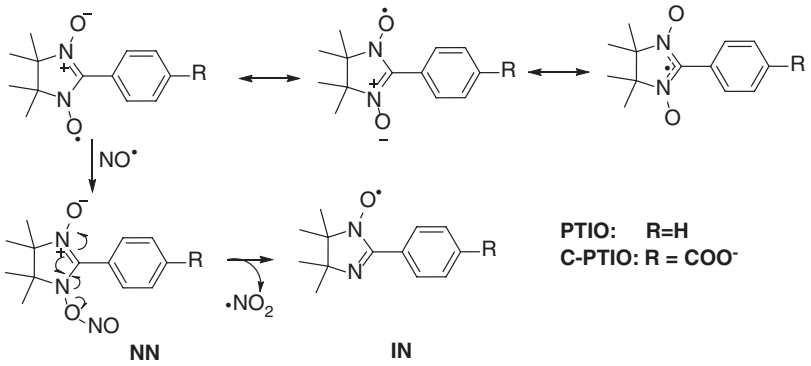


Figure 1.45 Reaction of nitric oxide with nitronyl nitroxides (NN), PTIO and C-PTIO, to form the imino nitroxide (IN).

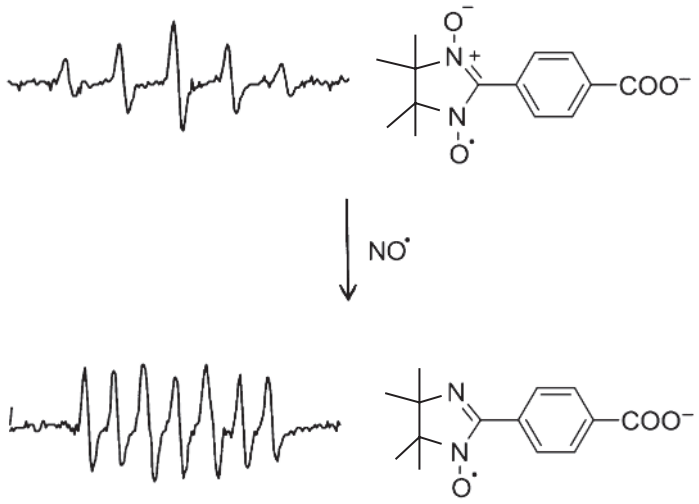


Figure 1.46 EPR spectrum of nitronyl nitroxides (NN) and imino nitroxide (IN) after reaction with NO•. (Adapted with permission from Ref. 254. Copyright 2010 American Chemical Society).

therefore requires careful consideration in the interpretation of the signal formed.[254,255] One main disadvantage of NN as probes for NO• is their ability to be reduced to EPR-silent hydroxylamine by reductants such as ascorbate or metal ions.

Several NO• traps such as Fe^{2+}-dithiocarbamate complexes have been developed that allow NO• detection using EPR (Figure 1.47). This technique was first introduced by Vanin et al.[256–258] *In vivo* EPR experiments using mice showed that NO• trapping by the hydrophobic Fe^{2+}-DETC is more efficient than by the hydrophilic Fe^{2+}-MGD due to the higher stability of the latter in animal tissues.[259] The redox state of Fe-dithiocarbamates plays a critical role in the detection of NO•. Under aerobic conditions, Fe^{2+} complex can be readily oxidized to form Fe^{3+}-dithiocarbamate. Reaction of ferric complex with NO• forms the EPR-silent NO-Fe^{3+}-MGD complex but can be converted to an EPR-detectable NO–Fe^{2+}-MGD by NO• itself with 50% yield and by reductants such as ascorbate, hydroquinone, or cysteine with conversion efficiency of up to 99.9%. The use of iron carbamate complexes involves pre-mixing of $FeSO_4$ with excess dithiocarbamate co-ligand. Water-insoluble $Fe(DETC)_2$ can be introduced as suspension with serum albumin[260] and has been reported to measure NO• in porcine aorta with high sensitivity of 10 pmol/ml. Detection of NO• in blood vessels as well as human umbilical endothelial cells has been successfully demonstrated using colloidal Fe^{2+}-DETC prepared by mixing DETC and Fe^{2+} in concentrated Krebs–HEPES solution.[261,262] Compared when using NN as probe for NO•, Fe dithiocarbamate complexes are better probes for the detection of NO• due to the stability of the adducts formed. Caution should be observed however since iron complexes also have been

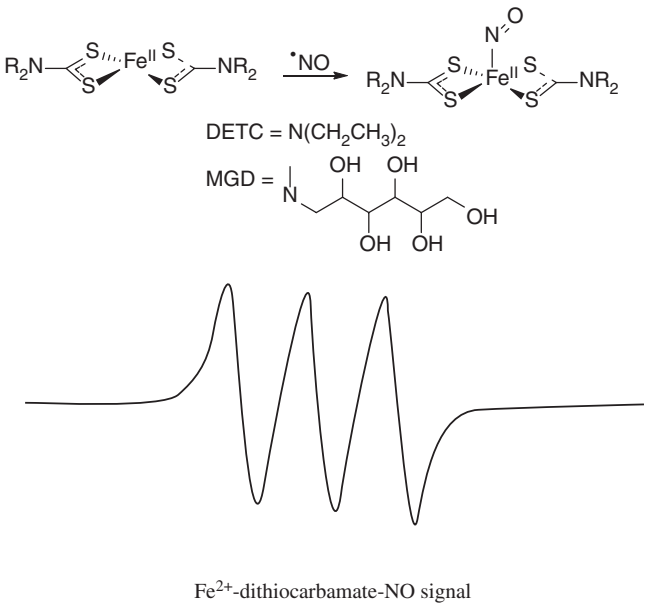


Figure 1.47 Complexation of nitric oxide with iron(II) dithiocarbamates, Fe-DETC and Fe-MGD, giving a triplet EPR signal.

shown to detect HNO, nitrite, and S-nitrosothiols. Dithiocarbamates have potential to chelate metals and may act as enzyme inhibitors. Through the use of NOS inhibitors, the triplet signal can be integrated to represent NOS-derived NO•.[263] Nitric oxide can be trapped by hemoglobin/myoglobin (Hb) as well and can be detected using EPR but with the disadvantage of cooling the sample to ~100 K to allow observation of the signal thus making Hb impractical for real-time monitoring of NO• production but proved useful in determining NO• production in tissues. However, deoxygenated ferrous heme forms HbNO and is detectable by EPR at normal conditions, and the complex formed is very stable.[263]

1.8.2 In Vivo

Formation of reactive species *in vivo* is conventionally determined through analysis of biomarkers by using various methods such as histochemical, immunocytochemical, or EPR imaging. It should be noted that samples taken *in vivo* can be analyzed using the same techniques mentioned above employed for the formation of reactive species in *in vitro*.

1.8.2.1 Histochemical Protein carbonyls are biomarkers of protein oxidation, and their detection can be accomplished by their derivatization using dinitrophenyldrazine to form the protein-bound hydrazone and by using the anti-2,4-dintirophenyl antibody. Another approach is through the use of biotin-hydrazide in which the protein-bound acyl hydrazone is detected by the enzyme-linked avidin or streptavidin.[264]

1.8.2.2 Immunocytochemical Methods Nitrotyrosine, lipid peroxidation end products, and DNA damage can be visualized in tissues using monoclonal or polyclonal antibodies for nitrotyrosine, HNE, and 8-OHG, respectively.[264,265] Nitrated tyrosine has been considered as biochemical marker of ONOO-induced damage to proteins and lipids. By employing two-dimensional polyacrylamide gel electrophoresis (2DE) and western blotting, coupled with mass spectroscopy, targets of protein nitration and HNE modification have been determined in protein systems.[218]

1.8.2.3 Low-frequency EPR Imaging The availability of low-frequency EPR instrumentation could limit the application of radical imaging to many investigators; however, it provides direct visualization of probe response to ROS formation or O_2 concentrations in whole animals.[266,267] The method involves the use of low-frequency, highly sensitive spectrometers, operating between 200 MHz and 1.5 GHz and paramagnetic probes. As mentioned earlier, probes such as nitroxides[250] and trityls react with ROS and show characteristic spectral behavior, that is, signal formation or its disappearance, respectively. Since ROS production has an inverse correlation with O_2 consumption, probes that respond to the pO_2 are very desirable such as trityl,[268] charcoal,[269] and pthalocyanines,[270,271] the latter two are stable enough from being metabolized. Significant advancements have already been achieved in the development of highly sensitive detectors, data acquisition, and analysis modalities. *In vivo* imaging of NO• has also been achieved using commonly use iron-dithiocarbamate spin traps.[272]

1.8.2.4 In Vivo Spin Trapping–Ex vivo EPR Measurement *In vivo* spin trapping of radical metabolites has been extensively employed using the commonly used spin traps, DMPO, PBN, or POBN. However, due to the susceptibility of the radical adducts to be reduced to diamagnetic hydroxylamine species, post-treatment of the samples is needed to re-oxidize the hydroxylamine back to the EPR-detectable nitroxide using mild oxidants such as potassium ferricyanide or bubbling with O_2. Carbon- or S-centered radicals have been detected from blood or biles samples after systemic injection of the xenobiotics. Spin traps have been extensively employed for the detection of transient radicals in animals.[251,273,274]

1.8.2.5 Immuno-spin Trapping Free radical production had been implicated in macromolecule radical

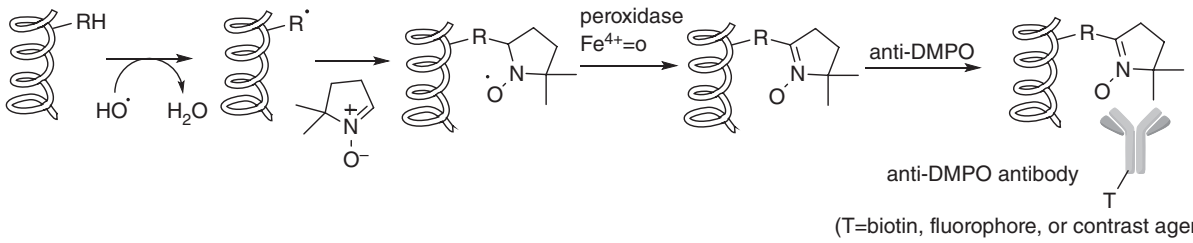


Figure 1.48 Mechanism of immune-spin-trapping reaction showing the formation of DMPO-macromolecular adduct and its binding to anti-DMPO antibody.

formation. Immuno-spin-trapping technique uses DMPO as spin trap to react with macromolecule radical to form a highly stable DMPO–protein or DMPO–nucleotide adduct. As shown in Figure 1.48, these DMPO–macromolecule adducts are different from a typical nitroxyl spin adduct as the former are oxidized nitroxides forming the conjugated DMPO through mild oxidation by ferryl or peroxidase. DMPO–macromolecule conjugate is a highly stable adduct which makes it an ideal antigen allowing for its detection in biological systems such as organelles, cells, tissues, and whole animals by binding to DMPO monoclonal antibody. In protein systems, DMPO–macromolecule adduct could be identified using mass spectrometry, while in cells and tissues, DMPO–macromolecule adduct could be detected using heterogenous immunoassay and confocal microscopy techniques using anti-DMPO-antibody tethered to a biotin and fluorophore moiety, respectively. The use of anti-DMPO conjugated to MRI gadolinium contrast agent made it possible to image DMPO–macromolecule adduct localization in tissues of whole animal.[275–277]

REFERENCES

1. Lelieveld, J. Atmospheric chemistry: a missing sink for radicals. *Nature*. **2010**, *466*, 925–926.
2. Baumgarten, M., Muellen, K. Radical ions: where organic chemistry meets materials sciences. *Top. Curr. Chem.* **1994**, *169*, 1–103.
3. Halliwell, B., Gutteridge, J.M.C. *Free Radicals in Biology and Medicine*, 4th ed. Oxford University Press, New York, **2007**.
4. Gomberg, M. An instance of trivalent carbon: triphenylmethyl. *J. Am. Chem. Soc.* **1900**, *22*, 757–771.
5. Adam, F.C., Weissman, S.I. Electron spin resonance and electronic structure of triphenylmethyl. *J. Am. Chem. Soc.* **1958**, *80*, 2057–2059.
6. Kazzaz, J.A., Xu, J., Palaia, T.A., Mantell, L., Fein, A.M., Horowitz, S. Cellular oxygen toxicity. Oxidant injury without apoptosis. *J. Biol. Chem.* **1996**, *271*, 15182–15186.
7. Song, Y., Wagner, B.A., Lehmler, H.J., Buettner, G.R. Semiquinone radicals from oxygenated polychlorinated biphenyls: electron paramagnetic resonance studies. *Chem. Res. Toxicol.* **2008**, *21*(7), 1359–1367.
8. Fu, H., Zhou, Y.-H., Chen, W.-L., Deqing, Z.-G., Tong, M.-L., Ji, L.-N., Mao, Z.-W. Complexation, structure, and superoxide dismutase activity of the imidazolate-bridged dinuclear copper moiety with beta -cyclodextrin and its guanidinium-containing derivative. *J. Am. Chem. Soc.* **2006**, *128*(15), 4924–4925.
9. Valgimigli, L., Amorati, R., Fumo, M.G., DiLabio, G.A., Pedulli, G.F., Ingold, K.U., Pratt, D.A. The unusual reaction of semiquinone radicals with molecular oxygen. *J. Org. Chem.* **2008**, *73*(5), 1830–1841.
10. Sawyer, D.T., Valentine, J.S. How super is superoxide? *Acc. Chem. Res.* **1981**, *14*(12), 393–400.
11. Evans, M.G., Uri, N. Dissociation constant of hydrogen peroxide and the electron affinity of the HO_2 radical. *J. Chem. Soc., Faraday Trans.* **1949**, *45*, 224–230.
12. Liu, G.-F., Filipovic, M., Ivanovic-Burmazovic, I., Beuerle, F., Witte, P., Hirsch, A. High catalytic activity of dendritic C_{60} monoadducts in metal-free superoxide dismutation. *Angew. Chem. Int. Ed.* **2008**, *47*(21), 3991–3994.
13. Ali, S.S., Hardt, J.I., Quick, K.L., Sook Kim-Han, J., Erlanger, B.F., Huang, T.-T., Epstein, C.J., Dugan, L.L. A biologically effective fullerene C_{60} derivative with superoxide dismutase mimetic properties. *Free Radic. Biol. Med.* **2004**, *37*(8), 1191–1202.
14. Osuna, S., Swart, M., Sola, M. On the mechanism of action of fullerene derivatives in superoxide dismutation. *Chem. Eur. J.* **2010**, *16*(10), 3207–3214, S3207/1–S3207/33.
15. Tietze, D., Tischler, M., Voigt, S., Imhof, D., Ohlenschlaeger, O., Goerlach, M., Buntkowsky, G. Development of a functional *cis*-prolyl bond biomimetic and mechanistic implications for nickel superoxide dismutase. *Chem. Eur. J.* **2010**, *16*(25), 7572–7578.
16. Batinic-Haberle, I., Spasojevic, I., Stevens, R.D., Hambright, P., Neta, P., Okado-Matsumoto, A., Fridovich, I. New class of potent catalysts of O $2^{\bullet-}$ dismutation. Mn (III) ortho-methoxyethylpyridyl- and di-ortho-methoxyethylimidazolyl porphyrins. *Dalton Trans.* **2004**, *11*, 1696–1702.
17. Riley, D.P., Weiss, R.H. Manganese macrocyclic ligand complexes as mimics of superoxide dismutase. *J. Am. Chem. Soc.* **1994**, *116*(1), 387–388.
18. Nagano, T., Hirano, T., Hirobe, M. Superoxide dismutase mimics based on iron *in vivo*. *J. Biol. Chem.* **1989**, *264*(16), 9243–9249.

19. Ivanovic-Burmazovic, I., van Eldik, R. Metal complex-assisted activation of small molecules. From NO to superoxide and peroxides. *Dalton Trans.* **2008**, 5259–5275.
20. Spasojevic, I., Batinic-Haberle, I., Reboucas, J.S., Idemori, Y.M., Fridovich, I. Electrostatic contribution in the catalysis of O 2· _ dismutation by superoxide dismutase mimics. Mn^{III}TE-2-PyP^{5+} versus $Mn^{III}Br_8$T-2-PyP^{+}. *J. Biol. Chem.* **2003**, *278*(9), 6831–6837.
21. Krishna, M.C., Grahame, D.A., Samuni, A., Mitchell, J.B., Russo, A. Oxoammonium cation intermediate in the nitroxide-catalyzed dismutation of superoxide. *Proc. Natl. Acad. Sci. U.S.A.* **1992**, *89*(12), 5537–5541.
22. Krishna, M.C., Russo, A., Mitchell, J.B., Goldstein, S., Dafni, H., Samuni, A. Do nitroxide antioxidants act as scavengers of superoxide radical or as SOD mimics? *J. Biol. Chem.* **1996**, *271*(42), 26026–26031.
23. Chern, C.-I., DiCosimo, R., De Jesus, R., San Filippo, J. Jr. A study of superoxide reactivity. Reaction of potassium superoxide with alkyl halides and tosylates. *J. Am. Chem. Soc.* **1978**, *100*(23), 7317–7327.
24. Davico, G.E., Bierbaum, V.M. Reactivity and secondary kinetic isotope effects in the S_N2 reaction mechanism: dioxygen radical anion and related nucleophiles. *J. Am. Chem. Soc.* **2000**, *122*(8), 1740–1748.
25. Das, A.B., Nagy, P., Abbott, H.F., Winterbourn, C.C., Kettle, A.J. Reactions of superoxide with the myoglobin tyrosyl radical. *Free Radic. Biol. Med.* **2004**, *48*(11), 1540–1547.
26. Winterbourn, C.C., Parsons-Mair, H.N., Gebicki, S., Gebicki, J.M., Davies, M.J. Requirements for superoxide-dependent tyrosine hydroperoxide formation in peptides. *Biochem. J.* **2004**, *381*(Pt 1), 241–248.
27. Field, S.M., Villamena, F.A. Theoretical and experimental studies of tyrosyl hydroperoxide formation in the presence of H-bond donors. *Chem. Res. Toxicol.* **2008**, *21*(10), 1923–1932.
28. Sawyer, D.T., Stamp, J.J., Menton, K.A. Reactivity of superoxide ion with ethyl pyruvate, a-diketones, and benzil in dimethylformamide. *J. Org. Chem.* **1983**, *48*, 3733–3736.
29. Rene, A., Abasq, M.-L., Hauchard, D., Hapiot, P. How do phenolic compounds react toward superoxide ion? A simple electrochemical method for evaluating antioxidant capacity. *Anal. Chem.* **2010**, *82*, 8703–8710.
30. Salazar, R., Navarrete-Encina, P.A., Squella, J.A., Camargo, C., Nunez-Vergara, L.J. Reactivity of C4-indolyl substituted 1,4-dihydropyridines toward superoxide anion ($O2^{\bullet}$) in dimethylsulfoxide. *J. Phys. Org. Chem.* **2009**, *22*, 569–577.
31. Winterbourn, C.C., Metodiewa, D. Reactivity of biologically important thiol compounds with superoxide and hydrogen peroxide. *Free Radic. Biol. Med.* **1999**, *27*(3/4), 322–328.
32. Cardey, B., Foley, S., Enescu, M. Mechanism of thiol oxidation by the superoxide radical. *J. Phys. Chem. A*. **2007**, *111*(50), 13046–13052.
33. Sutton, V.R., Stubna, A., Patschkowski, T., Munck, E., Beinert, H., Kiley, P.J. Superoxide destroys the $[2Fe\text{-}2S]^{2+}$ cluster of FNR from *Escherichia coli*. *Biochemistry*. **2004**, *43*(3), 791–798.
34. Flint, D.H., Tuminello, J.F., Emptage, M.H. The inactivation of Fe-S cluster containing hydro-lyases by superoxide. *J. Biol. Chem.* **1993**, *268*(30), 22369–22376.
35. Sawyer, D.T. The chemistry of dioxygen species (oxygen, super oxide radical anion, peroxide radical and hydrogen peroxide) and their activation by transition metals. *Int. Rev. Exp. Pathol.* **1990**, *31*, 109–131.
36. Cheng, Z., Li, Y. What is responsible for the initiating chemistry of iron-mediated lipid peroxidation: an update. *Chem. Rev.* **2007**, *107*(3), 748–766.
37. Czapski, G., Bielski, B.H.J. The formation and decay of H_2O_3 and HO_2 in electronirradiated aqueous solutions. *J. Phys. Chem.* **1963**, *67*(10), 2180–2184.
38. Haber, F., Weiss, J. The catalytic decomposition of hydrogen peroxide by iron salts. *Proc. R. Soc. London, Ser. A*. **1934**, *147*, 332.
39. Perez-Benito, J.F. Iron(III)-hydrogen peroxide reaction: kinetic evidence of a hydroxyl-mediated chain mechanism. *J. Phys. Chem. A*. **2004**, *108*, 4853–4858.
40. Furtmuller, P.G., Obinger, C., Hsuanyu, Y., Dunford, H.B. Mechanism of reaction of myeloperoxidase with hydrogen peroxide and chloride ion. *Eur. J. Biochem.* **2000**, *267*(19), 5858–5864.
41. Kettle, A.J., Winterbourn, C.C. A kinetic analysis of the catalase activity of myeloperoxidase. *Biochemistry*. **2001**, *40*(34), 10204–10212.
42. Silanikove, N., Shapiro, F., Silanikove, M., Merin, U., Leitner, G. Hydrogen peroxide-dependent conversion of nitrite to nitrate as a crucial feature of bovine milk catalase. *J. Agric. Food Chem.* **2009**, *57*(17), 8018–8025.
43. Robinson, K.M., Beckman, J.S. Synthesis of peroxynitrite from nitrite and hydrogen peroxide. *Methods Enzymol.* **2005**, *396*, 207–214.
44. Oury, T.D., Tatro, L., Ghio, A.J., Piantadosi, C.A. Nitration of tyrosine by hydrogen peroxide and nitrite. *Free Radic. Res.* **1995**, *23*, 537–547.
45. Adimora, N.J., Jones, D.P., Kemp, M.L. A model of redox kinetics implicates the thiol proteome in cellular hydrogen peroxide responses. *Antioxid. Redox Signal.* **2010**, *13*(6), 731–743.
46. Scrivens, G., Gilbert, B.C., Lee, T.C.P. EPR studies of the copper-catalysed oxidation of thiols with peroxides. *J. Chem. Soc., Perkin Trans. 2*. **1995**, 955–963.
47. Koppenol, W.H., Liebman, J.F. The oxidizing nature of the hydroxyl radical. A comparison with the ferryl ion (FeO^{2+}). *J. Phys. Chem.* **1984**, *88*, 99–101.
48. Li, H., Lawson, J.A., Reilly, M., Adiyaman, M., Hwang, S.W., Rokach, J., FitzGerald, G.A. Quantitative high performance liquid chromatography/tandem mass spectrometric analysis of the four classes of F_2-isoprostanes in human urine. *Proc. Natl. Acad. Sci. U.S.A.* **1999**, *96*(23), 13381–13386.
49. Song, Y., Buettner, G.R., Parkin, S., Wagner, B.A., Robertson, L.W., Lehmler, H.J. Chlorination increases the persistence of semiquinone free radicals derived from polychlorinated biphenyl hydroquinones and quinones. *J. Org. Chem.* **2008**, *73*(21), 8296–8304.

50. Buxton, G.V., Greenstock, C.L., Helman, W.P., Ross, A.B. Critical review of rate constants for reactions of hydrated electrons, hydrogen atoms and hydroxyl radicals (OH/O) in aqueous solution. *J. Phys. Chem. Ref. Data*. **1988**, *17*, 513–886.
51. Adhikari, S., Sprinz, H., Brede, O. Thiyl radical induced isomerization of unsaturated fatty acids: determination of equilibrium constants. *Res. Chem. Intermed.* **2001**, *27*, 549–559.
52. Alam, M.S., Rao, B.S.M., Janata, E. •OH reactions with aliphatic alcohols: evaluation of kinetics by direct optical absorption measurement. A pulse radiolysis study. *Radiat. Phys. Chem.* **2003**, *67*, 723–728.
53. Galano, A., Alvarez-Idaboy, J.R., Bravo-Pérez, G., Ruiz-Santoyo, M.E. Gas phase reactions of C1–C4 alcohols with the OH radical: a quantum mechanical approach. *Phys. Chem. Chem. Phys.* **2002**, *4*, 4648–4662.
54. Rachmilovich-Calis, S., Meyerstein, N., Meyerstein, D. A mechanistic study of the effects of antioxidants on the formation of malondialdehyde-like products in the reaction of hydroxyl radicals with deoxyribose. *Chem. Eur. J.* **2009**, *15*(31), 7717–7723.
55. Esterbauer, H., Schaur, R.J., Zollner, H. Chemistry and biochemistry of 4-hydroxynonenal, malonaldehyde and related aldehydes. *Free Radic. Biol. Med.* **1991**, *11*(1), 81–128.
56. Onyango, A.N., Baba, N. New hypotheses on the pathways of formation of malondialdehyde and isofurans. *Free Radic. Biol. Med.* **2010**, *49*(10), 1594–1600.
57. Bucknall, T., Edwards, H.E., Kemsley, K.G., Moore, J.S., Phillips, G.O. The formation of malonaldehyde in irradiated carbohydrates. *Carbohydr. Res.* **1978**, *62*, 49–59.
58. Gligorovski, S., Herrmann, H. Kinetics of reactions of OH with organic carbonyl compounds in aqueous solution. *Phys. Chem. Chem. Phys.* **2004**, *6*, 4118–4126.
59. Alvarez-Idaboy, J.R., Cruz-Torres, A., Galano, A., Ruiz-Santoyo, M.E. Structure-reactivity relationship in ketones + OH reactions: a quantum mechanical and TST. *J. Phys. Chem. A*. **2004**, *108*, 2740–2749.
60. Alvarez-Idaboy, J.R., Mora-Diez, N., Boyd, R.J., Vivier-Bunge, A. On the importance of prereactive complexes in molecule-radical reactions: hydrogen abstraction from aldehydes by OH. *J. Am. Chem. Soc.* **2001**, *123*, 2018–2024.
61. Ervens, B., Gligorovski, S., Herrmann, H. Temperature-dependent rate constants for hydroxyl radical reactions with organic compounds in aqueous solutions. *Phys. Chem. Chem. Phys.* **2003**, *5*, 1811–1824.
62. Morris, E. D.; Niki, H., Reactivity of hydroxyl radicals with olefins. *J. Phys. Chem.* **1971,** *75*(23), 3640–3641.
63. Atkinson, R. Kinetics and mechanisms of the gas-phase reactions of the hydroxyl radical with organic compounds under atmospheric conditions. *Chem. Rev.* **1985**, *85*, 69–201.
64. Poole, J.S., Shi, X., Hadad, C.M., Platz, M.S. Reaction of hydroxyl radical with aromatic hydrocarbons in non-aqueous solutions: a laser flash photolysis study in acetonitrile. *J. Phys. Chem. A*. **2005**, *109*, 2547–2551.
65. DeMatteo, M.P., Poole, J.S., Shi, X., Sachdeva, R., Hatcher, P.G., Hadad, C.M., Platz, M.S. On the electrophilicity of hydroxyl radical: a laser flash photolysis and computational study. *J. Am. Chem. Soc.* **2005**, *127*(19), 7094–7109.
66. Geeta, S., Rao, B.S.M., Mohan, H., Mittal, J.P. Radiation-induced oxidation of substituted benzaldehydes: a pulse radiolysis study. *J. Phys. Org. Chem.* **2004**, *17*, 194–198.
67. Enescu, M., Cardey, B. Mechanism of cysteine oxidation by a hydroxyl radical: a theoretical study. *Chem. Phys. Chem.* **2006**, *7*(4), 912–919.
68. Cruz-Torres, A., Galano, A. On the mechanism of gas-phase reaction of C1–C3 aliphatic thiols + OH radicals. *J. Phys. Chem. A*. **2007**, *111*(8), 1523–1529.
69. Karoui, H., Hogg, N., Frejaville, C., Tordo, P., Kalyanaraman, B. Characterization of sulfur-centered radical intermediates formed during the oxidation of thiols and sulfite by peroxynitrite. ESR-spin trapping and oxygen uptake studies. *J. Biol. Chem.* **1996**, *271*(11), 6000–6009.
70. DeRosa, M.C., Crutchley, R.J. Photosensitized singlet oxygen and its applications. *Coord. Chem. Rev.* **2002**, *233-234*, 351–371.
71. Wilkinson, F., Helman, W.P., Ross, A.B. Rate constants for the decay and reactions of the lowest electronically excited singlet state of molecular oxygen in solution. An expanded and revised compilation. *J. Phys. Chem. Ref. Data*. **1995**, *24*, 663–1021.
72. Greer, A. Christopher Foote's discovery of the role of singlet oxygen [$^1O_2$ ($^1\Delta_g$)] in photosensitized oxidation reactions. *Acc. Chem. Res.* **2006**, *39*(11), 797–804.
73. Sun, S., Bao, Z., Ma, H., Zhang, D., Zheng, X. Singlet oxygen generation from the decomposition of alpha-linolenic acid hydroperoxide by cytochrome c and lactoperoxidase. *Biochemistry*. **2007**, *46*(22), 6668–6673.
74. Escobar, J.A., Vasquez-Vivar, J., Cilento, G. Free radicals and excited species in the metabolism of indole-3-acetic acid and its ethyl ester by horseradish peroxidase and by neutrophils. *Photochem. Photobiol.* **1992**, *55*(6), 895–902.
75. King, M.M., Lai, E.K., McCay, P.B. Singlet oxygen production associated with enzyme-catalyzed lipid peroxidation in liver microsomes. *J. Biol. Chem.* **1975**, *250*(16), 6496–6502.
76. Kiryu, C., Makiuchi, M., Miyazaki, J., Fujinaga, T., Kakinuma, K. Physiological production of singlet molecular oxygen in the myeloperoxidase-H_2O_2-chloride system. *FEBS Lett.* **1999**, *443*(2), 154–158.
77. Medeiros, M.H., Wefers, H., Sies, H. Generation of excited species catalyzed by horseradish peroxidase or hemin in the presence of reduced glutathione and H_2O_2. *Free Radic. Biol. Med.* **1987**, *3*(2), 107–110.
78. Zacharia, I.G., Deen, W.M. Diffusivity and solubility of nitric oxide in water and saline. *Ann. Biomed. Eng.* **2005**, *33*, 214–222.
79. Zhao, Y.L., Bartberger, M.D., Goto, K., Shimada, K., Kawashima, T., Houk, K.N. Theoretical evidence for enhanced NO dimerization in aromatic hosts: implications for the role of the electrophile $(NO)_2$ in nitric oxide chemistry. *J. Am. Chem. Soc.* **2005**, *127*(22), 7964–7965.
80. Lewis, R.S., Deen, W.M. Kinetics of the reaction of nitric oxide with oxygen in aqueous solutions. *Chem. Res. Toxicol.* **1994**, *7*, 568–574.

81. Goldstein, S., Czapski, G. Kinetics of nitric oxide autoxidation in aqueous solution in the absence and presence of various reductants. The nature of the oxidizing intermediates. *J. Am. Chem. Soc.* **1995**, *117*, 12078–12084.
82. Czapski, G., Holcman, J., Bielski, B.H.J. Reactivity of nitric oxide with simple short-lived radicals in aqueous solutions. *J. Am. Chem. Soc.* **1994**, *116*, 11465–11469.
83. Batt, L., Rattray, G.N. The reaction of methoxy radicals with nitric oxide and nitrogen dioxide. *Int. J. Chem. Kin.* **1979**, *11*, 1183–1196.
84. Goldstein, S., Lind, J., Merenyi, G. Reaction of organic peroxyl radicals with NO_2 and NO in aqueous solution: intermediacy of organic peroxynitrate and peroxynitrite species. *J. Phys. Chem. A*. **2004**, *108*, 1719–1725.
85. Ford, P.C., Lorkovic, I.M. Mechanistic aspects of the reactions of nitric oxide with transition-metal complexes. *Chem. Rev.* **2002**, *102*(4), 993–1018.
86. Scheidt, W.R., Lee, Y.J., Hatano, K. Preparation and structural characterization of nitrosyl complexes of ferric porphyrinates. Molecular structure of aquonitrosyl(mesotetraphenylporphinato)iron(III) perchlorate and nitrosyl (octaethylporphinato)iron(III) perchlorate. *J. Am. Chem. Soc.* **1984**, *106*, 3191–3198.
87. Enami, S., Hoffmann, M.R., Colussi, A.J. Absorption of inhaled NO_2. *J. Phys. Chem. B*. **2009**, *113*(23), 7977–7981.
88. Huie, R.E. The reaction kinetics of NO_2. *Toxicology*. **1994**, *89*, 193–216.
89. Dutton, A.S., Fukuto, J.M., Houk, K.N. Theoretical reduction potentials for nitrogen oxides from CBS-QB3 energetics and (C)PCM solvation calculations. *Inorg. Chem.* **2005**, *44*(11), 4024–4028.
90. Napolitano, A., Camera, E., Picardo, M., d'Ischia, M. Acid-promoted reactions of ethyl linoleate with nitrite ions: formation and structural characterization of isomeric nitroalkene, nitrohydroxy, and novel 3-nitro-1,5-hexadiene and 1,5-dinitro-1, 3-pentadiene products. *J. Org. Chem.* **2000**, *65*(16), 4853–4860.
91. d'Ischia, M., Napolitano, A., Manini, P., Panzella, L. Secondary targets of nitrite-derived reactive nitrogen species: nitrosation/nitration pathways, antioxidant defense mechanisms and toxicological implications. *Chem. Res. Toxicol.* **2011**, *24*(12), 2071–2092.
92. Solar, S., Solar, W., Getoff, N. Reactivity of hydroxyl with tyrosine in aqueous solution studied by pulse radiolysis. *J. Phys. Chem.* **1984**, *88*, 2091–2095.
93. Prütz, W.A., Mönig, H., Butler, J., Land, E.J. Reactions of nitrogen dioxide in aqueous model systems: oxidation of tyrosine units in peptides and proteins. *Arch. Biochem. Biophys.* **1985**, *243*, 125–134.
94. Deeb, R.S., Resnick, M.J., Mittar, D., McCaffrey, T., Hajjar, D.P., Upmacis, R.K. Tyrosine nitration in prostaglandin H_2 synthase. *J. Lipid Res.* **2002**, *43*(10), 1718–1726.
95. Surmeli, N.B., Litterman, N.K., Miller, A.F., Groves, J.T. Peroxynitrite mediates active site tyrosine nitration in manganese superoxide dismutase. Evidence of a role for the carbonate radical anion. *J. Am. Chem. Soc.* **2010**, *132*(48), 17174–17185.
96. Abriata, L.A., Cassina, A., Tortora, V., Marin, M., Souza, J.M., Castro, L., Vila, A.J., Radi, R. Nitration of solvent-exposed tyrosine 74 on cytochrome c triggers heme iron-methionine 80 bond disruption. Nuclear magnetic resonance and optical spectroscopy studies. *J. Biol. Chem.* **2009**, *284*(1), 17–26.
97. Jourd'heuil, D., Jourd'heuil, F.L., Feelisch, M. Oxidation and nitrosation of thiols at low micromolar exposure to nitric oxide. Evidence for a free radical mechanism. *J. Biol. Chem.* **2003**, *278*(18), 15720–15726.
98. Hofstetter, D., Nauser, T., Koppenol, W.H. The glutathione thiyl radical does not react with nitrogen monoxide. *Biochem. Biophys. Res. Commun.* **2007**, *360*(1), 146–148.
99. Goldstein, S., Lind, J., Merenyi, G. Chemistry of peroxynitrites as compared to peroxynitrates. *Chem. Rev.* **2005**, *105*(6), 2457–2470.
100. Merenyi, G., Lind, J., Eriksen, T.E. The reactivity of superoxide ($O2^{-}$.) and its ability to induce chemiluminescence with luminol. *Photochem. Photobiol.* **1985**, *41*(2), 203–208.
101. Szabo, C., Ischiropoulos, H., Radi, R. Peroxynitrite: biochemistry, pathophysiology and development of therapeutics. *Nat. Rev. Drug Discov.* **2007**, *6*(8), 662–680.
102. Pearce, L.L., Martinez-Bosch, S., Manzano, E.L., Winnica, D.E., Epperly, M.W., Peterson, J. The resistance of electron-transport chain Fe-S clusters to oxidative damage during the reaction of peroxynitrite with mitochondrial complex II and rat-heart pericardium. *Nitric Oxide*. **2009**, *20*(3), 135–142.
103. Rubbo, H., Denicola, A., Radi, R. Peroxynitrite inactivates thiol-containing enzymes of Trypanosoma cruzi energetic metabolism and inhibits cell respiration. *Arch. Biochem. Biophys.* **1994**, *308*(1), 96–102.
104. Merényi, G., Lind, J., Czapski, G., Goldstein, S. Direct determination of the Gibbs' energy of formation of peroxynitrous acid. *Inorg. Chem.* **2003**, *42*, 3796–3800.
105. Lymar, S.V., Hurst, J.K. Rapid reaction between peroxonitrite ion and carbon dioxide: implications for biological activity. *J. Am. Chem. Soc.* **1995**, *117*, 8867–8868.
106. Bonini, M.G., Siraki, A.G., Atanassov, B.S., Mason, R.P. Immunolocalization of hypochlorite-induced, catalase-bound free radical formation in mouse hepatocytes. *Free Radic. Biol. Med.* **2007**, *42*(4), 530–540.
107. Zhang, R., Goldstein, S., Samuni, A. Kinetics of superoxide-induced exchange among nitroxide antioxidants and their oxidized and reduced forms. *Free Radic. Biol. Med.* **1999**, *26*, 1245–1252.
108. Massari, J., Tokikawa, R., Zanolli, L., Tavares, M.F.M., Assuncao, N.A., Bechara, E.J.H. Acetyl radical production by the methylglyoxal-peroxynitrite system: a possible route for L-lysine acetylation. *Chem. Res. Toxicol.* **2010**, *23*(11), 1762–1770.
109. Royer, L.O., Knudsen, F.S., De Oliveira, M.A., Tavares, M.F.M., Bechara, E.J.H. Peroxynitrite-initiated oxidation of acetoacetate and 2-methylacetoacetate esters by oxygen: potential sources of reactive intermediates in keto acidoses. *Chem. Res. Toxicol.* **2004**, *17*(12), 1725–1732.

110. Imaram, W., Gersch, C., Kim, K.M., Johnson, R.J., Henderson, G.N., Angerhofer, A. Radicals in the reaction between peroxynitrite and uric acid identified by electron spin resonance spectroscopy and liquid chromatography mass spectrometry. *Free Radic. Biol. Med.* **2010**, *49*(2), 275–281.
111. Imaram, W., Johnson, R.J., Angerhofer, A. ESR spin trapping of the reaction between urate and peroxynitrite: the hydrogen adduct. *Appl. Magn. Reson.* **2009**, *37*(1-4), 463–472.
112. Olson, L.P., Bartberger, M.D., Houk, K.N. Peroxynitrate and peroxynitrite: a complete basis set investigation of similarities and differences between these NO_x species. *J. Am. Chem. Soc.* **2003**, *125*(13), 3999–4006.
113. Goldstein, S., Saha, A., Lymar, S.V., Czapski, G. Oxidation of peroxynitrite by inorganic radicals: a pulse radiolysis study. *J. Am. Chem. Soc.* **1998**, *120*, 5549–5554.
114. Koppenol, W.H. Thermodynamics of reactions involving nitrogen-oxygen compounds. *Methods Enzymol.* **1996**, *268*, 7–12.
115. Trujillo, M., Radi, R. Peroxynitrite reaction with the reduced and the oxidized forms of lipoic acid: new insights into the reaction of peroxynitrite with thiols. *Arch. Biochem. Biophys.* **2002**, *397*(1), 91–98.
116. Radi, R., Beckman, J.S., Bush, K.M., Freeman, B.A. Peroxynitrite oxidation of sulfhydryls. The cytotoxic potential of superoxide and nitric oxide. *J. Biol. Chem.* **1991**, *266*, 4244–4250.
117. Dubuisson, M., Vander Stricht, D., Clippe, A., Etienne, F., Nauser, T., Kissner, R., Koppenol, W.H., Rees, J.F., Knoops, B. Human peroxiredoxin 5 is a peroxynitrite reductase. *FEBS Lett.* **2004**, *571*, 161–165.
118. Alvarez, B., Ferrer-Sueta, G., Freeman, B.A., Radi, R. Kinetics of peroxynitrite reaction with amino acids and human serum albumin. *J. Biol. Chem.* **1999**, *274*(2), 842–848.
119. Jursic, B.S. Reliability of hybrid density theory-semiempirical approach for evaluation of bond dissociation energies. *J. Chem. Soc., Perkin Trans. 2*. **1999**, 369–372.
120. Hoffman, M.Z., Hayon, E. Pulse radiolysis study of sulfhydryl compounds in aqueous solution. *J. Phys. Chem. Ref. Data*. **1973**, *77*, 990–996.
121. Folkes, L.K., Trujillo, M., Bartesaghi, S., Radi, R., Wardman, P. Kinetics of reduction of tyrosine phenoxyl radicals by glutathione. *Arch. Biochem. Biophys.* **2011**, *506*, 242–249.
122. Ferreri, C., Kratzsch, S., Landic, L., Bredeb, O. Thiyl radicals in biosystems: effects on lipid structures and metabolisms. *Cell. Mol. Life Sci.* **2005**, *62*, 834–847.
123. Chatgilialoglu, C., Altieri, A., Fischer, H. The kinetics of thiyl radical-induced reactions of monounsaturated fatty acid esters. *J. Am. Chem. Soc.* **2002**, *124*(43), 12816–12823.
124. Schöneich, C., Dillinger, U., von Bruchhausen, F., Asmus, K.-D. Oxidation of polyunsaturated fatty acids and lipids through thiyl and sulfonyl radicals: reaction kinetics, and influence of oxygen and structure of thiyl radicals. *Arch. Biochem. Biophys.* **1992**, *292*, 456–467.
125. Schoneich, C., Asmus, K.-D., Bonifacic, M. Determination of absolute rate constants for the reversible hydrogen-atom transfer between thiyl radicals and alcohols or ethers. *J. Chem. Soc., Faraday Trans.* **1995**, *91*, 1923–1193.
126. Nauser, T., Schoneich, C. Thiyl radicals abstract hydrogen atoms from the $^{\alpha}$C–H bonds in model peptides: absolute rate constants and effect of amino acid structure. *J. Am. Chem. Soc.* **2003**, *125*, 2042–2043.
127. Schoneich, C. Cysteine residues as catalysts for covalent peptide and protein modification: a role for thiyl radicals? *Biochem. Soc. Trans.* **2011**, *39*(5), 1254–1259.
128. Hofstetter, D., Nauser, T., Koppenol, W.H. Hydrogen exchange equilibria in glutathione radicals: rate constants. *Chem. Res. Toxicol.* **2010**, *23*(10), 1596–1600.
129. Pogocki, D., Schoneich, C. Thiyl radicals abstract hydrogen atoms from carbohydrates: reactivity and selectivity. *Free Radic. Biol. Med.* **2001**, *31*(1), 98–107.
130. Madej, E., Folkes, L.K., Wardman, P., Czapski, G., Goldstein, S. Thiyl radicals react with nitric oxide to form S-nitrosothiols with rate constants near the diffusion-controlled limit. *Free Radic. Biol. Med.* **2008**, *44*, 2013–2018.
131. Sevilla, M.D., Becker, D., Swarts, S., Herrington, J. Sulfinyl radical formation from the reaction of cysteine and glutathione thiyl radicals with molecular oxygen. *Biochem. Biophys. Res. Commun.* **1987**, *144*, 1037–1042.
132. Mönig, J., Asmus, K.D., Forni, L.G., Willson, R.L. On the reaction of molecular oxygen with thiyl radicals: a re-examination. *Int. J. Radiat. Biol. Relat. Stud. Phys. Chem. Med.* **1987**, *52*, 589–602.
133. Tamba, M., Simone, G., Quintiliani, M. Interactions of thiyl free radicals with oxygen: a pulse radiolysis study. *J. Radiat. Biol.* **1986**, *50*, 595–600.
134. Zhao, R., Lind, J., Merbnyi, G., Eriksen, T.E. Kinetics of one-electron oxidation of thiols and abstraction by thiyl radicals from α-amino C–H bonds. *J. Am. Chem. Soc.* **1994**, *116*, 12010–12015.
135. Hoffman, M.Z., Hayon, E. One-electron reduction of the disulfide linkage in aqueous solution. Formation, protonation, and decay kinetics of the RSSR anion radical. *J. Am. Chem. Soc.* **1972**, *94*, 7950–7957.
136. Quintiliani, M., Badiello, R., Tamba, M., Esfandi, A., Gorin, G. Radiolysis of glutathione in oxygen-containing solutions of pH 7. *Int. J. Radiat. Biol.* **1977**, *32*, 195–202.
137. Voronkov, M.G., Deryagin, E.N. Thermal reactions of thiyl radicals. *Russ. Chem. Rev.* **1990**, *59*, 778–791.
138. Guo, W., Pleasants, J., Rabenstein, D.L. Nuclear magnetic resonance studies of thiol/disulfide chemistry. 2. Kinetics of symmetrical thiol/disulfide interchange reactions. *J. Org. Chem.* **1990**, *55*, 373–376.
139. Trivedi, M.V., Laurence, J.S., Siahaan, T.J. The role of thiols and disulfides on protein stability. *Curr. Protein Pept. Sci.* **2009**, *10*(6), 614–625.
140. Giles, G.I., Tasker, K.M., Jacob, C. Hypothesis: the role of reactive sulfur species in oxidative stress. *Free Radic. Biol. Med.* **2001**, *31*(10), 1279–1283.
141. Racker, E. Glutathione reductase from baker's yeast and beef liver. *J. Biol. Chem.* **1955**, *217*, 855–866.

142. Collet, J.F., Messens, J. Structure, function, and mechanism of thioredoxin proteins. *Antioxid. Redox Signal.* **2010**, *13*(8), 1205–1216.

143. Singh, R., Lamoureux, G.V., Lees, W.J., Whitesides, G.M. Reagents for rapid reduction of disulfide bonds. *Methods Enzymol.* **1995**, *251*, 167–173.

144. Pattison, D.I., Davies, M.J. Reactions of myeloperoxidase-derived oxidants with biological substrates: gaining chemical insight into human inflammatory diseases. *Curr. Med. Chem.* **2006**, *13*(27), 3271–3290.

145. Khan, A.U., Kasha, M. Chemiluminescence arising from simultaneous transitions in pairs of singlet oxygen molecules. *J. Am. Chem. Soc.* **1970**, *92*, 3293–3300.

146. Long, C.A., Bielski, B.H.J. Rate of reaction of superoxide radical with chloride-containing species. *J. Phys. Chem.* **1980**, *84*, 555–557.

147. Zuo, Z., Katsumura, Y., Ueda, K., Ishigur, K. Reactions between some inorganic radicals and oxychlorides studied by pulse radiolysis and laser photolysis. *J. Chem. Soc., Faraday Trans.* **1997**, *93*, 1885–1891.

148. Miyamoto, S., Martinez, G.R., Rettori, D., Augusto, O., Medeiros, M.H., Di Mascio, P. Linoleic acid hydroperoxide reacts with hypochlorous acid, generating peroxyl radical intermediates and singlet molecular oxygen. *Proc. Natl. Acad. Sci. U.S.A.* **2006**, *103*(2), 293–298.

149. Eiserich, J.P., Cross, C.E., Jones, A.D., Halliwell, B., van der Vliet, A. Formation of nitrating and chlorinating species by reaction of nitrite with hypochlorous acid. A novel mechanism for nitric oxide-mediated protein modification. *J. Biol. Chem.* **1996**, *271*(32), 19199–19208.

150. Eiserich, J.P., Hristova, M., Cross, C.E., Jones, A.D., Freeman, B.A., Halliwell, B., van der Vliet, A. Formation of nitric oxide-derived inflammatory oxidants by myeloperoxidase in neutrophils. *Nature*. **1998**, *391*(6665), 393–397.

151. Fogelman, K.D., Walker, D.M., Margerum, D.W. Nonmetal redox kinetics: hypochlorite and hypochlorous acid reactions with sulfite. *Inorg. Chem.* **1989**, *28*, 986–993.

152. Chesney, J.A., Mahoney, J.R.J., Eaton, J.W. A spectrophotometric assay for chlorine-containing compounds. *Anal. Biochem.* **1991**, *196*, 262–266.

153. Folkes, L.K., Candeias, L.P., Wardma, P. Kinetics and mechanisms of hypochlorous acid reactions. *Arch. Biochem. Biophys.* **1995**, *323*, 120–126.

154. Hawkins, C.L., Davie, M.J. Reaction of HOCl with amino acids and peptides: EPR evidence for rapid rearrangement and fragmentation reactions of nitrogen-centred radicals. *J. Chem. Soc., Perkin Trans. 2*. **1998**, 1937–1945.

155. Peskin, A.V., Winterbourn, C.C. Kinetics of the reactions of hypochlorous acid and amino acid chloramines with thiols, methionine, and ascorbate. *Free Radic. Biol. Med.* **2001**, *30*(5), 572–579.

156. Carr, A.C., Winterbourn, C.C. Oxidation of neutrophil glutathione and protein thiols by myeloperoxidase-derived hypochlorous acid. *Biochem. J.* **1997**, *327*, 275–281.

157. Peskin, A.V., Turner, R., Maghzal, G.J., Winterbourn, C.C., Kettle, A.J. Oxidation of methionine to dehydromethionine by reactive halogen species generated by neutrophils. *Biochemistry*. **2009**, *48*(42), 10175–10182.

158. Fu, S., Wang, H., Davies, M., Dean, R. Reactions of hypochlorous acid with tyrosine and peptidyl-tyrosyl residues give dichlorinated and aldehydic products in addition to 3-chlorotyrosine. *J. Biol. Chem.* **2000**, *275*(15), 10851–10858.

159. Prutz, W.A., Kissner, R., Nauser, T., Koppenol, W.H. On the oxidation of cytochrome c by hypohalous acids. *Arch. Biochem. Biophys.* **2001**, *389*(1), 110–122.

160. Winterbourn, C.C., van den Berg, J.J.M., Roitman, E., Kuypers, F.A. Chlorohydrin formation from unsaturated fatty acids reacted with hypochlorous acid. *Arch. Biochem. Biophys.* **1992**, *296*, 547–555.

161. Hawkins, C.L., Davies, M.J. Hypochlorite-induced damage to nucleosides: formation of chloramines and nitrogen-centered radicals. *Chem. Res. Toxicol.* **2001**, *14*(8), 1071–1081.

162. Stanley, N.R., Pattison, D.I., Hawkins, C.L. Ability of hypochlorous acid and N-chloramines to chlorinate DNA and its constituents. *Chem. Res. Toxicol.* **2010**, *23*(7), 1293–1302.

163. Whiteman, M., Jenner, A., Halliwell, B. Hypochlorous acid-induced base modifications in isolated calf thymus DNA. *Chem. Res. Toxicol.* **1997**, *10*(11), 1240–1246.

164. Prutz, W.A., Kissner, R., Koppenol, W.H., Ruegger, H. On the irreversible destruction of reduced nicotinamide nucleotides by hypohalous acids. *Arch. Biochem. Biophys.* **2000**, *380*(1), 181–191.

165. Koppenol, W.H., Stanbury, D.M., Bounds, P.L. Electrode potentials of partially reduced oxygen species, from dioxygen to water. *Free Radic. Biol. Med.* **2010**, *49*(3), 317–322.

166. Koppenol, W.H., Butler, J. Energetics of interconversion reactions of oxyradicals. *Adv. Free Radic. Biol. Med.* **1985**, *1*, 91–131.

167. Pfeiffer, S., Mayer, B., Janoschek, R. Gibbs energies of reactive species involved in peroxynitrite chemistry calculated by density functional theory. *J. Mol. Struct.* **2003**, *623*, 95–103.

168. Lagager, T., Sehested, K. Formation and decay of peroxynitrous acid: a pulse radiolysis study. *J. Phys. Chem.* **1993**, *97*, 6664–6669.

169. Buettner, G.R. The pecking order of free radicals and antioxidants: lipid peroxidation, α-tocopherol, and ascorbate. *Arch. Biochem. Biophys.* **1993**, *300*, 535–543.

170. Hotamisligil, G.S. Endoplasmic reticulum stress and the inflammatory basis of metabolic disease. *Cell*. **2010**, *140*(6), 900–917.

171. Jiang, Z., Hu, Z., Zeng, L., Lu, W., Zhang, H., Li, T., Xiao, H. The role of the Golgi apparatus in oxidative stress: is this organelle less significant than mitochondria? *Free Radic. Biol. Med.* **2011**, *50*, 907–917.

172. Quinn, M.T., Gauss, K.A. Structure and regulation of the neutrophil respiratory burst oxidase: comparison with nonphagocyte oxidases. *J. Leukoc. Biol.* **2004**, *76*, 760–781.

173. Berry, C.E., Hare, J.M. Xanthine oxidoreductase and cardiovascular disease: molecular mechanisms and

pathophysiological implications. *J. Physiol.* **2004**, *555* (Pt 3), 589–606.

174. Cadenas, E., Davies, K.J.A. Mitochondrial free radical generation, oxidative stress, and aging. *Free Radic. Biol. Med.* **2000**, *29*, 222–230.
175. Barja, G. Mitochondrial oxygen radical generation and leak: sites of production in states 4 and 3, organ specificity, and relation to aging and longevity. *J. Bioenerg. Biomembr.* **1999**, *31*(4), 347–366.
176. Rifkind, J.M., Ramasamy, S., Manoharan, P.T., Nagababu, E., Mohanty, J.G. Redox reactions of hemoglobin *Antioxid. Redox Signal.* **2004**, *6*, 657–666.
177. Wei, C.-C., Crane, B.R., Stuehr, D.J. Tetrahydrobiopterin radical enzymology. *Chem. Rev.* **2003**, *103*, 2365–2384.
178. Surawatanawong, P., Tye, J.W., Hall, M.B. Density functional theory applied to a difference in pathways taken by the enzymes cytochrome P450 and superoxide reductase: spin states of ferric hydroperoxo intermediates and hydrogen bonds from water. *Inorg. Chem.* **2010**, *49*, 188–198.
179. Kuthan, H., Tsuji, H., Graf, H., Ullrich, V., Werringloer, J., Estabrook, R.W. Generation of superoxide anion as a source of hydrogen peroxide in a reconstituted monooxygenase system. *FEBS Lett.* **1978**, *91*, 343–345.
180. Roy, P., Roy, S.K., Mitra, A., Kulkarni, A.P. Superoxide generation by lipoxygenase in the presence of NADH and NADPH. *Biochem. Biophys. Acta, Lipids Lipid Metab.* **1994**, *1214*, 171–179.
181. Gross, E., Sevier, C.S., Heldman, N., Vitu, E., Bentzur, M., Kaiser, C.A., Thorpe, C., Fass, D. Generating disulfides enzymatically: reaction products and electron acceptors of the endoplasmic reticulum thiol oxidase Ero1p. *Proc. Natl. Acad. Sci. U.S.A.* **2006**, *103*(2), 299–304.
182. Bielski, B.H.J., Richter, H.W. A study of the superoxide radical chemistry by stopped-flow radiolysis and radiation induced oxygen consumption. *J. Am. Chem. Soc.* **1977**, *99*, 3019–3023.
183. Holroyd, R.A., Bielski, B.H.J. Photochemical generation of superoxide radicals in aqueous solutions. *J. Am. Chem. Soc.* **1978**, *100*, 5796–5800.
184. Hochanadel, C.J. Photolysis of dilute H_2O_2 solution in the presence of dissolved H_2 and O_2. Evidence relating to the nature of the OH radical and the H atom produced in the radiolysis of H_2O. *Radiat. Res.* **1962**, *17*, 286–301.
185. Joshi, A., Yang, G.C. Spin trapping of radicals generated in the UV photolysis of alkyl disulfides. *J. Org. Chem.* **1981**, *46*, 3736–3738.
186. Misik, V., Miyoshi, N., Riesz, P. EPR spin-trapping study of the sonolysis of H_2O/D_2O mixtures: probing the temperatures of cavitation regions. *J. Phys. Chem.* **1995**, *99*, 3605–3611.
187. Makino, K., Mossoba, M.M., Riesz, P. Chemical effects of ultrasound on aqueous solutions. Formation of hydroxyl radicals and hydrogen atoms. *J. Phys. Chem.* **1983**, *87*, 1369–1377.
188. Misik, V., Riesz, P. Free radical intermediates in sonodynamic therapy. *Ann. N. Y. Acad. Sci.* **2000**, *899*, 335–348.
189. Draper, W.M., Crosby, D.G. Photochemical generation of superoxide radical anion in water. *J. Agric. Food Chem.* **1983**, *31*, 734–737.
190. Maurette, M.-T., Oliveros, E., Infelta, P.P., Ramsteiner, K., Braun, A.M. Singlet oxygen and superoxide: experimental differentiation and analysis. *Helv. Chim. Acta*. **1983**, *66*, 722–732.
191. Yamakoshi, Y., Sueyoshi, S., Fukuhara, K., Miyata, N. OH and O_2 generation in aqueous C_{60} and C_{70} solutions by photoirradiation: an EPR study. *J. Am. Chem. Soc.* **1998**, *120*, 12363–12364.
192. Garg, S., Rose, A.L., Waite, T.D. Production of reactive oxygen species on photolysis of dilute aqueous quinone solutions. *Photochem. Photobiol.* **2007**, *83*(4), 904–913.
193. Matsumoto, F., Okajima, T., Uesugi, S., Koura, N., Ohsaka, T. Electrogeneration of superoxide ion and its mechanism at thiol-modified Au electrodes in alkaline aqueous solution. *Electrochemistry*. **2003**, *71*, 266–273.
194. Merritt, M.V., Sawyer, D.T. Electrochemical studies of the reactivity of superoxide ion with several alkyl halides in dimethyl sulfoxide. *J. Org. Chem.* **1970**, *35*, 2157–2159.
195. Maricle, D.L., Hodgson, W.G. Reduction of oxygen to superoxide in aprotic solvents. *Anal. Chem.* **1965**, *37*, 1562–1565.
196. Martiz, B., Keyrouz, R., Gmouh, S., Vaultier, M., Jouikov, V. Superoxide-stable ionic liquids: new and efficient media for electrosynthesis of functional siloxanes. *Chem. Commun.* **2004**, *6*, 674–675.
197. Bohle, D.S., Sagan, E.S., Koppenol, W.H., Kissner, R. Tetramethylammonium salts of superoxide and peroxynitrite. *Inorg. Synth.* **2004**, *34*, 36–42.
198. McElroy, A.D., Hashman, J.S. Synthesis of tetramethylammonium superoxide. *Inorg. Chem.* **1964**, *3*, 1798–1799.
199. Bolton, J.L., Trush, M.A., Penning, T.M., Dryhurst, G., Monks, T.J. Role of quinones in toxicology. *Chem. Res. Toxicol.* **2000**, *13*, 135–160.
200. Wang, P.G., Xian, M., Tang, X., Wu, X., Wen, Z., Cai, T., Janczuk, A.J. Nitric oxide donors: chemical activities and biological applications. *Chem. Rev.* **2002**, *102*(4), 1091–1134.
201. Pryor, W.A., Cueto, R., Jin, X., Koppenol, W.H., Ngu-Schwemlein, M., Squadrito, G.L., Uppu, P.L., Uppu, R.M. A practical method for preparing peroxynitrite solutions of low ionic strength and free of hydrogen peroxide. *Free Radic. Biol. Med.* **1995**, *18*(1), 75–83.
202. Uppu, R.M. Synthesis of peroxynitrite using isoamyl nitrite and hydrogen peroxide in a homogeneous solvent system. *Anal. Biochem.* **2006**, *354*(2), 165–168.
203. Wahl, R.U.R. Decomposition mechanism of 3-*N*-morpholinosydnonimine (SIN-1)—a density functional study on intrinsic structures and reactivities. *J. Mol. Model.* **2004**, *10*, 121–129.
204. Wardman, P. Fluorescent and luminescent probes for measurement of oxidative and nitrosative species in cells and tissues: progress, pitfalls, and prospects. *Free Radic. Biol. Med.* **2007**, *43*(7), 995–1022.

205. Zhao, H., Joseph, J., Fales, H.M., Sokoloski, E.A., Levine, R.L., Vasquez-Vivar, J., Kalyanaraman, B. Detection and characterization of the product of hydroethidine and intracellular superoxide by HPLC and limitations of fluorescence. *Proc. Natl. Acad. Sci. U.S.A.* **2005**, *102*(16), 5727–5732.

206. Miller, E.W., Chang, C.J. Fluorescent probes for nitric oxide and hydrogen peroxide in cell signaling. *Curr. Opin. Chem. Biol.* **2007**, *11*(6), 620–625.

207. Sikora, A., Zielonka, J., Lopez, M., Joseph, J., Kalyanaraman, B. Direct oxidation of boronates by peroxynitrite: mechanism and implications in fluorescence imaging of peroxynitrite. *Free Radic. Biol. Med.* **2009**, *47*(10), 1401–1407.

208. Nagano, T. Bioimaging probes for reactive oxygen species and reactive nitrogen species. *J. Clin. Biochem. Nutr.* **2009**, *45*(2), 111–124.

209. Fontijn, A., Sabadell, A.J., Ronco, R.J. Homogeneous chemiluminescent measurement of nitric oxide with ozone: implications for continuous selective monitoring of gaseous air pollutants. *Anal. Chem.* **1970**, *42*, 575–579.

210. Afanasev, I. Detection of superoxide in cells, tissues and whole organisms. *Front. Biosci.* **2009**, *E1*, 153–160.

211. Archer, S. Measurement of nitric oxide in biological models. *FASEB J.* **1993**, *7*, 349–360.

212. Kleinbongard, P., Rassaf, T., Dejam, A., Kerber, S., Kelm, M. Griess method for nitrite measurement of aqueous and protein-containing samples. *Methods Enzymol.* **2002**, *359*, 158–168.

213. Thomas, E.L., Grisham, M.B., Jefferson, M.M. Preparation and characterization of chloramines. *Methods Enzymol.* **1986**, *132*, 569–585.

214. Dypbukt, J.M., Bishop, C., Brooks, W.M., Thong, B., Eriksson, H., Kettle, A.J. A sensitive and selective assay for chloramine production by myeloperoxidase. *Free Radic. Biol. Med.* **2005**, *39*(11), 1468–1477.

215. Floyd, R.A., West, M.S., Eneff, K.L., Hogsett, W.E., Tingey, D.T. Hydroxyl free radical mediated formation of 8-hydroxyguanine in isolated DNA. *Arch. Biochem. Biophys.* **1988**, *262*(1), 266–272.

216. Freinbichler, W., Bianchi, L., Colivicchi, M.A., Ballini, C., Tipton, K.F., Linert, W., Corte, L.D. The detection of hydroxyl radicals *in vivo*. *J. Inorg. Biochem.* **2008**, *102* (5-6), 1329–1333.

217. Rebrin, I., Bregere, C., Gallaher, T.K., Sohal, R.S. Detection and characterization of peroxynitrite-induced modifications of tyrosine, tryptophan, and methionine residues by tandem mass spectrometry. *Methods Enzymol.* **2008**, *441*, 283–294.

218. Sultana, R., Reed, T., Butterfield, D.A. Detection of 4-hydroxy-2-nonenal- and 3-nitrotyrosine-modified proteins using a proteomics approach. *Methods Mol. Biol.* **2009**, *519*, 351–361.

219. Butt, Y.K., Lo, S.C. Detecting nitrated proteins by proteomic technologies. *Methods Enzymol.* **2008**, *440*, 17–31.

220. Nourooz-Zadeh, J., Tajaddini-Sarmadi, J., Ling, K.L., Wolff, S.P. Low-density lipoprotein is the major carrier of lipid hydroperoxides in plasma. Relevance to determination of total plasma lipid hydroperoxide concentrations. *Biochem. J.* **1996**, *313*(Pt 3), 781–786.

221. Fukuzawa, K., Fujisaki, A., Akai, K., Tokumura, A., Terao, J., Gebicki, J.M. Measurement of phosphatidylcholine hydroperoxides in solution and in intact membranes by the ferric-xylenol orange assay. *Anal. Biochem.* **2006**, *359*(1), 18–25.

222. Gieseg, S.P., Pearson, J., Firth, C.A. Protein hydroperoxides are a major product of low density lipoprotein oxidation during copper, peroxyl radical and macrophage-mediated oxidation. *Free Radic. Res.* **2003**, *37*(9), 983–991.

223. Winterbourn, C.C., Pichorner, H., Kettle, A.J. Myeloperoxidase-dependent generation of a tyrosine peroxide by neutrophils. *Arch. Biochem. Biophys.* **1997**, *338*(1), 15–21.

224. O'Donnell, V.B., Eiserich, J.P., Chumley, P.H., Jablonsky, M.J., Krishna, N.R., Kirk, M., Barnes, S., Darley-Usmar, V.M., Freeman, B.A. Nitration of unsaturated fatty acids by nitric oxide-derived reactive nitrogen species peroxynitrite, nitrous acid, nitrogen dioxide, and nitronium ion. *Chem. Res. Toxicol.* **1999**, *12*(1), 83–92.

225. Janero, D.R. Malondialdehyde and thiobarbituric acid-reactivity as diagnostic indices of lipid peroxidation and peroxidative tissue injury. *Free Radic. Biol. Med.* **1990**, *9*(6), 515–540.

226. Lawson, J.A., Rokach, J., FitzGerald, G.A. Isoprostanes: formation, analysis and use as indices of lipid peroxidation *in vivo*. *J. Biol. Chem.* **1999**, *274*(35), 24441–24444.

227. Mason, R.P. Using anti-5,5-dimethyl-1-pyrroline N-oxide (anti-DMPO) to detect protein radicals in time and space with immuno-spin trapping. *Free Radic. Biol. Med.* **2004**, *36*(10), 1214–1223.

228. Ramirez, D.C., Chen, Y.R., Mason, R.P. Immunochemical detection of hemoglobin-derived radicals formed by reaction with hydrogen peroxide: involvement of a protein-tyrosyl radical. *Free Radic. Biol. Med.* **2003**, *34*(7), 830–839.

229. Detweiler, C.D., Lardinois, O.M., Deterding, L.J., de Montellano, P.R., Tomer, K.B., Mason, R.P. Identification of the myoglobin tyrosyl radical by immuno-spin trapping and its dimerization. *Free Radic. Biol. Med.* **2005**, *38*(7), 969–976.

230. Ramirez, D.C., Gomez Mejiba, S.E., Mason, R.P. Mechanism of hydrogen peroxide-induced Cu, Zn-superoxide dismutase-centered radical formation as explored by immuno-spin trapping: the role of copper- and carbonate radical anion-mediated oxidations. *Free Radic. Biol. Med.* **2005**, *38*(2), 201–214.

231. Ehrenshaft, M., Mason, R.P. Protein radical formation on thyroid peroxidase during turnover as detected by immuno-spin trapping. *Free Radic. Biol. Med.* **2006**, *41*(3), 422–430.

232. Ranguelova, K., Suarez, J., Magliozzo, R.S., Mason, R.P. Spin trapping investigation of peroxide- and isoniazid-induced radicals in *Mycobacterium tuberculosis* catalase-peroxidase. *Biochemistry*. **2008**, *47*(43), 11377–11385.

233. Ramirez, D.C., Mejiba, S.E., Mason, R.P. Immuno-spin trapping of DNA radicals. *Nat. Methods*. **2006**, *3*(2), 123–127.

234. Ramirez, D.C., Gomez-Mejiba, S.E., Mason, R.P. Immuno-spin trapping analyses of DNA radicals. *Nat. Protoc.* **2007**, *2*(3), 512–522.

235. Gomez-Mejiba, S.E., Zhai, Z., Akram, H., Deterding, L.J., Hensley, K., Smith, N., Towner, R.A., Tomer, K.B., Mason, R.P., Ramirez, D.C. Immuno-spin trapping of protein and DNA radicals: "tagging" free radicals to locate and understand the redox process. *Free Radic. Biol. Med.* **2009**, *46*(7), 853–865.

236. Kutala, V.K., Villamena, F.A., Ilangovan, G., Maspoch, D., Roques, N., Veciana, J., Rovira, C., Kuppusamy, P. Reactivity of superoxide anion radical with a perchlorotriphenylmethyl (trityl) radical. *J. Phys. Chem. B*. **2008**, *112*(1), 158–167.

237. Rizzi, C., Samouilov, A., Kutala, V.K., Parinandi, N.L., Zweier, J.L., Kuppusamy, P. Application of a trityl-based radical probe for measuring superoxide. *Free Radic. Biol. Med.* **2003**, *35*(12), 1608–1618.

238. Ballester, M., Riera-Figueras, J., Castaner, J., Badfa, C., Monso, J.M. Inert carbon free radicals. I. Perchlorodiphenylmethyl and perchlorotriphenylmethyl radical series. *J. Am. Chem. Soc.* **1971**, *93*(9), 2215–2225.

239. Dikalov, S., Skatchkov, M., Bassenge, E. Quantification of peroxynitrite, superoxide, and peroxyl radicals by a new spin trap hydroxylamine 1-hydroxy-2,2,6,6-tetramethyl-4 -oxo-piperidine. *Biochem. Biophys. Res. Commun.* **1997**, *230*(1), 54–57.

240. Saito, K., Takeshita, K., Anzai, K., Ozawa, T. Pharmacokinetic study of acyl-protected hydroxylamine probe, 1-a cetoxy-3-carbamoyl-2,2,5,5-tetramethylpyrrolidine, for *in vivo* measurements of reactive oxygen species. *Free Radic. Biol. Med.* **2004**, *36*(4), 517–525.

241. Dikalov, S., Grigor'ev, I.A., Voinov, M., Bassenge, E. Detection of superoxide radicals and peroxynitrite by 1-hydroxy-4-phosphonooxy-2,2,6,6-tetramethylpiperidin e: quantification of extracellular superoxide radicals formation. *Biochem. Biophys. Res. Commun.* **1998**, *248*(2), 211–215.

242. Zang, L.Y., Misra, B.R., van Kuijk, F.J., Misra, H.P. EPR studies on the kinetics of quenching singlet oxygen. *Biochem. Mol. Biol. Int.* **1995**, *37*(6), 1187–1195.

243. Villamena, F.A., Das, A., Nash, K.M. Potential implication of the chemical properties and bioactivity of nitrone spin traps for therapeutics. *Future Med. Chem.* **2012**, *4*(9), 1171–1207.

244. Britigan, B.E., Pou, S., Rosen, G.M., Lilleg, D.M., Buettner, G.R. Hydroxyl radical is not a product of the reaction of xanthine oxidase and xanthine. The confounding problem of adventitious iron bound to xanthine oxidase. *J. Biol. Chem.* **1990**, *265*(29), 17533–17538.

245. Du, G., Mouithys-Mickalad, A., Sluse, F.E. Generation of superoxide anion by mitochondria and impairment of their functions during anoxia and reoxygenation *in vitro*. *Free Radic. Biol. Med.* **1998**, *25*(9), 1066–1074.

246. Nohl, H., Jordan, W., Hegner, D. Identification of free hydroxyl radicals in respiring rat heart mitochondria by spin trapping with the nitrone DMPO. *FEBS Lett.* **1981**, *123*(2), 241–244.

247. Bannister, J.V., Bellavite, P., Serra, M.C., Thornalley, P.J., Rossi, F. An EPR study of the production of superoxide radicals by neutrophil NADPH oxidase. *FEBS Lett.* **1982**, *145*(2), 323–326.

248. Shi, H., Timmins, G., Monske, M., Burdick, A., Kalyanaraman, B., Liu, Y., Clement, J.-L., Burchiel, S., Liu, K.J. Evaluation of spin trapping agents and trapping conditions for detection of cell-generated reactive oxygen species. *Arch. Biochem. Biophys.* **2005**, *437*(1), 59–68.

249. Britigan, B.E., Cohen, M.S., Rosen, G.M. Detection of the production of oxygen-centered free radicals by human neutrophils using spin trapping techniques: a critical perspective. *J. Leukoc. Biol.* **1987**, *41*(4), 349–362.

250. Hirata, H., He, G., Deng, Y., Salikhov, I., Petryakov, S., Zweier, J.L. A loop resonator for slice-selective *in vivo* EPR imaging in rats. *J. Magn. Reson.* **2008**, *190*(1), 124–134.

251. Jiang, J.J., Liu, K.J., Jordan, S.J., Swartz, H.M., Mason, R.P. Detection of free radical metabolite formation using *in vivo* EPR spectroscopy: evidence of rat hemoglobin thiyl radical formation following administration of phenylhydrazine. *Arch. Biochem. Biophys.* **1996**, *330*(2), 266–270.

252. Kadiiska, M.B., Burkitt, M.J., Xiang, Q.H., Mason, R.P. Iron supplementation generates hydroxyl radical *in vivo*. An ESR spin-trapping investigation. *J. Clin. Invest.* **1995**, *96*(3), 1653–1657.

253. Bolli, R., Jeroudi, M.O., Patel, B.S., DuBose, C.M., Lai, E.K., Roberts, R., McCay, P.B. Direct evidence that oxygen-derived free radicals contribute to postischemic myocardial dysfunction in the intact dog. *Proc. Natl. Acad. Sci. U.S.A.* **1989**, *86*(12), 4695–4699.

254. Samuni, U., Samuni, Y., Goldstein, S. On the distinction between nitroxyl and nitric oxide using nitronyl nitroxides. *J. Am. Chem. Soc.* **2010**, *132*(24), 8428–8432.

255. Goldstein, S., Russo, A., Samuni, A. Reactions of PTIO and Carboxy-PTIO with .bul.NO, .bul.NO2, and O2-.bul. *J. Biol. Chem.* **2003**, *278*(51), 50949–50955.

256. Mordvintcev, P., Mulsch, A., Busse, R., Vanin, A.F. On-line detection of nitric oxide formation in liquid aqeous phase by EPR. *Anal. Biochem.* **1991**, *199*, 142.

257. Vanin, A.F., Huisman, A., Van Faassen, E.E. Iron dithiocarbamate as spin trap for nitric oxide detection: pitfalls and successes. *Methods Enzymol.* **2002**, *359*(Nitric Oxide, Part D), 27–42.

258. Vanin, A.F. Iron diethyldithiocarbamate as spin trap for nitric oxide detection. *Methods Enzymol.* **1999**, *301*, 269–279.

259. Mikoyan, V.D., Kubrina, L.N., Serezhenkov, V.A., Stukan, R.A., Vanin, A.F. Complexes of Fe(II) with diethyldithiocarbamate or N-methyl-D-glucamine dithiocarbamate as traps of nitric oxide in animal tissues: comparative investigations. *Biochim. Biophys. Acta*. **1997**, *1336*, 225–234.

260. Tsuchiya, K., Takasugi, M., Minakuchi, K., Fukuzawa, K. Senstitive quantification of nitric oxide by EPR spectroscopy. *Free Radic. Biol. Med.* **1996**, *21*, 733–737.

261. Kleschyov, A.L., Munzel, T. Advanced spin trapping of vascular nitric oxide using colloid iron dithiocarbamate. *Methods Enzymol.* **2002**, *359*, 43–51.

262. Kleschyov, A.L., Hanke Mollnau, H., Oelze, M., Meinertz, T., Huang, Y., Harrison, D.G., Munzel, T. Spin trapping of vascular nitric oxide using colloidal Fe(II)-diethyldithiocarbamate. *Biochim. Biophys. Res. Commun.* **2000**, *275*, 672–677.

263. Hogg, N. Detection of nitric oxide by electron paramagnetic resonance spectroscopy. *Free Radic. Biol. Med.* **2010**, *49*(2), 122–129.

264. Moreira, P.I., Sayre, L.M., Zhu, X., Nunomura, A., Smith, M.A., Perry, G. Detection and localization of markers of oxidative stress by in situ methods: application in the study of Alzheimer disease. *Methods Mol. Biol.* **2010**, *610*, 419–434.

265. Celes, M.R., Torres-Duenas, D., Prado, C.M., Campos, E.C., Moreira, J.E., Cunha, F.Q., Rossi, M.A. Increased sarcolemmal permeability as an early event in experimental septic cardiomyopathy: a potential role for oxidative damage to lipids and proteins. *Shock*. **2010**, *33*(3), 322–331.

266. Kuppusamy, P., Zweier, J.L. Cardiac applications of EPR imaging. *NMR Biomed.* **2004**, *17*(5), 226–239.

267. Jackson, S.K., Thomas, M.P., Smith, S., Madhani, M., Rogers, S.C., James, P.E. *In vivo* EPR spectroscopy: biomedical and potential diagnostic applications. *Faraday Discuss.* **2004**, *126*, 103–117; discussion 169–83.

268. Liu, Y., Villamena, F.A., Sun, J., Wang, T.Y., Zweier, J.L. Esterified trityl radicals as intracellular oxygen probes. *Free Radic. Biol. Med.* **2009**, *46*(7), 876–883.

269. He, G., Shankar, R.A., Chzhan, M., Samouilov, A., Kuppusamy, P., Zweier, J.L. Noninvasive measurement of anatomic structure and intraluminal oxygenation in the gastrointestinal tract of living mice with spatial and spectral EPR imaging. *Proc. Natl. Acad. Sci. U.S.A.* **1999**, *96*(8), 4586–4591.

270. Pandian, R.P., Chacko, S.M., Kuppusamy, M.L., Rivera, B.K., Kuppusamy, P. Evaluation of lithium naphthalocyanine (LiNc) microcrystals for biological EPR oximetry. *Adv. Exp. Med. Biol.*, *701*, 29–36.

271. Khan, N., Williams, B.B., Hou, H., Li, H., Swartz, H.M. Repetitive tissue pO_2 measurements by electron paramagnetic resonance oximetry: current status and future potential for experimental and clinical studies. *Antioxid. Redox Signal.* **2007**, *9*(8), 1169–1182.

272. Berliner, L.J., Fujii, H. *In vivo* spin trapping of nitric oxide. *Antioxid. Redox Signal.* **2004**, *6*(3), 649–656.

273. Sentjurc, M., Mason, R.P. Inhibition of radical adduct reduction and reoxidation of the corresponding hydroxylamines in *in vivo* spin trapping of carbon tetrachloride-derived radicals. *Free Radic. Biol. Med.* **1992**, *13*(2), 151–160.

274. Chamulitrat, W., Jordan, S.J., Mason, R.P. Fatty acid radical formation in rats administered oxidized fatty acids: *in vivo* spin trapping investigation. *Arch. Biochem. Biophys.* **1992**, *299*(2), 361–367.

275. Gomez-Mejiba, S.E., Ramirez, D.C. Trapping of DNA radicals with the nitrone spin trap 5,5-dimethyl-1-pyrroline N-oxide and genotoxic damage: recent advances using the immuno-spin trapping technology. *Mutat. Res. Rev. Mutat. Res.* **2019**, *782*, 108283.

276. Mason, R.P. Imaging free radicals in organelles, cells, tissue, and *in vivo* with immuno-spin trapping. *Redox Biol.* **2016**, *8*, 422–429.

277. Ahn, B., Smith, N., Saunders, D., Ranjit, R., Kneis, P., Towner, R.A., Van Remmen, H. Using MRI to measure *in vivo* free radical production and perfusion dynamics in a mouse model of elevated oxidative stress and neurogenic atrophy. *Redox Biol.* **2019**, *26*, 101308.

278. Simic, M.G., Jovanovi, S.V. Antioxidation mechanisms of uric acid? *J. Am. Chem. Soc.* **1989**, *111*, 5718–5182.

279. Lancaster, J.R. Jr. Nitroxidative, nitrosative, and nitrative stress: kinetic predictions of reactive nitrogen species chemistry under biological conditions. *Chem. Res. Toxicol.* **2006**, *19*(9), 1160–1174.